5

SPIN WAVES IN THE FERROMAGNETIC
HEAVY RARE EARTHS

As discussed in Section 1.5, the exchange interaction dominates the magnetic behaviour of the heavy rare earth metals, and the ordered moments at low temperatures are consequently close to the saturation values. The excitations of such a system are *spin waves*, which may be viewed semiclassically as coupled precessions of the moments about their equilibrium directions, with well-defined frequencies which are determined by the phase relations between the precessing moments on different sites. From the viewpoint of quantum mechanics, these modes are *magnons*, which are linear combinations of single-ion excitations from the ground state to the first excited molecular-field state, which is to a good approximation $|J_z = J - 1>$, with phase factors between the coefficients for different ions which determine the dispersion relation $E_{\mathbf{q}}$ for the magnon energy. A useful review of the excitations of magnetic systems has been given by Stirling and McEwen (1987).

These spin waves have been very extensively studied in the heavy rare earths, both experimentally and theoretically. In this chapter, we consider the simplest case of the *ferromagnet*, in which all the sites are equivalent. Since the magnetic heavy rare earths are all hcp, we begin by extending the earlier treatment of the linear response of the isotropic Heisenberg ferromagnet to this structure. These results are immediately applicable to Gd, where the anisotropy is indeed negligible, with the consequence that the excitation spectrum is the simplest to be found among the magnetic rare earths. Crystal-field and magnetoelastic anisotropies modify the excitation spectrum significantly, inducing an *elliptical polarization* of the precessing moments, and a *spin-wave energy gap* at long wavelengths. To treat such systems, we employ *linear spin-wave theory*, determining the magnon energies via the *Holstein–Primakoff transformation*. We consider in particular the basal-plane ferromagnet, comparing the calculated excitation spectrum throughout with experimental measurements on Tb, which has been very comprehensively studied. The magnon energies and their temperature dependence are discussed, and the energy gap associated with the uniform spin-wave mode is treated in some detail and related to the macroscopic magnetic anisotropy. The contribution to this energy gap of the *magnetoelastic coupling*, via the *static* deformation of the crystal, is then

calculated and its *dynamic* manifestation in the *magnon–phonon* interaction is discussed. *Anisotropic two-ion coupling* between the moments alters the form of the dispersion relations, both quantitatively and, on occasions, qualitatively. The classical *dipole–dipole interaction*, though weak, is highly anisotropic and long-ranged, and may therefore have an important influence at long wavelengths. Since its form is known exactly, we can calculate its effects in detail, but we can say much less about the two-ion anisotropy in general. Its possible origins and symmetry are however discussed, and examples of observable effects to which it gives rise are presented. The mutual solubility of the rare earths allows the formation of an enormous variety of *binary alloys*, with magnetic properties which may be adjusted with the concentration. We show how the excitation spectrum of such systems can be calculated by the *virtual crystal approximation* and the *coherent potential approximation*, and illustrate the phenomena which may be observed by experiments on Tb alloys. Finally, we consider the interaction between the conduction electrons and the localized $4f$ moments, and its influence on both the spin waves and the conduction electrons themselves. The *indirect-exchange interaction* is derived more rigorously than in Section 1.4, and the lifetime of the magnons due to electron scattering is deduced. The *mass enhancement* of the conduction electrons is determined, and the effects of magnetic ordering on the band structure, and of magnetic scattering on the conductivity, are discussed.

5.1 The ferromagnetic hcp-crystal

In Chapter 3, we considered the linear response of a system of magnetic moments placed on a Bravais lattice and coupled by the Heisenberg interaction. We shall now generalize this treatment to the hexagonal close-packed crystal structure of the heavy rare earth metals, in which there is a basis of two ions per unit cell, constituting two identical sublattices which, for convenience, we number 1 and 2. The surroundings of the atoms belonging to each of the two sublattices are identical, except for an inversion. Introducing the following Fourier transforms:

$$\mathcal{J}_{ss'}(\mathbf{q}) = \sum_{j\in s'-subl.} \mathcal{J}(ij)\, e^{-i\mathbf{q}\cdot(\mathbf{R}_i-\mathbf{R}_j)} \qquad ; \quad i\in s\text{-sublattice},$$

$$(5.1.1a)$$

we have, for an hcp crystal,

$$\mathcal{J}_1(\mathbf{q}) \equiv \mathcal{J}_{11}(\mathbf{q}) = \mathcal{J}_{22}(\mathbf{q})$$
$$\mathcal{J}_2(\mathbf{q}) \equiv \mathcal{J}_{12}(\mathbf{q}) = \mathcal{J}_{21}(-\mathbf{q}) = \mathcal{J}_{21}^*(\mathbf{q}),$$

$$(5.1.1b)$$

where $\mathcal{J}_1(\mathbf{q})$ is real. Defining the four Fourier transforms $\overline{\overline{\chi}}_{ss'}(\mathbf{q},\omega)$ of the susceptibility tensor equivalently to $(5.1.1a)$, we obtain from the

RPA equation (3.5.7):

$$\overline{\overline{\chi}}_{11}(\mathbf{q},\omega) = \overline{\overline{\chi}}^{o}(\omega)\left\{1 + \mathcal{J}_{11}(\mathbf{q})\overline{\overline{\chi}}_{11}(\mathbf{q},\omega) + \mathcal{J}_{12}(\mathbf{q})\overline{\overline{\chi}}_{21}(\mathbf{q},\omega)\right\}$$
$$\overline{\overline{\chi}}_{21}(\mathbf{q},\omega) = \overline{\overline{\chi}}^{o}(\omega)\left\{\mathcal{J}_{21}(\mathbf{q})\overline{\overline{\chi}}_{11}(\mathbf{q},\omega) + \mathcal{J}_{22}(\mathbf{q})\overline{\overline{\chi}}_{21}(\mathbf{q},\omega)\right\},$$
(5.1.2)

assuming that the MF susceptibility $\overline{\overline{\chi}}^{o}(\omega)$ is the same for all the sites, as in a paramagnet or a ferromagnet. These matrix equations may be solved straightforwardly, and using (5.1.1b) we find

$$\overline{\overline{\chi}}_{11}(\mathbf{q},\omega) = \overline{\overline{D}}(\mathbf{q},\omega)^{-1}\{1 - \overline{\overline{\chi}}^{o}(\omega)\,\mathcal{J}_{1}(\mathbf{q})\}\,\overline{\overline{\chi}}^{o}(\omega)$$
$$\overline{\overline{\chi}}_{21}(\mathbf{q},\omega) = \overline{\overline{D}}(\mathbf{q},\omega)^{-1}\left\{\overline{\overline{\chi}}^{o}(\omega)\right\}^{2}\,\mathcal{J}_{2}(-\mathbf{q}),$$
(5.1.3a)

where

$$\overline{\overline{D}}(\mathbf{q},\omega) = \left\{1 - \overline{\overline{\chi}}^{o}(\omega)\,\mathcal{J}_{1}(\mathbf{q})\right\}^{2} - \left\{\overline{\overline{\chi}}^{o}(\omega)\,|\mathcal{J}_{2}(\mathbf{q})|\right\}^{2}$$
$$= \left(1 - \overline{\overline{\chi}}^{o}(\omega)\left\{\mathcal{J}_{1}(\mathbf{q}) + |\mathcal{J}_{2}(\mathbf{q})|\right\}\right)\left(1 - \overline{\overline{\chi}}^{o}(\omega)\left\{\mathcal{J}_{1}(\mathbf{q}) - |\mathcal{J}_{2}(\mathbf{q})|\right\}\right),$$
(5.1.3b)

and, by symmetry,

$$\overline{\overline{\chi}}_{22}(\mathbf{q},\omega) = \overline{\overline{\chi}}_{11}(\mathbf{q},\omega) \qquad \text{and} \quad \overline{\overline{\chi}}_{12}(\mathbf{q},\omega) = \overline{\overline{\chi}}_{21}(-\mathbf{q},\omega). \qquad (5.1.3c)$$

If $\overline{\overline{\chi}}^{o}(\omega)$ contains only one pole, as in the case of the Heisenberg ferromagnet, then $\overline{\overline{D}}(\mathbf{q},\omega)^{-1}$ in (5.1.3a) generates two poles, corresponding to the existence of both an *acoustic* and an *optical* mode at each $\mathbf{q}$-vector. $\mathcal{J}_{2}(\mathbf{0})$ must be real and, since it is also positive in a ferromagnet, the acoustic mode arises from the zero of the first factor in (5.1.3b), its energy therefore being determined by the effective coupling parameter $\mathcal{J}_{1}(\mathbf{q}) + |\mathcal{J}_{2}(\mathbf{q})|$. On the other hand, if $\mathcal{J}_{2}(\mathbf{0})$ is negative, as it is in paramagnetic Pr, it is the second factor which gives the acoustic mode. The nomenclature results from the circumstance that the deviations of the moments from their equilibrium values are in phase in the acoustic mode in the limit of $\mathbf{q} \to \mathbf{0}$, and it therefore dominates the neutron cross-section. The inelastic neutron scattering is determined by (4.2.2) and (4.2.3), i.e. by

$$\overline{\overline{\chi}}(\boldsymbol{\kappa},\omega) = \frac{1}{N}\sum_{ij}\overline{\overline{\chi}}(ij,\omega)\,e^{-i\boldsymbol{\kappa}\cdot(\mathbf{R}_{i}-\mathbf{R}_{j})} = \frac{1}{2}\sum_{ss'}\overline{\overline{\chi}}_{ss'}(\boldsymbol{\kappa},\omega)$$
$$= \overline{\overline{D}}(\boldsymbol{\kappa},\omega)^{-1}\left\{1 - \overline{\overline{\chi}}^{o}(\omega)\left(\mathcal{J}_{1}(\boldsymbol{\kappa}) - \tfrac{1}{2}[\mathcal{J}_{2}(\boldsymbol{\kappa}) + \mathcal{J}_{2}(-\boldsymbol{\kappa})]\right)\right\}\overline{\overline{\chi}}^{o}(\omega),$$
(5.1.4)

where $N = 2N_{0}$ is the number of atoms. Introducing $\boldsymbol{\kappa} = \mathbf{q} + \boldsymbol{\tau}$, with $\mathbf{q}$ lying in the primitive zone, we may write this result as a sum of the acoustic and optical response functions:

$$\overline{\overline{\chi}}_{\text{Ac}}(\mathbf{q},\omega) = \left\{1 - \overline{\overline{\chi}}^{o}(\omega)(\mathcal{J}_{1}(\mathbf{q}) + \nu|\mathcal{J}_{2}(\mathbf{q})|)\right\}^{-1}\overline{\overline{\chi}}^{o}(\omega)$$
$$\overline{\overline{\chi}}_{\text{Op}}(\mathbf{q},\omega) = \left\{1 - \overline{\overline{\chi}}^{o}(\omega)(\mathcal{J}_{1}(\mathbf{q}) - \nu|\mathcal{J}_{2}(\mathbf{q})|)\right\}^{-1}\overline{\overline{\chi}}^{o}(\omega),$$
(5.1.5)

where $\nu = \pm 1$ denotes the sign of $\mathcal{J}_2(\mathbf{0})$. $\mathcal{J}_1(\boldsymbol{\kappa}) = \mathcal{J}_1(\mathbf{q})$ is real, whereas

$$\mathcal{J}_2(\boldsymbol{\kappa}) = \mathcal{J}_2(\mathbf{q})\, e^{i\boldsymbol{\tau}\cdot\boldsymbol{\rho}} = \nu|\mathcal{J}_2(\mathbf{q})|e^{i\varphi}, \qquad (5.1.6a)$$

defining the phase $\varphi = \varphi(\boldsymbol{\kappa})$, and $\boldsymbol{\rho} = \mathbf{d}_2 - \mathbf{d}_1$ is the vector joining the two sublattices. In terms of these quantities, the susceptibility (5.1.4) may be written

$$\overline{\overline{\chi}}(\mathbf{q}+\boldsymbol{\tau},\omega) = \tfrac{1}{2}(1+\cos\varphi)\,\overline{\overline{\chi}}_{\mathrm{Ac}}(\mathbf{q},\omega) + \tfrac{1}{2}(1-\cos\varphi)\,\overline{\overline{\chi}}_{\mathrm{Op}}(\mathbf{q},\omega). \quad (5.1.6b)$$

The phase φ vanishes in the limit $\mathbf{q} \to \mathbf{0}$ if $\boldsymbol{\tau} = \mathbf{0}$, and the scattering cross-section then only depends on the isolated pole in the acoustic response function, in accordance with our definition above. Introducing the following lattice vectors of the hexagonal lattice:

$$\mathbf{a}_1 = (a,0,0) \qquad \mathbf{a}_2 = \left(-\frac{a}{2}, \frac{\sqrt{3}a}{2}, 0\right) \qquad \mathbf{a}_3 = (0,0,c), \quad (5.1.7a)$$

we find the corresponding reciprocal lattice vectors:

$$\mathbf{b}_1 = \left(\frac{2\pi}{a}, \frac{2\pi}{\sqrt{3}a}, 0\right) \qquad \mathbf{b}_2 = \left(0, \frac{4\pi}{\sqrt{3}a}, 0\right) \qquad \mathbf{b}_3 = \left(0, 0, \frac{2\pi}{c}\right). \quad (5.1.7b)$$

Since $\boldsymbol{\rho} = \left(\frac{a}{2}, \frac{a}{2\sqrt{3}}, \frac{c}{2}\right)$,

$$\boldsymbol{\tau}\cdot\boldsymbol{\rho} = \frac{4\pi}{3}h + \frac{2\pi}{3}k + \pi l \qquad \text{with} \quad \boldsymbol{\tau} = (hkl) = h\mathbf{b}_1 + k\mathbf{b}_2 + l\mathbf{b}_3. \quad (5.1.8)$$

If $\mathbf{q}$ is parallel to the c-axis, $\mathcal{J}_2(\mathbf{q})$ is real. The phase φ in (5.1.6) is then $\boldsymbol{\tau}\cdot\boldsymbol{\rho}$ and, if the Miller indices h and k are both zero, $\varphi = \boldsymbol{\tau}\cdot\boldsymbol{\rho} = l\pi$. In this case, with $\boldsymbol{\kappa}$ in the c-direction, the inelastic scattering detects only the acoustic or the optical excitations, depending on whether l is respectively even or odd, and no energy gap appears at the zone boundary, even though l changes, because $\mathcal{J}_2(\mathbf{b}_3/2) = 0$ by symmetry. We may therefore use a *double-zone representation*, in which the dispersion relation for the excitations is considered as comprising a single branch extending twice the distance to the Brillouin zone boundary, corresponding to an effective unit cell of height $c/2$. We shall generally use this representation when discussing excitations propagating in the c-direction.
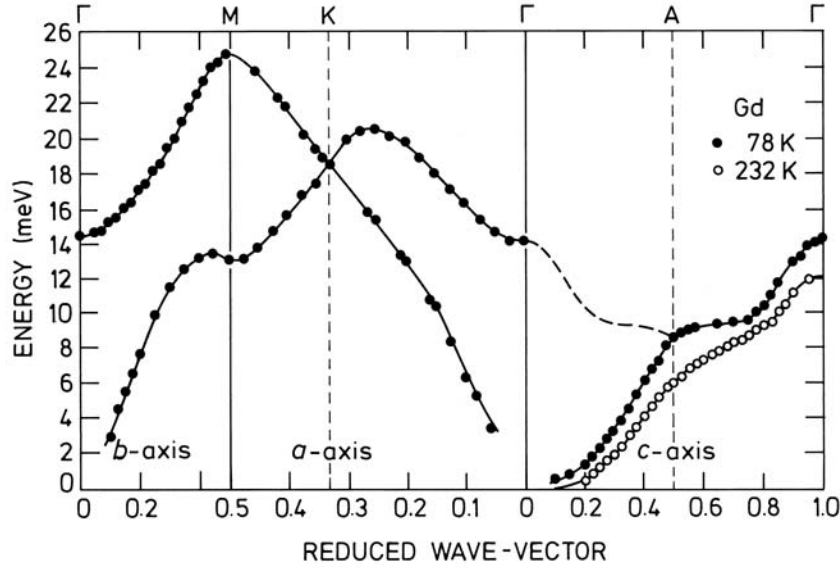
Fig. 5.1.   Spin-wave dispersion relations for Gd, after Koehler *et al.* (1970). The two atoms of the hcp structure give rise to acoustic and optical branches. Since the single-ion anisotropy is negligible, the acoustic mode rises quadratically from the origin.

Because $L = 0$, so that $J = S$, anisotropy effects are small in Gd, and it is therefore a good approximation to a Heisenberg ferromagnet. Using the above procedure to generalize (3.5.26) to the hcp structure, we obtain the two branches of the excitation spectrum

$$E_{\mathbf{q}}^{\text{Ac}} = \langle J_z \rangle \big\{ \mathcal{J}_1(\mathbf{0}) + \mathcal{J}_2(\mathbf{0}) - \mathcal{J}_1(\mathbf{q}) - |\mathcal{J}_2(\mathbf{q})| \big\}$$
$$E_{\mathbf{q}}^{\text{Op}} = \langle J_z \rangle \big\{ \mathcal{J}_1(\mathbf{0}) + \mathcal{J}_2(\mathbf{0}) - \mathcal{J}_1(\mathbf{q}) + |\mathcal{J}_2(\mathbf{q})| \big\}, \tag{5.1.9}$$

since $\mathcal{J}_2(\mathbf{0})$ is positive. The dispersion relations measured by inelastic neutron scattering by Koehler *et al.* (1970) are shown in Fig. 5.1. This figure illustrates the use of the double-zone representation when $\mathbf{q}$ is along the c-axis, resulting in a single spin-wave branch. The renormalization predicted by the simple RPA theory, that $E_{\mathbf{q}}(T)$ is proportional to σ, is not followed very precisely. σ changes from about 0.97 at 78 K to 0.66 at 232 K. As may be seen from Fig. 5.1, and from more extensive studies by Cable *et al.* (1985), the energies in the c-direction vary approximately like $\sigma^{0.5}$ at the largest wave-vectors, like σ in the middle of the branch, and faster than σ at small wave-vectors. However, it is also evident from the figure that the form of $\mathcal{J}(\mathbf{q})$ changes with decreasing magnetization, so some of the discrepancy between the simple

prediction and the observed behaviour at low temperatures may be due to changes of $\mathcal{J}(\mathbf{q})$. At higher temperatures, the RPA renormalization breaks down completely. The spin-wave energy at the zone boundary has only fallen by about a factor two at $292\,\mathrm{K}$, very close to T_C. Furthermore, strongly-broadened neutron peaks are observed even at $320\,\mathrm{K}$, well above the transition, close to the zone boundary in the basal plane, with energies of about $k_B T_C$. On the other hand, the low-energy spin waves progressively broaden out into diffusive peaks as T_C is approached from below.

5.2 Spin waves in the anisotropic ferromagnet

In the heavy rare earth metals, the two-ion interactions are large and of long range. They induce magnetically-ordered states at relatively high temperatures, and the ionic moments approach closely their saturation values at low temperatures. These circumstances allow us to adopt a somewhat different method, *linear spin-wave theory*, from those discussed previously in connection with the derivation of the correlation functions. We shall consider the specific case of a hexagonal close-packed crystal ordered ferromagnetically, with the moments lying in the basal plane, corresponding to the low-temperature phases of both Tb and Dy. For simplicity, we shall initially treat only the anisotropic effects introduced by the single-ion crystal-field Hamiltonian so that, in the case of hexagonal symmetry, we have

$$\mathcal{H} = \sum_i \left[\sum_{l=2,4,6} B_l^0 Q_l^0(\mathbf{J}_i) + B_6^6 Q_6^6(\mathbf{J}_i) - g\mu_B \mathbf{J}_i \cdot \mathbf{H} \right] - \frac{1}{2} \sum_{i \neq j} \mathcal{J}(ij)\, \mathbf{J}_i \cdot \mathbf{J}_j.$$
(5.2.1)

The system is assumed to order ferromagnetically at low temperatures, a sufficient condition for which is that the maximum of $\mathcal{J}(\mathbf{q})$ occurs at $\mathbf{q} = \mathbf{0}$. $Q_l^m(\mathbf{J}_i)$ denotes the Stevens operator of the ith ion, but defined in terms of (J_ξ, J_η, J_ζ) instead of (J_x, J_y, J_z), where the (ξ, η, ζ)-axes are fixed to be along the symmetry a-, b- and c-directions, respectively, of the hexagonal lattice. The (x, y, z)-coordinate system is chosen such that the z-axis is along the magnetization axis, specified by the polar angles (θ, ϕ) in the (ξ, η, ζ)-coordinate system. Choosing the y-axis to lie in the basal plane, we obtain the following relations:

$$\begin{aligned}
J_\xi &= J_z \sin\theta \cos\phi - J_x \cos\theta \cos\phi + J_y \sin\phi \\
J_\eta &= J_z \sin\theta \sin\phi - J_x \cos\theta \sin\phi - J_y \cos\phi \\
J_\zeta &= J_z \cos\theta + J_x \sin\theta,
\end{aligned}$$
(5.2.2)

from which

$$Q_2^0 = 3\{J_z^2 \cos^2\theta + J_x^2 \sin^2\theta + (J_z J_x + J_x J_z)\cos\theta \sin\theta\} - J(J+1). \quad (5.2.3)$$

Initially we assume that $\langle J_z \rangle = J$ at $T = 0$, which implies that the ground state is the product of $|J_z = J>$-states of the single ions. In this case, we find, consistently with eqn (2.2.14),

$$\langle Q_2^0 \rangle = <J\,|\,Q_2^0\,|\,J> = J^{(2)}(3\cos^2\theta - 1),$$

where, as before, $J^{(n)} = J(J - \frac{1}{2})\cdots(J - \frac{n-1}{2})$, and we have used the expectation values $\langle J_z^2 \rangle = J^2$, $\langle J_x^2 \rangle = \frac{1}{2}J$ and $\langle J_z J_x \rangle = 0$. Analogously, though with considerably more labour, we can show that, for instance,

$$\langle Q_6^6 \rangle = <J\,|\,\tfrac{1}{2}(J_\xi + iJ_\eta)^6 + \tfrac{1}{2}(J_\xi - iJ_\eta)^6\,|\,J> = J^{(6)}\sin^6\theta\cos 6\phi. \quad (5.2.4)$$

For simplicity, we neglect for the moment B_4^0 and B_6^0, and specifying the direction of the magnetic field by the polar angles (θ_H, ϕ_H), we find that the ground-state energy is, within this approximation,

$$U(T = 0) \simeq N\big[B_2^0 J^{(2)}(3\cos^2\theta - 1) + B_6^6 J^{(6)}\sin^6\theta\cos 6\phi$$
$$- g\mu_B JH\{\cos\theta\cos\theta_H + \sin\theta\sin\theta_H\cos(\phi - \phi_H)\} - \tfrac{1}{2}\mathcal{J}(\mathbf{0})\,J^2\big],$$
$$(5.2.5)$$

where θ and ϕ are determined so that they minimize this expression. In zero magnetic field, $H = 0$, (5.2.5) only gives two possibilities for θ, viz. $\theta = 0$ for $B_2^0 J^{(2)} < -\frac{1}{3}|B_6^6|J^{(6)}$ or $\theta = \frac{\pi}{2}$ for $B_2^0 J^{(2)} > -\frac{1}{3}|B_6^6|J^{(6)}$. We shall here be concerned with the second case of $\theta = \frac{\pi}{2}$, i.e. the basal-plane ferromagnet. In this case, the angle ϕ is determined by the sign of B_6^6. The magnetic moments will be along an a- or a b-axis ($\phi = 0$ or $\phi = \frac{\pi}{2}$) if B_6^6 is respectively negative or positive. Having specified the (approximate) ground state, we turn to the excitations, i.e. the spin waves.

Instead of utilizing the standard-basis operators, defined by (3.5.11), we shall introduce a Bose operator a_i for the ith ion, satisfying

$$[a_i\,,\,a_j^+] = \delta_{ij} \qquad ; \qquad [a_i\,,\,a_j] = [a_i^+\,,\,a_j^+] = 0, \qquad (5.2.6)$$

which acts on the $|J_z>$-state vector of this ion (the site index is suppressed) in the following way:

$$a\,|\,J> = 0 \qquad ; \qquad a\,|\,J - m> = \sqrt{m}\,|\,J - m + 1> \qquad (5.2.7)$$

Holstein and Primakoff (1940) introduced the following representation of the angular momentum operators:

$$J_z = J - a^+ a$$
$$J_+ = \big(2J - a^+ a\big)^{\frac{1}{2}} a \qquad\qquad (5.2.8)$$
$$J_- = a^+\big(2J - a^+ a\big)^{\frac{1}{2}}.$$

If the usual basis vectors in the Hilbert space created by the Bose operators are denoted by $|n)$, i.e. $a|n) = \sqrt{n}|n-1)$ where $n = 0, 1, 2, \cdots, \infty$, then by the definition (5.2.7), $|n) = |J_z = J - n>$ for $n = 0, 1, 2, \cdots, 2J$, but there is no physical $|J_z>$-state corresponding to $|n)$ when $n > 2J$. It is straightforward to see that the Bose representation (5.2.8) produces the right matrix-elements of the angular momentum operators, as long as $|n)$ is restricted to the physical part of the Hilbert space, $n \leq 2J$, but this representation presupposes the presence of an infinite number of states. In the ferromagnetic case, the unphysical states are at high energies, if J is large and T is low, and their influence on the thermal averages is negligible. In this regime of J and T, the *Holstein–Primakoff transformation* is useful and the results derived from it are trustworthy.

In order to be able to treat the Bose operators under the square roots in eqn (5.2.8), we shall utilize $1/J$ as an expansion parameter. This means that, instead of the $J_{\pm}$ given by (5.2.8), we shall use

$$J_+ = (J_-)^{\dagger} \simeq \sqrt{2J}\left(a - \frac{1}{4J}a^+aa\right). \qquad (5.2.9)$$

It is important here to realize that the expansion parameter is $1/J$ and not, for instance, 'the number of deviation operators'. If the latter were the case, a well-ordered expansion of J_+ (Lindgård and Danielsen 1974) would suggest instead $J_+ = \sqrt{2J}\{a - (1 - \sqrt{1 - 1/2J})a^+aa + \cdots\}$, corresponding to a replacement of $\frac{1}{4J}$ in (5.2.9) by $\frac{1}{4J}(1 + \frac{1}{8J} + \cdots)$. We emphasize that we shall be expanding the *reduced* operators $(1/J^{(l)})O_l^m$, leaving no ambiguities either in (5.2.9) or in the following. Using eqn (5.2.9) and $J_z = J - a^+a$, it is straightforward to express the Stevens operators in terms of the Bose operators. For O_2^0, we get

$$\begin{aligned} O_2^0 &= 3J_z^2 - J(J+1) = 3(J - a^+a)^2 - J(J+1) \\ &= 2J(J - \tfrac{1}{2}) - 6(J - \tfrac{1}{2})\,a^+a + 3a^+a^+aa \\ &= 2J^{(2)}\Big\{1 - \frac{3}{J}\,a^+a + \frac{3}{2J^2}\,a^+a^+aa + \mathcal{O}(1/J^3)\Big\}. \end{aligned} \qquad (5.2.10)$$

Here we have used $[a\,,\,a^+] = 1$ to arrange the operators in 'well-ordered' products, with all the creation operators to the left, and in the last line $1/J^{(2)}$ has been replaced by $1/J^2$ in the term of second order in $1/J$. In the same way, we obtain

$$\begin{aligned} O_2^2 &= \tfrac{1}{2}(J_+^2 + J_-^2) = J^{(2)}\Big\{\frac{1}{J}(a^+a^+ + aa) \\ &\quad + \frac{1}{4J^2}(a^+a^+ + aa - 2a^+a^+a^+a - 2a^+aaa) + \mathcal{O}(1/J^3)\Big\}. \end{aligned} \qquad (5.2.11)$$

The expression for Q_2^0 is then determined using $Q_2^0(\theta = \frac{\pi}{2}) = -\frac{1}{2}O_2^0 + \frac{3}{2}O_2^2$. For the case of Q_6^6, we refer to Lindgård and Danielsen (1974), who have established the Bose operator expansion of the tensor operators up to the eighth rank. Introducing these expansions into (5.2.1), and grouping the terms together according to their order in $1/J$, we may write the Hamiltonian

$$\mathcal{H} = \mathcal{H}_0 + \mathcal{H}_1 + \mathcal{H}_2 + \cdots + \mathcal{H}', \qquad (5.2.12)$$

where $\mathcal{H}_0 = U_0$ is the zero-order term, and

$$U_0 = N\big[-B_2^0 J^{(2)} + B_6^6 J^{(6)} \cos 6\phi - g\mu_B JH \cos(\phi - \phi_H) - \tfrac{1}{2}J^2 \mathcal{J}(\mathbf{0})\big], \qquad (5.2.13)$$

corresponding to (5.2.5), when we restrict ourselves to the case $\theta = \theta_H = \pi/2$. $\mathcal{H}_1$ comprises the terms of first order in $1/J$, and is found to be

$$\mathcal{H}_1 = \sum_i \big[A\, a_i^+ a_i + B\, \tfrac{1}{2}(a_i^+ a_i^+ + a_i a_i)\big] - \sum_{ij} J\mathcal{J}(ij)(a_i^+ a_j - a_i^+ a_i), \qquad (5.2.14)$$

where the parameters A and B are

$$A = \frac{1}{J}\big\{3B_2^0 J^{(2)} - 21 B_6^6 J^{(6)} \cos 6\phi + g\mu_B JH \cos(\phi - \phi_H)\big\}$$
$$B = \frac{1}{J}\big\{3B_2^0 J^{(2)} + 15 B_6^6 J^{(6)} \cos 6\phi\big\}. \qquad (5.2.15)$$

If we consider only the zero- and first-order part of the Hamiltonian, i.e. assume $\mathcal{H} \simeq \mathcal{H}_0 + \mathcal{H}_1$, it can be brought into diagonal form via two transformations. The first step is to introduce the spatial Fourier transforms of $\mathcal{J}(ij)$, eqn (3.4.2), and of a_i:

$$a_{\mathbf{q}} = \frac{1}{\sqrt{N}} \sum_i a_i\, e^{-i\mathbf{q}\cdot\mathbf{R}_i} \qquad ; \qquad a_{\mathbf{q}}^+ = \frac{1}{\sqrt{N}} \sum_i a_i^+\, e^{i\mathbf{q}\cdot\mathbf{R}_i}, \qquad (5.2.16)$$

for which the commutators are

$$[a_{\mathbf{q}}, a_{\mathbf{q}'}^+] = \frac{1}{N} \sum_i e^{-i(\mathbf{q}-\mathbf{q}')\cdot\mathbf{R}_i} = \delta_{\mathbf{q}\mathbf{q}'}.$$

In the case of an hcp lattice, with its two ions per unit cell, the situation is slightly more complex, as discussed in the previous section. However, this complication is inessential in the present context, and for simplicity we consider a Bravais lattice in the rest of this section, so that the results which we obtain are only strictly valid for excitations propagating in

the c-direction, for which the double-zone representation may be used. Introducing the Fourier transforms, we may write

$$\mathcal{H}_1 = \sum_{\mathbf{q}} \left[A_{\mathbf{q}}\, a_{\mathbf{q}}^+ a_{\mathbf{q}} + B\, \tfrac{1}{2}(a_{\mathbf{q}}^+ a_{-\mathbf{q}}^+ + a_{\mathbf{q}} a_{-\mathbf{q}}) \right], \qquad (5.2.17)$$

with

$$A_{\mathbf{q}} = A + J\{\mathcal{J}(\mathbf{0}) - \mathcal{J}(\mathbf{q})\}. \qquad (5.2.18)$$

$\mathcal{H}_1$ is quadratic in the Bose operators, and it can be diagonalized by performing a *Bogoliubov transformation*. A new Bose operator $\alpha_{\mathbf{q}}$ is introduced, such that

$$a_{\mathbf{q}} = u_{\mathbf{q}}\alpha_{\mathbf{q}} - v_{\mathbf{q}}\alpha_{-\mathbf{q}}^+ \quad ; \quad |u_{\mathbf{q}}|^2 - |v_{\mathbf{q}}|^2 = 1, \qquad (5.2.19)$$

in terms of which $\mathcal{H}_0 + \mathcal{H}_1$ is transformed into

$$\mathcal{H}_0 + \mathcal{H}_1 = U_0 + U_1 + \sum_{\mathbf{q}} E_{\mathbf{q}}\, \alpha_{\mathbf{q}}^+ \alpha_{\mathbf{q}}, \qquad (5.2.20)$$

when $u_{\mathbf{q}}$ and $v_{\mathbf{q}}$ are adjusted appropriately. Here they can both be chosen to be real quantities, and are determined by the equation

$$(u_{\mathbf{q}} \pm v_{\mathbf{q}})^2 = (A_{\mathbf{q}} \pm B)/E_{\mathbf{q}}. \qquad (5.2.21)$$

The energy parameters are

$$U_1 = \frac{1}{2} \sum_{\mathbf{q}} (E_{\mathbf{q}} - A_{\mathbf{q}}) \quad ; \quad E_{\mathbf{q}} = \sqrt{A_{\mathbf{q}}^2 - B^2}. \qquad (5.2.22)$$

When B is different from zero, as occurs if either B_2^0 or B_6^6 is non-zero, the product of the $|J_{iz} = J> = |0)_i$-states is no longer the (MF) ground state. Q_2^0 and Q_6^6 give rise to couplings between the single-ion states $|J>$, $|J-2>$ etc. as reflected in the term proportional to B in (5.2.17). The new ground state established by the Bogoliubov transformation has the energy $U_0 + U_1$ $(= U_0 - \sum_{\mathbf{q}} B^2/4E_{\mathbf{q}}$ to leading order in $B)$, which is always smaller than U_0. The admixture of (predominantly) the $|J-2>$-state into the ground state implies that the system is no longer fully polarized at $T = 0$, as assumed in (5.2.5). Using (5.2.19) and the conditions $\langle \alpha_{\mathbf{q}} \alpha_{\mathbf{q}} \rangle = \langle \alpha_{\mathbf{q}}^+ \alpha_{\mathbf{q}}^+ \rangle = 0$, whereas

$$\langle \alpha_{\mathbf{q}}^+ \alpha_{\mathbf{q}} \rangle = n_{\mathbf{q}} = \frac{1}{e^{\beta E_{\mathbf{q}}} - 1} \qquad (5.2.23)$$

is the usual Bose population-factor, we find to first order in $1/J$:

$$\langle J_z \rangle = \Big\langle J - \frac{1}{N} \sum_{\mathbf{q}} a_{\mathbf{q}}^+ a_{\mathbf{q}} \Big\rangle = J(1 - m), \qquad (5.2.24)$$

with

$$m = \frac{1}{N} \sum_{\mathbf{q}} \frac{1}{J} \langle a_{\mathbf{q}}^+ a_{\mathbf{q}} \rangle = \frac{1}{N} \sum_{\mathbf{q}} m_{\mathbf{q}}$$

and

$$\begin{aligned} m_{\mathbf{q}} &= \frac{1}{J} \langle (u_{\mathbf{q}} \alpha_{\mathbf{q}}^+ - v_{\mathbf{q}} \alpha_{-\mathbf{q}})(u_{\mathbf{q}} \alpha_{\mathbf{q}} - v_{\mathbf{q}} \alpha_{-\mathbf{q}}^+) \rangle \\ &= \frac{1}{J} \big\{ u_{\mathbf{q}}^2 n_{\mathbf{q}} + v_{\mathbf{q}}^2 (n_{\mathbf{q}} + 1) \big\} \\ &= \frac{1}{J} \Big\{ \frac{A_{\mathbf{q}}}{E_{\mathbf{q}}} \big(n_{\mathbf{q}} + \tfrac{1}{2} \big) - \tfrac{1}{2} \Big\}, \end{aligned} \qquad (5.2.25)$$

which is positive and non-zero, even when $n_{\mathbf{q}} = 0$ at $T = 0$.

The second-order contribution to the Hamiltonian is

$$\begin{aligned} \mathcal{H}_2 = \sum_i &\Big[B \frac{1}{8J} (a_i^+ a_i^+ + a_i a_i) + C_1 a_i^+ a_i^+ a_i a_i \\ &+ C_2 (a_i^+ a_i^+ a_i^+ a_i + a_i^+ a_i a_i a_i) + C_3 (a_i^+ a_i^+ a_i^+ a_i^+ + a_i a_i a_i a_i) \Big] \\ &- \tfrac{1}{4} \sum_{ij} \mathcal{J}(ij) \big(2a_i^+ a_j^+ a_i a_j - a_i^+ a_j^+ a_j a_j - a_i^+ a_i^+ a_i a_j \big), \quad (5.2.26) \end{aligned}$$

with

$$\begin{aligned} C_1 &= -\frac{1}{J^2} \big(\tfrac{3}{2} B_2^0 J^{(2)} - 105 B_6^6 J^{(6)} \cos 6\phi \big) \\ C_2 &= -\frac{1}{J^2} \big(\tfrac{3}{4} B_2^0 J^{(2)} + \tfrac{195}{4} B_6^6 J^{(6)} \cos 6\phi \big) \qquad (5.2.27) \\ C_3 &= \frac{1}{J^2} \tfrac{15}{4} B_6^6 J^{(6)} \cos 6\phi. \end{aligned}$$

Introducing the Fourier transforms of the Bose operators in $\mathcal{H}_2$, we find straightfwardly that

$$i\hbar \partial a_{\mathbf{q}} / \partial t = [a_{\mathbf{q}}, \mathcal{H}] \simeq [a_{\mathbf{q}}, \mathcal{H}_1 + \mathcal{H}_2] = A_{\mathbf{q}} a_{\mathbf{q}} + B \big(1 + \frac{1}{4J} \big) a_{-\mathbf{q}}^+ +$$

$$\frac{1}{N} \sum_{\mathbf{k}, \mathbf{k}'} \Big[\big\{ -\mathcal{J}(\mathbf{q} - \mathbf{k}') + \tfrac{1}{2} \mathcal{J}(\mathbf{k}') + \tfrac{1}{4} \mathcal{J}(\mathbf{k}) + \tfrac{1}{4} \mathcal{J}(\mathbf{q}) + 2C_1 \big\} a_{\mathbf{k}}^+ a_{\mathbf{k}'} a_{\mathbf{q}+\mathbf{k}-\mathbf{k}'}$$

$$+ C_2 \big\{ 3 a_{\mathbf{k}}^+ a_{-\mathbf{k}'}^+ a_{\mathbf{q}+\mathbf{k}-\mathbf{k}'} + a_{-\mathbf{k}} a_{\mathbf{k}'} a_{\mathbf{q}+\mathbf{k}-\mathbf{k}'} \big\} + 4C_3 \, a_{\mathbf{k}}^+ a_{-\mathbf{k}'}^+ a_{-\mathbf{q}-\mathbf{k}+\mathbf{k}'}^+ \Big],$$

$$(5.2.28)$$

for the operator $[a_{\mathbf{q}}, \mathcal{H}]$, which appears in the equation of motion of, for instance $\langle\langle a_{\mathbf{q}} ; a_{\mathbf{q}}^+ \rangle\rangle$. When the thermal averages of terms due to $\mathcal{H}_2$

are considered, the replacement of $\mathcal{H}$ by $\mathcal{H}_0 + \mathcal{H}_1$ in the density matrix only gives rise to errors of higher-order in $1/J$. Because $\mathcal{H}_0 + \mathcal{H}_1$ is quadratic in the Bose operators, this replacement results in a decoupling of the $\mathcal{H}_2$-terms (according to *Wick's theorem*) which is equivalent to the RPA decoupling utilized previously. Hence, when considering thermal averages, we have to leading order in $1/J$, for instance,

$$a_{\mathbf{k}}^+ a_{\mathbf{k}'} a_{\mathbf{q+k-k}'} \simeq a_{\mathbf{k}}^+ \langle a_{\mathbf{k}'} a_{\mathbf{q+k-k}'} \rangle + a_{\mathbf{k}'} \langle a_{\mathbf{k}}^+ a_{\mathbf{q+k-k}'} \rangle + a_{\mathbf{q+k-k}'} \langle a_{\mathbf{k}} a_{\mathbf{k}'} \rangle$$
$$= \delta_{\mathbf{k},-\mathbf{q}} a_{-\mathbf{q}}^+ \langle a_{\mathbf{k}'} a_{-\mathbf{k}'} \rangle + \delta_{\mathbf{k}',\mathbf{q}} a_{\mathbf{q}} \langle a_{\mathbf{k}}^+ a_{\mathbf{k}} \rangle + \delta_{\mathbf{k},\mathbf{k}'} a_{\mathbf{q}} \langle a_{\mathbf{k}}^+ a_{\mathbf{k}} \rangle,$$
$$(5.2.29)$$

where the last line follows from the diagonality of $\mathcal{H}_0 + \mathcal{H}_1$ in reciprocal space. We note that it is convenient here that the single-ion operators are expressed as products of Bose operators which are well-ordered. When this decoupling is introduced in (5.2.28), it reduces to

$$[a_{\mathbf{q}}, \mathcal{H}] = \widetilde{A}_{\mathbf{q}}(T) a_{\mathbf{q}} + \widetilde{B}_{\mathbf{q}}(T) a_{-\mathbf{q}}^+, \qquad (5.2.30)$$

where the effective, renormalized parameters are

$$\widetilde{A}_{\mathbf{q}}(T) = A + 4JC_1 m + 6JC_2 b + J\{\mathcal{J}(\mathbf{0}) - \mathcal{J}(\mathbf{k})\}(1 - m)$$
$$+ \frac{1}{N} \sum_{\mathbf{k}} J\{\mathcal{J}(\mathbf{k}) - \mathcal{J}(\mathbf{k} - \mathbf{q})\} m_{\mathbf{k}} \qquad (5.2.31a)$$

and

$$\widetilde{B}_{\mathbf{q}}(T) = B\left(1 + \frac{1}{4J}\right) + 2JC_1 b + 6JC_2 m + 12JC_3 b - \tfrac{1}{2}J\{\mathcal{J}(\mathbf{0}) - \mathcal{J}(\mathbf{q})\}b$$
$$+ \frac{1}{2N} \sum_{\mathbf{k}} J\{\mathcal{J}(\mathbf{0}) - \mathcal{J}(\mathbf{k})\}b_{\mathbf{k}} + \frac{1}{N} \sum_{\mathbf{k}} J\{\mathcal{J}(\mathbf{k}) - \mathcal{J}(\mathbf{k} - \mathbf{q})\}b_{\mathbf{k}}.$$
$$(5.2.31b)$$

$m_{\mathbf{k}}$ and $b_{\mathbf{k}}$ are respectively the correlation functions $(1/J)\langle a_{\mathbf{k}}^+ a_{\mathbf{k}} \rangle$ and $(1/J)\langle a_{\mathbf{k}}^+ a_{-\mathbf{k}}^+ \rangle = (1/J)\langle a_{\mathbf{k}} a_{-\mathbf{k}} \rangle$, and m and b are the corresponding averages over $\mathbf{k}$. Equation (5.2.30) implies that the operator $[a_{\mathbf{q}}, \mathcal{H}]$, in the equations of motion of any Green function involving $a_{\mathbf{q}}$, can be replaced by the expression on the right-hand side. The same result is obtained if, instead, $\mathcal{H}_2$ is neglected, and $A_{\mathbf{q}}$ and B in $\mathcal{H}_1$ are replaced by $\widetilde{A}_{\mathbf{q}}(T)$ and $\widetilde{B}_{\mathbf{q}}(T)$ in (5.2.17). Consequently, the system behaves as if the Hamiltonian $\mathcal{H}_0 + \mathcal{H}_1 + \mathcal{H}_2$ is replaced by $\widetilde{\mathcal{H}}_0 + \widetilde{\mathcal{H}}_1$, which is similar to $\mathcal{H}_0 + \mathcal{H}_1$ except for the introduction of the effective, temperature-dependent parameters. The RPA decoupling (5.2.29) introduces errors in the Green functions, but only in the third order of $1/J$, and as it leads to an effective Hamiltonian which is quadratic in the Bose operators, it is a valid procedure. This internal consistency of the theory to second order in

$1/J$ means that the RPA contributions to the correlation functions are reliably estimated, and that all second-order contributions are included when $\widetilde{\mathcal{H}}_0 + \widetilde{\mathcal{H}}_1$ is used, instead of $\mathcal{H}_0 + \mathcal{H}_1$, in the calculation of the thermal averages. We shall therefore use the following self-consistent expressions for the characteristic correlation functions, $m_{\mathbf{k}}$ and $b_{\mathbf{k}}$, determined straightforwardly by utilizing the correspondence between $\mathcal{H}_0 + \mathcal{H}_1$ and $\widetilde{\mathcal{H}}_0 + \widetilde{\mathcal{H}}_1$:

$$m_{\mathbf{k}} = \frac{1}{J}\left\{\frac{\widetilde{A}_{\mathbf{k}}(T)}{E_{\mathbf{k}}(T)}\left(n_{\mathbf{k}} + \tfrac{1}{2}\right) - \tfrac{1}{2}\right\}, \qquad (5.2.32a)$$

corresponding to (5.2.25), and

$$b_{\mathbf{k}} = -\frac{1}{J}\frac{\widetilde{B}_{\mathbf{k}}(T)}{E_{\mathbf{k}}(T)}\left(n_{\mathbf{k}} + \tfrac{1}{2}\right). \qquad (5.2.32b)$$

In order to express the result in a convenient form, we rewrite one of the second-order terms in $\widetilde{B}_{\mathbf{q}}(T)$ as

$$\frac{1}{2N}\sum_{\mathbf{k}} J\{\mathcal{J}(\mathbf{0}) - \mathcal{J}(\mathbf{k})\}b_{\mathbf{k}} = -\tfrac{1}{2}B\left(m + \tfrac{1}{2J}\right) - \tfrac{1}{2}A\,b + \mathcal{O}(1/J^3), \quad (5.2.33)$$

since, to leading order, $J\{\mathcal{J}(\mathbf{0}) - \mathcal{J}(\mathbf{k})\} = \widetilde{A}_{\mathbf{k}}(T) - A$, and $\widetilde{B}_{\mathbf{k}}(T)$ in $b_{\mathbf{k}}$ can be approximated by B. We note that $A_{\mathbf{q}}$ and B are parameters of the order $1/J$, as are m and b (at low temperatures). In addition to introducing (5.2.33) into (5.2.31b), it is adequate for calculating the spin-wave energies to define a transformed set of parameters:

$$\begin{aligned} A_{\mathbf{q}}(T) &= \widetilde{A}_{\mathbf{q}}(T) + \tfrac{1}{2}\widetilde{B}_{\mathbf{q}}(T)\,b \\ B_{\mathbf{q}}(T) &= \widetilde{B}_{\mathbf{q}}(T) + \tfrac{1}{2}\widetilde{A}_{\mathbf{q}}(T)\,b \end{aligned} \qquad (5.2.34)$$

and these are then, to the order considered,

$$\begin{aligned} A_{\mathbf{q}}(T) = {}& A + 4JC_1 m + 6JC_2 b + \tfrac{1}{2}Bb \\ &+ J\{\mathcal{J}(\mathbf{0}) - \mathcal{J}(\mathbf{q})\}(1 - m) + \frac{1}{N}\sum_{\mathbf{k}} J\{\mathcal{J}(\mathbf{k}) - \mathcal{J}(\mathbf{k} - \mathbf{q})\}m_{\mathbf{k}} \end{aligned}$$
$$(5.2.35a)$$

and

$$\begin{aligned} B_{\mathbf{q}}(T) = {}& B + 2JC_1 b + 6JC_2 m + 12JC_3 b - \tfrac{1}{2}Bm \\ &+ \frac{1}{N}\sum_{\mathbf{k}} J\{\mathcal{J}(\mathbf{k}) - \mathcal{J}(\mathbf{k} - \mathbf{q})\}b_{\mathbf{k}}. \end{aligned} \qquad (5.2.35b)$$

This transformation leaves the expression for the excitation energies unchanged, i.e.

$$E_{\mathbf{q}}(T) = \left\{[A_{\mathbf{q}}(T) + B_{\mathbf{q}}(T)][A_{\mathbf{q}}(T) - B_{\mathbf{q}}(T)]\right\}^{\frac{1}{2}}, \qquad (5.2.36)$$

when higher-order corrections are neglected. Inserting the eqns (5.2.15), (5.2.18), and (5.2.27) into (5.2.35), we finally obtain, at zero wave-vector,

$$A_{\mathbf{0}}(T) - B_{\mathbf{0}}(T) = \frac{1}{J}\big\{-36B_6^6 J^{(6)}(1 - 20m + 15b)\cos 6\phi$$
$$+ g\mu_B JH\cos(\phi - \phi_H)\big\} \qquad (5.2.37a)$$

and

$$A_{\mathbf{0}}(T) + B_{\mathbf{0}}(T) = \frac{1}{J}\big\{6B_2^0 J^{(2)}(1 - 2m - b)$$
$$- 6B_6^6 J^{(6)}(1 - 20m + 5b)\cos 6\phi + g\mu_B JH\cos(\phi - \phi_H)\big\}, \quad (5.2.37b)$$

and, at non-zero wave-vector,

$$A_{\mathbf{q}}(T) = A_{\mathbf{0}}(T) + J\{\mathcal{J}(\mathbf{0}) - \mathcal{J}(\mathbf{q})\}(1-m) + \frac{1}{N}\sum_{\mathbf{k}} J\{\mathcal{J}(\mathbf{k}) - \mathcal{J}(\mathbf{k}-\mathbf{q})\}m_{\mathbf{k}}$$
$$(5.2.38a)$$

and

$$B_{\mathbf{q}}(T) = B_{\mathbf{0}}(T) + \frac{1}{N}\sum_{\mathbf{k}} J\{\mathcal{J}(\mathbf{k}) - \mathcal{J}(\mathbf{k} - \mathbf{q})\}b_{\mathbf{k}}. \qquad (5.2.38b)$$

The spin-wave energies deduced here, to second order in the expansion in $1/J$, depend on temperature and on the crystal-field mixing of the J_z-eigenstates, and both dependences are introduced via the two correlation functions $m_{\mathbf{k}}$ and $b_{\mathbf{k}}$, given self-consistently by (5.2.32) in terms of the energy parameters. $B_{\mathbf{q}}(T)$ vanishes if there is no anisotropy, i.e. if B_2^0 and B_6^6 are zero. In the case of single-ion anisotropy, $B_{\mathbf{q}}(T)$ is independent of $\mathbf{q}$ if the small second-order term in (5.2.38b) is neglected, nor does it depend on the magnetic field, except for the slight field-dependence which may occur via the correlation functions m and b.

When the spin-wave excitation energies have been calculated, it is a straightforward matter to obtain the corresponding response functions. Within the present approximation, the xx-component of the susceptibility is

$$\chi_{xx}(\mathbf{q},\omega) = -\frac{1}{4N}\sum_{ij}\langle\langle(J_+ + J_-)_i\, e^{-i\mathbf{q}\cdot\mathbf{R}_i}\,;\,(J_+ + J_-)_j\, e^{i\mathbf{q}\cdot\mathbf{R}_j}\rangle\rangle$$
$$= -\frac{J}{2}\big(1 - \tfrac{1}{2}m - \tfrac{1}{4}b\big)^2\langle\langle a_{\mathbf{q}} + a_{-\mathbf{q}}^+\,;\,a_{\mathbf{q}}^+ + a_{-\mathbf{q}}\rangle\rangle.$$
$$(5.2.39)$$

The Bogoliubov transformation, eqns (5.2.19) and (5.2.21), with the parameters replaced by renormalized values, then leads to

$$\chi_{xx}(\mathbf{q},\omega) = -\frac{J}{2}\big(1 - m - \tfrac{1}{2}b\big)\frac{\widetilde{A}_{\mathbf{q}}(T) - \widetilde{B}_{\mathbf{q}}(T)}{E_{\mathbf{q}}(T)}\langle\langle \alpha_{\mathbf{q}} + \alpha_{-\mathbf{q}}^+\,;\,\alpha_{\mathbf{q}}^+ + \alpha_{-\mathbf{q}}\rangle\rangle,$$

which is a simple combination of Bose Green-functions determined by (5.2.20), with $E_{\mathbf{q}}$ replaced by $E_{\mathbf{q}}(T)$. Introducing these functions and the parameters given by (5.2.34), we finally obtain

$$\chi_{xx}(\mathbf{q},\omega) = J(1-m)\frac{A_{\mathbf{q}}(T)-B_{\mathbf{q}}(T)}{E_{\mathbf{q}}^2(T)-(\hbar\omega)^2}, \qquad (5.2.40a)$$

neglecting third-order terms. A rotation of the coordinate system by $\pi/2$ around the z-axis changes the sign of $B_{\mathbf{q}}(T)$, and hence we have

$$\chi_{yy}(\mathbf{q},\omega) = J(1-m)\frac{A_{\mathbf{q}}(T)+B_{\mathbf{q}}(T)}{E_{\mathbf{q}}^2(T)-(\hbar\omega)^2}. \qquad (5.2.40b)$$

These results show that the ratio between the neutron-scattering intensities due to the spin-wave at $\mathbf{q}$, neglecting $S_{zz}(\mathbf{q},\omega)$, in the two cases where the scattering vector is perpendicular to the basal y–z plane and to the x–z plane is

$$R_{\mathbf{q}}(T) = \frac{S_{xx}(\mathbf{q},\omega)}{S_{yy}(\mathbf{q},\omega)}\Bigg|_{\hbar\omega=\pm E_{\mathbf{q}}(T)} = \frac{\chi_{xx}(\mathbf{q},0)}{\chi_{yy}(\mathbf{q},0)} = \frac{A_{\mathbf{q}}(T)-B_{\mathbf{q}}(T)}{A_{\mathbf{q}}(T)+B_{\mathbf{q}}(T)}.$$
$$(5.2.41)$$

The measured intensities from Tb, which differ substantially from those calculated for the Heisenberg ferromagnet, agree well with this expression, especially if the correction for anisotropic two-ion coupling is taken into account (Jensen *et al.* 1975).

In the Heisenberg ferromagnet without rotational anisotropy, corresponding to $B_{\mathbf{q}}(T) = 0$, the elementary excitations at low temperatures are *circularly* polarized spin waves, in which the local moments precess in circles around the equilibrium direction. In the presence of anisotropy, $R_{\mathbf{q}}(T)$ differs from unity, and the excitations become *elliptically* polarized spin waves. The eccentricity of the ellipse depends on the wavevector of the excited spin wave, and by definition $R_{\mathbf{q}}(T)$ is the square of the ratio of the lengths of the principal axes which, at least to the order in $1/J$ which we have considered, is equal to the ratio between the corresponding static susceptibility components. So the static anisotropy is reflected, in a direct way, in the normal modes of the system. The result (5.2.41) justifies the transformation (5.2.34) by attributing observable effects to the parameters $A_{\mathbf{q}}(T)\pm B_{\mathbf{q}}(T)$, whereas the parameters which are defined via the Hamiltonian alone, here $\widetilde{A}_{\mathbf{q}}(T)\pm\widetilde{B}_{\mathbf{q}}(T)$, depend on the particular Bose representation which is employed.

The longitudinal correlation function $S_{zz}(\mathbf{q},\omega)$, which is neglected above, contains a diffusive mode at zero frequency, but no well-defined normal modes of non-zero frequency. There is inelastic scattering, but

the inelastic response, as well as the elastic mode, are purely of second order in $1/J$ and we shall not consider the longitudinal fluctuations further here.

The method developed in this section may be utilized, essentially unchanged, to calculate the MF susceptibility $\overline{\overline{\chi}}^o(\omega)$ of the *single* sites. The result to first order in $1/J$ is:

$$\chi_{xx}^o(\omega) = \langle J_z \rangle \frac{A - B + h_{\mathrm{ex}}}{E_{\mathrm{ex}}^2 - (\hbar\omega)^2}$$

$$\chi_{yy}^o(\omega) = \langle J_z \rangle \frac{A + B + h_{\mathrm{ex}}}{E_{\mathrm{ex}}^2 - (\hbar\omega)^2} \qquad\qquad (5.2.42a)$$

$$\chi_{xy}^o(\omega) = -\chi_{yx}^o(\omega) = \langle J_z \rangle \frac{i\hbar\omega}{E_{\mathrm{ex}}^2 - (\hbar\omega)^2},$$

where $\langle J_z \rangle$ is the MF expectation value of J_z, h_{ex} is the exchange field, and E_{ex} is the energy of the first excited MF state:

$$h_{\mathrm{ex}} = \langle J_z \rangle \mathcal{J}(\mathbf{0}) \qquad ; \qquad E_{\mathrm{ex}}^2 = (A + h_{\mathrm{ex}})^2 - B^2. \qquad (5.2.42b)$$

Introducing this expression for $\overline{\overline{\chi}}^o(\omega)$ into the RPA equation (3.5.8), we may derive $\overline{\overline{\chi}}(\mathbf{q}, \omega)$ by the same method as was used for the Heisenberg ferromagnet in Section 3.5.2, in which case $A = B = 0$. The results for the xx- and yy-components are then found to agree with eqn (5.2.40) to leading order in $1/J$. To the next order in $1/J$, the parameters are replaced by renormalized values, but this procedure is not here easily generalized so as to become fully self-consistent. However, most of the corrections may be included by substituting $A_{\mathbf{0}}(T) \pm B_{\mathbf{0}}(T)$ for $A \pm B$ in the expression for $\overline{\overline{\chi}}^o(\omega)$, and the self-consistent value of $\langle J_z \rangle$ for its MF value. The only terms which are not included in $\overline{\overline{\chi}}(\mathbf{q}, \omega)$ by this procedure, as we may see by a comparison with eqn (5.2.40), are the $\mathbf{q}$-dependent contributions to $A_{\mathbf{q}}(T) \pm B_{\mathbf{q}}(T)$ determined by the $\mathbf{k}$-sums in (5.2.38). At low temperatures, these contributions are small and may safely be neglected in systems with long-range interactions. This formulation therefore represents a valid alternative, which is useful for generalizing the linear spin-wave theory to the hcp structure, discussed in Section 5.1, or to the helically or conically ordered systems which we will consider in Chapter 6.

As an example of the *magnon dispersion relations* for the anisotropic basal-plane ferromagnet, we show in Fig. 5.2 experimental measurements on Tb at 4 K (Mackintosh and Bjerrum Møller 1972). The principal differences between these results and the corresponding excitations for Gd in Fig. 5.1 are the pronounced interactions which are observed between the magnons and phonons, which we shall discuss in some detail in
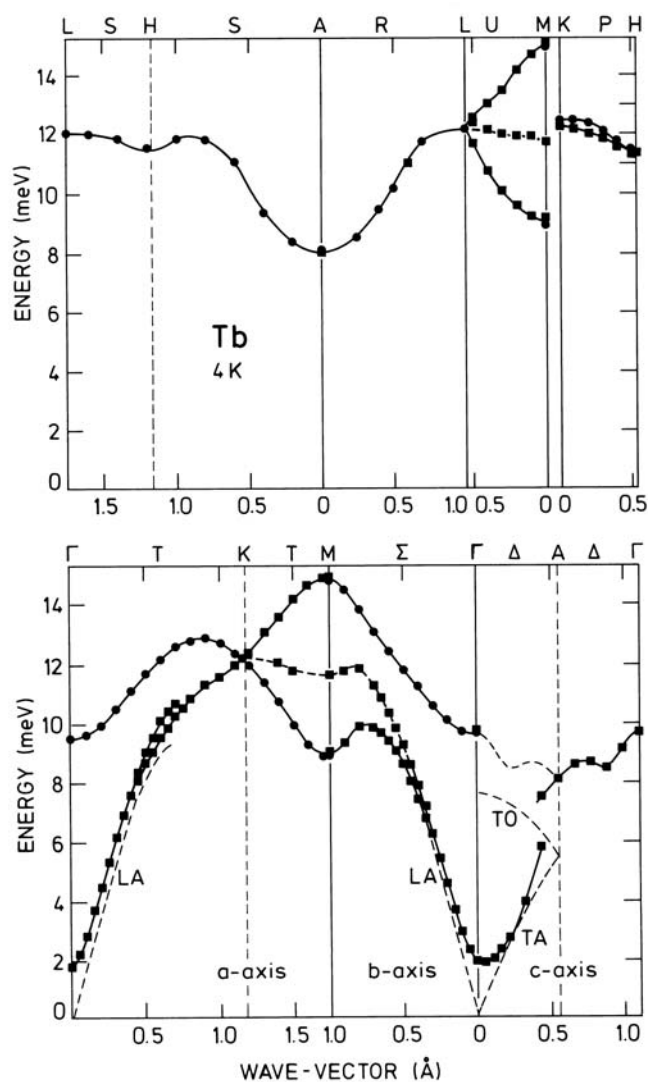
Fig. 5.2. The spin-wave dispersion relations along the symmetry lines in the Brillouin zone for Tb. In contrast to Gd, the anisotropy gives rise to an energy gap at the origin, and there are large effects due to interactions with the phonons. The third branch along, for example, ΓM may also be due to phonon interactions, or it may be a manifestation of the breaking of the hexagonal symmetry by the ordered moment in a particular domain, in the multi-domain sample.The lifting of the double degeneracy along the line KH provides evidence for anisotropic two-ion coupling.

Section 5.4.2, and the appearance of an energy gap at long wavelengths. This gap has its origin in the magnetic anisotropy. Even though the exchange energy required to excite a magnon vanishes in the long-wavelength limit, work is still required to turn the moments away from the easy direction against the anisotropy forces. If we neglect the small terms due to the sums over $\mathbf{k}$ in (5.2.38), the dispersion relation along the c-axis in zero field becomes, from eqns (5.2.36–38),

$$
\begin{aligned}
E_{\mathbf{q}}(T) = \big\{ &[A_{\mathbf{0}}(T) + B_{\mathbf{0}}(T) + \langle J_z\rangle\{\mathcal{J}(\mathbf{0}) - \mathcal{J}(\mathbf{q})\}] \\
&\times [A_{\mathbf{0}}(T) - B_{\mathbf{0}}(T) + \langle J_z\rangle\{\mathcal{J}(\mathbf{0}) - \mathcal{J}(\mathbf{q})\}]\big\}^{\frac{1}{2}}.
\end{aligned}
\tag{5.2.43}
$$

For an arbitrary direction in the zone, this relation is generalized analogously to eqn (5.1.9), giving rise again to acoustic and optical modes. From the dispersion relations, the *magnon density of states* and $\mathcal{J}(\mathbf{q})$ may readily be determined and hence, by a Fourier transform, the nominal Heisenberg exchange interaction $\mathcal{J}(ij)$ between moments on different atomic sites (Houmann 1968). The energy gap at zero wave-vector is given by

$$
E_{\mathbf{0}}(T) = \big\{[A_{\mathbf{0}}(T) + B_{\mathbf{0}}(T)][A_{\mathbf{0}}(T) - B_{\mathbf{0}}(T)]\big\}^{\frac{1}{2}},
\tag{5.2.44}
$$

and as we shall see in the next section, it is proportional to the geometrical mean of the axial- and hexagonal-anisotropy energies. We shall return to the dependence of this energy gap on the temperature and the magnetoelastic effects in the following two sections.

5.3 The uniform mode and spin-wave theory

The spin-wave mode at zero wave-vector is of particular interest. In comparison with the Heisenberg ferromagnet, the non-zero energy of this mode is the most distinct feature in the excitation spectrum of the anisotropic ferromagnet. In addition, the magnitude of the energy gap at $\mathbf{q} = \mathbf{0}$ is closely related to the bulk magnetic properties, which may be measured by conventional techniques. We shall first explore the connection between the static magnetic susceptibility and the energy of the uniform mode, leading to an expression for the temperature dependence of the energy gap. In the light of this discussion, we will then consider the general question of the validity of the spin-wave theory which we have presented in this chapter.

5.3.1 The magnetic susceptibility and the energy gap

The static-susceptibility components of the bulk crystal may be determined as the second derivatives of the free energy

$$
F = U - TS = -\frac{1}{\beta}\ln Z.
\tag{5.3.1}
$$

The specific heat C may be derived in a simple way, within our current spin-wave approximation, by noting that the excitation spectrum is the same as that for a non-interacting Bose system, so that the entropy is fully determined by the statistics of independent bosons of energies $E_{\mathbf{q}}(T)$:

$$S = k_B \sum_{\mathbf{q}} \left[(1 + n_{\mathbf{q}}) \ln (1 + n_{\mathbf{q}}) - n_{\mathbf{q}} \ln n_{\mathbf{q}} \right], \qquad (5.3.2)$$

and hence

$$C = T \partial S / \partial T = k_B T \sum_{\mathbf{q}} (dn_{\mathbf{q}}/dT) \ln \left\{ (1 + n_{\mathbf{q}})/n_{\mathbf{q}} \right\},$$

or, with $n_{\mathbf{q}} = \left[e^{\beta E_{\mathbf{q}}(T)} - 1 \right]^{-1}$,

$$
\begin{aligned}
C &= \sum_{\mathbf{q}} E_{\mathbf{q}}(T) \, dn_{\mathbf{q}}/dT \\
&= \beta \sum_{\mathbf{q}} n_{\mathbf{q}}(1 + n_{\mathbf{q}}) E_{\mathbf{q}}(T) \left\{ E_{\mathbf{q}}(T)/T - \partial E_{\mathbf{q}}(T)/\partial T \right\},
\end{aligned}
\qquad (5.3.3)
$$

as in (3.4.17).

The first derivative of F with respect to the angles θ and ϕ can be obtained in two ways. The first is to introduce S, as given by (5.3.2) into (5.3.1), so that

$$
\begin{aligned}
\frac{\partial F}{\partial \theta} &= \frac{\partial U}{\partial \theta} - \sum_{\mathbf{q}} E_{\mathbf{q}}(T) \frac{\partial n_{\mathbf{q}}}{\partial \theta} \\
&= \frac{\partial U}{\partial \theta} \bigg|_{m_{\mathbf{q}}, b_{\mathbf{q}}} + \sum_{\mathbf{q}} \left(\frac{\partial U}{\partial m_{\mathbf{q}}} \frac{\partial m_{\mathbf{q}}}{\partial \theta} + \frac{\partial U}{\partial b_{\mathbf{q}}} \frac{\partial b_{\mathbf{q}}}{\partial \theta} - E_{\mathbf{q}}(T) \frac{\partial n_{\mathbf{q}}}{\partial \theta} \right) \\
&= \frac{\partial U}{\partial \theta} \bigg|_{m_{\mathbf{q}}, b_{\mathbf{q}}},
\end{aligned}
\qquad (5.3.4)
$$

as it can be shown that $\partial U/\partial m_{\mathbf{q}} = J\widetilde{A}_{\mathbf{q}}(T)$ and $\partial U/\partial b_{\mathbf{q}} = J\widetilde{B}_{\mathbf{q}}(T)$, when $U = \langle \mathcal{H}_0 + \mathcal{H}_1 + \mathcal{H}_2 \rangle$, and hence that each term in the sum over $\mathbf{q}$ in the second line of (5.3.4) vanishes, when (5.2.32) is used. This result is only valid to second order in $1/J$. However, a result of general validity is

$$\partial F/\partial \theta = \langle \partial \mathcal{H}/\partial \theta \rangle, \qquad (5.3.5)$$

as discussed in Section 2.1, in connection with eqn (2.1.5). The two different expressions for $\partial F/\partial \theta$, and corresponding expressions for $\partial F/\partial \phi$, agree if $\mathcal{H}$ in (5.3.5) is approximated by $\mathcal{H}_0 + \mathcal{H}_1 + \mathcal{H}_2$, i.e. to second order in $1/J$. However, the results obtained up to now are based on the

additional assumption, which we have not stated explicitly, that $\mathcal{H}'$ in the starting Hamiltonian (5.2.12) is negligible. $\mathcal{H}'$ is the sum of the terms proportional to Stevens operators O_l^m with m odd, and it includes for instance the term $3B_2^0(J_z J_x + J_x J_z)\cos\theta\sin\theta$ associated with $B_2^0 Q_2^0$ in eqn (5.2.3). $\mathcal{H}'$ vanishes by symmetry if the magnetization is along a high-symmetry direction, i.e. $\theta = 0$ or $\pi/2$ and ϕ is a multiple of $\pi/6$. In these cases, the results obtained previously are valid. If the magnetization is not along a high-symmetry direction, $\mathcal{H}'$ must be taken into account. The first-order contributions arise from terms proportional to $(1/J)^{1/2}$ in $\mathcal{H}'$, which can be expressed effectively as a linear combination of J_x and J_y. In this order, $\langle\partial\mathcal{H}'/\partial\theta\rangle = 0$ therefore, because $\langle J_x\rangle = \langle J_y\rangle = 0$ by definition. For a harmonic oscillator, corresponding in this system to the first order in $1/J$, the condition for the elimination of terms in the Hamiltonian linear in a and a^+ coincides with the equilibrium condition $\partial F/\partial\theta = \partial F/\partial\phi = 0$. Although the linear terms due to $\mathcal{H}'$ can be removed from the Hamiltonian by a suitable transformation, terms cubic in the Bose operators remain. Second-order perturbation theory shows that, if $\mathcal{H}'$ is non-zero, $\langle\partial\mathcal{H}'/\partial\theta\rangle$ and the excitation energies include contributions of the order $1/J^2$. Although it is straightforward to see that $\mathcal{H}'$ makes contributions of the order $1/J^2$, it is not trivial to calculate them. The effects of $\mathcal{H}'$ have not been discussed in this context in the literature, but we refer to the recent papers of Rastelli *et al.* (1985, 1986), in which they analyse the equivalent problem in the case of a helically ordered system.

In order to prevent $\mathcal{H}'$ from influencing the $1/J^2$-contributions derived above, we may restrict our discussion to cases where the magnetization is along high-symmetry directions. This does not, however, guarantee that $\mathcal{H}'$ is unimportant in, for instance, the second derivatives of F. In fact $\partial\langle\partial\mathcal{H}'/\partial\theta\rangle/\partial\theta \propto \mathcal{O}(1/J^2)$ may also be non-zero when $\theta = 0$ or $\pi/2$, and using (5.3.4) we may write

$$F_{\theta\theta} = \frac{\partial^2 F}{\partial\theta^2} = \frac{\partial^2 U}{\partial\theta^2}\bigg|_{m_\mathbf{q}, b_\mathbf{q}} + \mathcal{O}(1/J^2)$$
$$= \Big\langle\frac{\partial^2}{\partial\theta^2}(\mathcal{H}_0 + \mathcal{H}_1 + \mathcal{H}_2)\Big\rangle + \mathcal{O}(1/J^2) \qquad ; \quad \theta = 0,\ \frac{\pi}{2}, \tag{5.3.6a}$$

and similarly

$$F_{\phi\phi} = \Big\langle\frac{\partial^2}{\partial\phi^2}(\mathcal{H}_0 + \mathcal{H}_1 + \mathcal{H}_2)\Big\rangle + \mathcal{O}(1/J^2) \qquad ; \quad \phi = p\,\frac{\pi}{6}, \tag{5.3.6b}$$

where the corrections of order $1/J^2$ are exclusively due to $\mathcal{H}'$. Here we have utilized the condition that the first derivatives of $m_\mathbf{q}$ and $b_\mathbf{q}$ vanish when the magnetization is along a symmetry direction.

The derivatives $F_{\theta\theta}$ and $F_{\phi\phi}$ are directly related to the static susceptibilities, as shown in Section 2.2.2. When $\theta_0 = \frac{\pi}{2}$, we obtain from eqn (2.2.18)

$$\chi_{xx}(\mathbf{0},0) = N\langle J_z\rangle^2/F_{\theta\theta} \qquad ; \quad \chi_{yy}(\mathbf{0},0) = N\langle J_z\rangle^2/F_{\phi\phi}. \qquad (5.3.7)$$

These results are of general validity, but we shall proceed one step further and use $F(\theta,\phi)$ for estimating the frequency dependence of the bulk susceptibilities. When considering the uniform behaviour of the system, we may to a good approximation assume that the equations of motion for all the different moments are the same:

$$\hbar\partial\langle\mathbf{J}\rangle/\partial t = \langle\mathbf{J}\rangle \times \mathbf{h}(\mathrm{eff}). \qquad (5.3.8)$$

By equating it to the average field, we may determine the effective field from

$$F = F(0) - N\langle\mathbf{J}\rangle \cdot \mathbf{h}(\mathrm{eff}), \qquad (5.3.9a)$$

corresponding to N isolated moments placed in the field $\mathbf{h}(\mathrm{eff})$. The free energy is

$$F = F(\theta_0,\phi_0) + \tfrac{1}{2}F_{\theta\theta}(\delta\theta)^2 + \tfrac{1}{2}F_{\phi\phi}(\delta\phi)^2 - N\langle\mathbf{J}\rangle \cdot \mathbf{h}, \qquad (5.3.9b)$$

and, to leading order, $\delta\theta = -\langle J_x\rangle/\langle J_z\rangle$ and $\delta\phi = -\langle J_y\rangle/\langle J_z\rangle$. Hence

$$h_x(\mathrm{eff}) = -\frac{1}{N}\frac{\partial F}{\partial\langle J_x\rangle} = h_x - \frac{1}{N}F_{\theta\theta}\frac{\langle J_x\rangle}{\langle J_z\rangle^2}, \qquad (5.3.10a)$$

and similarly

$$h_y(\mathrm{eff}) = h_y - \frac{1}{N}F_{\phi\phi}\frac{\langle J_y\rangle}{\langle J_z\rangle^2}. \qquad (5.3.10b)$$

Introducing a harmonic field applied perpendicular to the z-axis into eqn (5.3.8), we have

$$i\hbar\omega\langle J_x\rangle = \frac{1}{N\langle J_z\rangle}F_{\phi\phi}\langle J_y\rangle - h_y\langle J_z\rangle$$
$$i\hbar\omega\langle J_y\rangle = -\frac{1}{N\langle J_z\rangle}F_{\theta\theta}\langle J_x\rangle - h_x\langle J_z\rangle, \qquad (5.3.11)$$

and $\partial\langle J_z\rangle/\partial t = 0$, to leading order in $\mathbf{h}$. Solving the two equations for $h_x = 0$, we find

$$\chi_{yy}(\mathbf{0},\omega) = \langle J_y\rangle/h_y = \frac{1}{N}\frac{F_{\theta\theta}}{E_0^2(T) - (\hbar\omega)^2}, \qquad (5.3.12a)$$

and, when $h_y = 0$,

$$\chi_{xx}(\mathbf{0}, \omega) = \frac{1}{N} \frac{F_{\phi\phi}}{E_{\mathbf{0}}^2(T) - (\hbar\omega)^2}, \qquad (5.3.12b)$$

where the uniform-mode energy is

$$E_{\mathbf{0}}(T) = \frac{1}{N\langle J_z \rangle} \left\{ F_{\theta\theta} F_{\phi\phi} \right\}^{1/2}. \qquad (5.3.13)$$

This result for the uniform mode in an anisotropic ferromagnet was derived by Smit and Beljers (1955). It may be generalized to an arbitrary magnetization direction by defining (θ, ϕ) to be in a coordinate system in which the polar axis is *perpendicular* to the z-axis (as is the case here), and by replacing $F_{\theta\theta} F_{\phi\phi}$ by $F_{\theta\theta} F_{\phi\phi} - F_{\theta\phi}^2$ if $F_{\theta\phi} \neq 0$.

The introduction of the averaged effective-field in (5.3.8) corresponds to the procedure adopted in the RPA, and a comparison of the results (5.3.12–13) with the RPA result (5.2.40), at $\mathbf{q} = \mathbf{0}$ and $\omega = 0$, shows that the relations

$$A_{\mathbf{0}}(T) - B_{\mathbf{0}}(T) = \frac{1}{N\langle J_z \rangle} F_{\phi\phi}$$

$$A_{\mathbf{0}}(T) + B_{\mathbf{0}}(T) = \frac{1}{N\langle J_z \rangle} F_{\theta\theta} \qquad (5.3.14)$$

must be valid to second order in $1/J$. In this approximation, $A_{\mathbf{0}}(T) \pm B_{\mathbf{0}}(T)$ are directly determined by that part of the time-averaged two-dimensional potential, experienced by the single moments, which is quadratic in the components of the moments perpendicular to the magnetization axis. The excitation energy of the uniform mode is thus proportional to the geometric mean of the two force constants characterizing the parabolic part of this potential. Since $A_{\mathbf{0}}(T) \pm B_{\mathbf{0}}(T)$ are parameters of order $1/J$, the second-order contributions of $\mathcal{H}'$ in (5.3.6), which are not known, appear only in order $1/J^3$ in (5.3.14), when the magnetization is along a high-symmetry direction.

B_2^0 does not appear in $A_{\mathbf{0}}(T) - B_{\mathbf{0}}(T)$, and this is in accordance with eqn (5.3.14), as Q_2^0 is independent of ϕ. Considering instead the θ-dependence, we find that the contribution to $F_{\theta\theta}$ is determined by

$$\left\langle \frac{\partial^2 Q_2^0}{\partial \theta^2} \right\rangle = \left\langle -6(J_z^2 - J_x^2)\cos 2\theta - 6(J_z J_x + J_x J_z)\sin 2\theta \right\rangle_{\theta=\pi/2}$$

$$= 3\langle O_2^0 - O_2^2 \rangle. \qquad (5.3.15)$$

From (5.2.10) and (5.2.11), the thermal average is found to be

$$\langle O_2^0 - O_2^2 \rangle = 2J^{(2)} \Big\langle 1 - \frac{3}{J} a^+ a + \frac{3}{2J^2} a^+ a^+ aa$$

$$- \frac{1}{2J}\left(1 + \frac{1}{4J}\right)(aa + a^+ a^+) + \frac{1}{4J^2}(a^+ aaa + a^+ a^+ a^+ a) \Big\rangle,$$

or

$$\langle O_2^0 - O_2^2 \rangle = 2J^{(2)}\{1 - 3m + 3m^2 + \tfrac{3}{2}b^2 - (1 + \tfrac{1}{4J})b + \tfrac{3}{2}mb + \mathcal{O}(1/J^3)\}. \tag{5.3.16}$$

Hence, according to (5.3.6a) and (5.3.14), the B_2^0-term contributes to the spin-wave parameter $A_{\mathbf{0}}(T) + B_{\mathbf{0}}(T)$ by

$$3B_2^0 \langle O_2^0 - O_2^2 \rangle / \langle J_z \rangle \simeq 6B_2^0 J^{(2)}(1 - 3m - b)/J(1 - m)$$
$$\simeq 6B_2^0 J^{(2)}(1 - 2m - b)/J,$$

in agreement with (5.2.37b). When b is zero, this result is consistent with the classical Zener power-law (Zener 1954), $\langle O_l^m \rangle \propto \delta_{m0}\, \sigma^{l(l+1)/2}$, where $\sigma = 1 - m$ is the relative magnetization, since, to the order considered, $\langle O_2^0 - O_2^2 \rangle_{b=0} = \langle O_2^0 \rangle_{b=0} = 2J^{(2)}(1 - m)^3$. If we include the diagonal contribution of third order in m or $1/J$ to $\langle O_2^0 \rangle$ in (5.3.16), the result differs from the Zener power-law, but agrees, at low temperatures, with the more accurate theory of Callen and Callen (1960, 1965) discussed in Section 2.2. The results of the linear spin-wave theory obtained above can be utilized for generalizing the theory of Callen and Callen to the case of an anisotropic ferromagnet. The elliptical polarization of the spin waves introduces corrections to the thermal expectation values, which we express in the form

$$\langle O_2^0 - O_2^2 \rangle = 2J^{(2)} \hat{I}_{5/2}[\sigma]\, \eta_+^{-1}, \tag{5.3.17}$$

where the factor $\hat{I}_{l+1/2}[\sigma]$ represents the result (2.2.5) of Callen and Callen, and where $\eta_\pm$ differs from 1 if b is non-zero. The two correlation functions m and b are determined through eqn (5.2.32), in terms of the intermediate parameters $\widetilde{A}_{\mathbf{k}}(T) \pm \widetilde{B}_{\mathbf{k}}(T)$, but it is more appropriate to consider instead

$$m_o = \frac{1}{NJ} \sum_{\mathbf{k}} \left\{ \frac{A_{\mathbf{k}}(T)}{E_{\mathbf{k}}(T)}\left(n_{\mathbf{k}} + \tfrac{1}{2}\right) - \tfrac{1}{2} \right\}$$
$$b_o = -\frac{1}{NJ} \sum_{\mathbf{k}} \frac{B_{\mathbf{k}}(T)}{E_{\mathbf{k}}(T)}\left(n_{\mathbf{k}} + \tfrac{1}{2}\right), \tag{5.3.18}$$

defined in terms of the more fundamental parameters. The transformation (5.2.34) then leads to the following relations:

$$m_o + \tfrac{1}{2J} = m + \tfrac{1}{2J} - \tfrac{1}{2}b^2 \qquad \text{and} \quad b_o = b - \tfrac{1}{2}b(m + \tfrac{1}{2J}).$$

Separating the two contributions in (5.3.16), we find

$$\widetilde{b} \equiv \langle O_2^2 \rangle / \langle O_2^0 \rangle \simeq (1 + \tfrac{1}{4J})b(1 - m)^{-3/2}, \tag{5.3.19a}$$

which, to the order calculated, may be written

$$\widetilde{b} = \left(1 - \frac{1}{2J}\right)^{-1} \frac{b_o}{\sigma^2}, \qquad (5.3.19b)$$

where

$$\sigma = \langle J_z \rangle / J = 1 - m = 1 - m_o - \tfrac{1}{2} b_o \widetilde{b}. \qquad (5.3.20)$$

The function $\eta_\pm$ is then determined in terms of $\widetilde{b}$ as

$$\eta_\pm = (1 \pm \widetilde{b})(1 - \tfrac{1}{2}\widetilde{b}^2). \qquad (5.3.21)$$

The spin-wave theory determines the correlation functions σ and $\eta_\pm$ to second order in $1/J$, but for later convenience we have included some higher-order terms in (5.3.20) and (5.3.21). It may be straightforwardly verified that the thermal expectation values of $\langle O_2^0 - O_2^2 \rangle$ given by (5.3.16) and (5.3.17) agree with each other to order $1/J^2$. In the absence of anisotropy, the latter has a wider temperature range of validity than the former, extending beyond the regime where the excitations can be considered to be bosons. This should still be true in the presence of anisotropy, as long as $\widetilde{b}$ is small.

The combination of the spin-wave theory and the theory of Callen and Callen has thus led to an improved determination of the thermal averages of single-ion Stevens operators, as shown in Figs. 2.2 and 2.3. The quantity $O_2^0 - O_2^2$ was chosen as an example, but the procedure is the same for any other single-ion average. It is tempting also to utilize this improvement in the calculation of the excitation energies, and the relation (5.3.14) between the free energy and the spin-wave parameters $A_{\mathbf{0}}(T) \pm B_{\mathbf{0}}(T)$ is useful for this purpose. Neglecting the modifications due to $\mathcal{H}'$ in (5.3.6), i.e. using $F_{\theta\theta} \simeq \langle \partial^2 \mathcal{H} / \partial \theta^2 \rangle$ and similarly for $F_{\phi\phi}$, we find from (5.3.14) the following results:

$$A_{\mathbf{0}}(T) - B_{\mathbf{0}}(T) = -\frac{1}{J\sigma} 36 B_6^6 J^{(6)} \hat{I}_{13/2}[\sigma] \eta_-^{-15} \cos 6\phi + g\mu_B H \cos(\phi - \phi_H) \tag{5.3.22a}$$

and

$$
\begin{aligned}
A_{\mathbf{0}}(T) + B_{\mathbf{0}}(T) = \frac{1}{J\sigma} \Big[& 6 B_2^0 J^{(2)} \hat{I}_{5/2}[\sigma] \eta_+^{-1} - 60 B_4^0 J^{(4)} \hat{I}_{9/2}[\sigma] \eta_-^7 \eta_+^{-1} \\
& + 210 B_6^0 J^{(6)} \hat{I}_{13/2}[\sigma] \eta_-^{18} \eta_+^{-1} - 6 B_6^6 J^{(6)} \hat{I}_{13/2}[\sigma] \eta_-^{-30} \eta_+^{-25} \cos 6\phi \Big] \\
& + g\mu_B H \cos(\phi - \phi_H), \qquad (5.3.22b)
\end{aligned}
$$

which for completeness include all contributions from the starting Hamiltonian (5.2.1). The spin-wave spectrum at non-zero wave-vectors is adjusted accordingly by inserting $A_{\mathbf{0}}(T) \pm B_{\mathbf{0}}(T)$ given above, instead

of (5.2.37), in eqns (5.2.36), (5.2.38), and (5.2.40). If the out-of-plane anisotropy is stronger than the in-plane anisotropy, as in Tb and Dy, B is positive and $\widetilde{b}$ is negative. This means that η_+ and η_- are respectively smaller and greater than 1 (for small $\widetilde{b}$), with the result that the axial contributions to $A_{\mathbf{0}}(T) + B_{\mathbf{0}}(T)$ are increased, whereas the planar contribution to $A_{\mathbf{0}}(T) - B_{\mathbf{0}}(T)$ is diminished, due to $\widetilde{b}$. This is consistent with the fact that the out-of-plane fluctuations are suppressed in comparison with the in-plane fluctuations by the anisotropy. Hence we find, as a general result, that the elliptical polarization of the spin waves enhances, in a self-consistent fashion, the effects of the anisotropy. We note that Q_6^6, which depends on both θ and ϕ, contributes to both anisotropy parameters, but that the anisotropy of the fluctuations affects the two contributions differently.

If $\widetilde{b}$ and the $\mathbf{k}$-sums in (5.2.38) are neglected, the above result for the spin-wave energies $E_{\mathbf{q}}(T)$ reduces to that derived by Cooper (1968b). The modifications due to the non-spherical precession of the moments, $\widetilde{b} \neq 0$, were considered first by Brooks *et al.* (1968) and Brooks (1970), followed by the more systematic and comprehensive analysis of Brooks and Egami (1973). They utilized directly the equations of motion of the angular-momentum operators, without introducing a Bose representation. Their results are consistent with those above, except that they did not include all the second-order modifications considered here. We also refer to Tsuru (1986), who has more recently obtained a result corresponding to eqn (5.2.31), when B_6^6 is neglected, using a variational approach. The procedure outlined above essentially follows that of Lindgård and Danielsen (1974, 1975), which was further developed by Jensen (1975). This account only differs from that given by Jensen in the use of $\eta_\pm$ instead of $\widetilde{b}$ as the basis for the 'power-law' generalization (and by the alternative choice of sign for B and $\widetilde{b}$) and, more importantly, by the explicit use of $1/J$ as the expansion parameter.

As illustrated in Fig. 5.1 for Gd, and in Fig. 5.3 for Tb, the observed temperature dependence of the spin-wave spectrum is indeed substantial, both in the isotropic and the anisotropic ferromagnet. In the case of Tb, the variation of the exchange contribution is augmented by the temperature dependence of the anisotropy terms, which is reflected predominantly in the rapid variation of the energy gap at $\mathbf{q} = \mathbf{0}$. A comparison of Figs. 5.1 and 5.3 shows that the change in the form of $\mathcal{J}(\mathbf{q})$ appears to be more pronounced in Tb than in Gd. In Tb, the variation of $\mathcal{J}(\mathbf{q})$ with $\mathbf{q}$ at a particular temperature is also modified if the magnetization vector is rotated from the b-axis to a hard a-axis (Jensen *et al.* 1975). Most of these changes with magnetization can be explained as the result of two-ion anisotropy, which we will consider in Section 5.5. Anisotropic two-ion terms may also affect the energy gap. In addition,
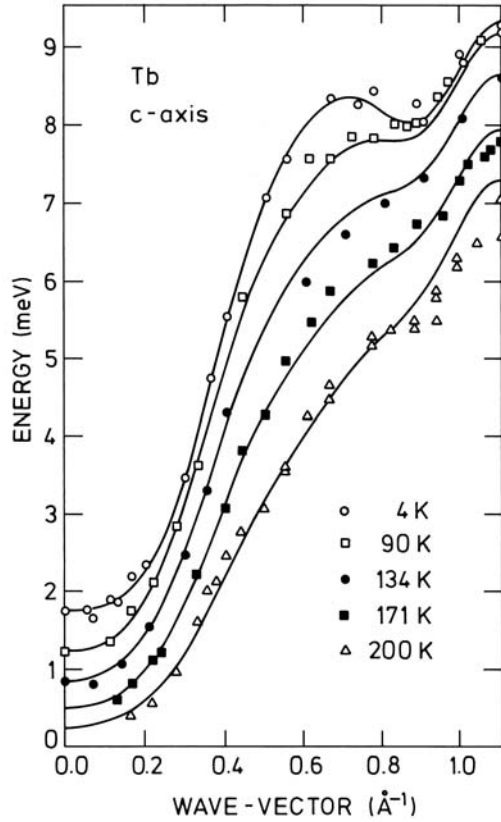
Fig. 5.3.   The temperature dependence of the dispersion relations for the unperturbed spin waves in the *c*-direction in Tb. Both the energy gap and the **q**-dependence renormalize with temperature. The results have been corrected for the magnon–phonon interaction, and the lines show the calculated energies.

the magnetoelastic coupling introduces qualitatively new effects, not describable by eqn (5.3.22), to which we will return after a short digression to summarize our understanding of the spin-wave theory.

5.3.2 The validity of the spin-wave theory

In presenting the spin-wave theory, we have neglected phenomena which first appear in the third order of $1/J$, most importantly the finite lifetimes of the excitations. In the presence of anisotropy, when B is different from zero, the total moment is not a conserved quantity, since $[\sum_i J_{iz}, \mathcal{H}] \neq 0$, unlike in the Heisenberg model. On the microscopic

plane, this means that the number of spin-wave excitations, i.e. magnons, is not necessarily conserved in a scattering process. In contrast to the behaviour of the isotropic ferromagnet, the linewidths do not therefore vanish at zero temperature, although energy conservation, combined with the presence of an energy gap in the magnon spectrum, strongly limit the importance of the allowed decay processes at low temperatures.

The two-ion interactions are assumed to involve only tensor operators of the lowest rank, so that these terms in the $1/J$-expansion only have small numerical factors multiplying the Bose operator products. Therefore, if J is large, as in heavy rare earth-ions, the third-order terms due to the exchange coupling, which are neglected in the spin-wave theory, are expected to be small, as long as the number of excited magnons is not very large. The weak influence, at low temperatures, of the higher-order contributions of the exchange coupling is also indicated by a comparison with the low-temperature expansion of Dyson (1956) of the free energy in a Heisenberg ferromagnet with only nearest-neighbour interactions, also discussed by Rastelli and Lindgård (1979). If $A = B = 0$, the results derived earlier, to second order in $1/J$, are consistent with those of Dyson, except that we have only included the leading-order contribution, in the Born approximation or in powers of $1/J$, to the T^4-term in the magnetization and in the specific heat. The higher-order corrections to the T^4-term are significant if $J = \frac{1}{2}$, but if $J = 6$ as in Tb, for example, they only amount to a few per cent of this term and can be neglected.

If only the two-ion terms are considered, the RPA decoupling of the Bose operator products (5.2.29) is a good approximation at large J and at low temperatures. However, this decoupling also involves an approximation to the single-ion terms, and these introduce qualitatively new features into the spin-wave theory in the third order of $1/J$. For example, the C_3-term in (5.2.26) directly couples the $|J_z = J>$ state and $|J - 4>$, leading to an extra modification of the ground state not describable in terms of B or $\eta_\pm$. Furthermore, the Bogoliubov transformation causes the (J_x, J_y)-matrix elements between the ground state and the third excited state to become non-zero. This coupling then leads to the appearance of a new pole in the transverse susceptibilities, in addition to the spin-wave pole, at an energy which, to leading order, is roughly independent of $\mathbf{q}$ and close to that of the third excited MF level, i.e. $3E_{\mathbf{q}_o}(T)$, with $\mathbf{q}_o$ defined as a wave-vector at which $\mathcal{J}(\mathbf{q}_o) = 0$. A qualitative analysis indicates that the third-order contribution to e.g. $\chi_{xx}(\mathbf{0}, 0)$, due to this pole, must cancel the second-order contribution of $\mathcal{H}'$ to $F_{\theta\theta}$ in the relation (5.3.12b) between the two quantities. Hence the approximation $F_{\theta\theta} \simeq \langle \partial^2 \mathcal{H}/\partial\theta^2 \rangle$, used in (5.3.22), corresponds to the neglect of this additional pole.

The higher-order exchange contributions can thus be neglected at low temperatures, if J is large. This condition is not, however, sufficient to guarantee that the additional MF pole is unimportant, and the spin-wave result (5.3.22), combined with (5.2.36), (5.2.38), and (5.2.40), can only be trusted as long as the modification of the ground state, due to the single-ion anisotropy, is weak. This condition is equivalent to the requirement that $|\widetilde{b}|$ be much less than 1. The regime within which the spin-wave theory is valid can be examined more closely by a comparison with the MF-RPA theory. In the latter, only the two-ion interactions are treated approximately, whereas the MF Hamiltonian is diagonalized exactly. The MF-RPA decoupling utilized in Section 3.5 leads here to a cancellation of the **k**-sums in (5.3.38), and to a replacement of the correlation functions m_o and b_o by their MF values

$$m_o \simeq m_o^{\mathrm{MF}} = \frac{1}{J}\left\{ \frac{A_{\mathbf{q}_o}(T)}{E_{\mathbf{q}_o}(T)}\left(n_{\mathbf{q}_o} + \tfrac{1}{2}\right) - \tfrac{1}{2} \right\}, \qquad (5.3.23)$$

with a similar expression for b_o^{MF}. The wave-vector $\mathbf{q}_o$ is defined as above, such that $\mathcal{J}(\mathbf{q}_o) = 0$. If the single-ion anisotropy is of second rank only, including possibly a Q_2^2-term as well as the Q_2^0-term of our specific model, all the predictions obtained with the MF-RPA version of the spin-wave theory agree extremely well with the numerical results obtained by diagonalizing the MF Hamiltonian exactly, even for relatively large values of $|b_o^{\mathrm{MF}}|$ (≈ 0.1). Even though $1/J$ is the expansion parameter, the replacement of $(1 + \frac{1}{2J})$ by $(1 - \frac{1}{2J})^{-1}$ in (5.3.19b) extends the good agreement to the limit $J = 1$, in which case the MF Hamiltonian can be diagonalized analytically.

The applicability of the $1/J$-expansion for the anisotropy is much more restricted if terms of high rank, such as Q_6^6, dominate. This is a simple consequence of the relatively greater importance of the contributions of higher-order in $1/J$, like for instance the C_3-term in (5.2.26), for higher-rank anisotropy terms. We have analysed numerically models corresponding to the low-temperature phases of Tb and Er, which include various combinations of anisotropy terms with ranks between 2 and 6. In the case of the basal-plane ferromagnet Tb, we find that the $1/J$-expansion leads to an accurate description of the crystal-field effects on both the ground-state properties and the excitation energies. The MF-RPA excitation-energies calculated with the procedure of Section 3.5 differ relatively only by $\sim 10^{-3}$ at $T = 0$ from those of the spin-wave theory (Jensen 1976c). We furthermore find that this good agreement extends to non-zero temperatures, and that the $1/J$-expansion is still acceptably accurate when $\sigma \simeq 0.8$. Consequently, the effective power-laws predicted by the spin-wave theory at low temperatures (Jensen 1975) are valid.

The renormalization of the anisotropy parameters appearing in the spin-wave energies, in the second order of $1/J$, is expected to be somewhat more important in the conical phase of Er than in Tb. In Er, the moments are not along a symmetry direction (they make an angle of about $28°$ with the c-axis) and the second-order modifications due to $\mathcal{H}'$ in (5.2.12) might be expected to be important. The $1/J$-results do not allow a precise estimate of the second-order contributions, but by introducing two scaling parameters, one multiplying the exchange terms by σ, and the other scaling the constant crystal-field contribution in the $1/J$-expression for the spin-wave energies in the cone phase, it is possible (Jensen 1976c) to give an accurate account of the excitation energies derived by diagonalizing the MF Hamiltonian exactly, the relative differences being only of the order 10^{-2}. The two scaling parameters are found to have the expected magnitudes, although σ turns out to be slightly smaller ($\simeq 0.94$ in the model considered) than the relative magnetization predicted by the MF Hamiltonian ($\sigma^{\mathrm{MF}} \simeq 0.98$). An analysis of the MF Hamiltonian shows that the excitations can be described in terms of an elliptical precession of the single moments, as expected, but surprisingly the ellipsoid lies in a plane with its normal making an angle ($\simeq 33°$) with the c-axis which differs from the equilibrium cone-angle ($\simeq 28°$), so the polarization of the spin waves is not purely transverse. In terms of the $1/J$-expansion, this modification of the excited states can only be produced by $\mathcal{H}'$. This observation indicates that $\mathcal{H}'$ has significant effects in Er, since it explains the difference between σ and σ^{MF}, as σ becomes equal to σ^{MF} if the angle appearing in the renormalized spin-wave energies is considered to be that defining the excited states, i.e. $33°$, rather than the equilibrium value.

We may conclude that the $1/J$-expansion is a valid procedure for describing the low-temperature magnetic properties of the heavy rare earth metals. This is an important conclusion for several reasons. To first order in $1/J$, the theory is simple and transparent. It is therefore feasible to include various kinds of complication in the model calculations and to isolate their consequences. This simplicity is retained in the second order of $1/J$, as long as $\mathcal{H}'$ can be neglected, in which case the first-order parameters are just renormalized. Accurate calculations of the amount of renormalization of the different terms may be quite involved, but because of the long range of the two-ion interactions in the rare earth metals, the MF values of m_o and b_o utilized above normally provide good estimates. The spin-wave theory in the harmonic approximation, to first order in $1/J$, has been employed quite extensively in the literature, both for analysing experimental results and in various theoretical developments. It is therefore fortunate that these analyses are not invalidated, but only modified, or renormalized, by the

presence of moderate anisotropy. However, it is necessary to be aware that the renormalization itself may cause special effects not expected in the harmonic approximation, as the amount of renormalization may change when the system is perturbed by an external magnetic field or pressure, or when the temperature is altered.

There have been attempts (Lindgård 1978, and references therein) to construct an analytical spin-wave theory starting with a diagonalization of the MF Hamiltonian. In principle, this should be an appropriate starting-point, since the ground state is closer to the MF ground-state than to the fully polarized state, as soon as the planar anisotropy becomes significant. As in the model calculations discussed above, the MF Hamiltonian can be diagonalized numerically without difficulty, but in this form the method is non-analytical and the results are not easily interpretable. In order to diagonalize the MF Hamiltonian analytically, one is forced to make a perturbative expansion, unless J is small. If the MF Hamiltonian is expressed in the $|J_z>$-basis, the natural expansion parameter is $\sim |B_{\mathbf{q}_o}/A_{\mathbf{q}_o}| \simeq 2J|b_o|$ at $T = 0$. The use of this expansion parameter and the $1/J$-expansion considered above lead to identical results in the limit $2J|b_o| \ll 1$ (Rastelli and Lindgård 1979). However, the expansion parameter is not small when the anisotropy is moderately large ($2J|b_o| \simeq 0.35$ in Tb at $T = 0$), which severely limits the usefulness of this procedure as applied by Lindgård (1978, 1988) to the analysis of the spin waves in the anisotropic heavy rare earths. It gives rise to a strong renormalization of all the leading-order spin-wave-energy parameters, which are thus quite sensitive, for example, to an external magnetic field, and it is extremely difficult to obtain a reasonable estimate of the degree of renormalization. In contrast, the $1/J$-expansion leads, at low temperatures, to results in which only the high-rank terms (which are quite generally of smaller magnitude than the low-rank terms) are renormalized appreciably, and the amount of renormalization can be determined with fair accuracy. In the numerical example corresponding to Tb, the B_6^6-term is renormalized by -38% at $T = 0$, according to the spin-wave theory, which agrees with the value obtained by diagonalizing the MF Hamiltonian exactly, as indicated in Fig. 2.3.

To recapitulate, we have developed a self-consistent RPA theory for the elementary excitations in a ferromagnet, i.e. the spin waves, valid when the magnetization is close to its saturation value. The major complication is the occurrence of anisotropic single-ion interactions, which were treated by performing a systematic expansion in $1/J$. To first order in $1/J$, the theory is transparent and simple, and it is straightforwardly generalized to different physical situations. Much of the simplicity is retained in second order, as long as the magnetization is along a

symmetry axis, but the first-order parameters are replaced by effective values. These effective parameters are determined self-consistently in terms of the spin-wave parameters $A_{\mathbf{q}}(T) \pm B_{\mathbf{q}}(T)$, which depend on T, and on an eventual applied magnetic field. One advantage of the use of $1/J$ as the expansion parameter is that the second-order modifications are smallest for the low-rank couplings, which are quite generally also the largest terms. If the magnetization is not along a symmetry axis, the elementary excitations may no longer be purely transverse. This additional second-order phenomenon may, however, be very difficult to detect experimentally within the regime of validity of the second-order spin-wave theory.

5.4 Magnetoelastic effects

The magnetoelastic coupling between the magnetic moments and the lattice modifies the spin waves in two different ways. The *static* deformations of the crystal, induced by the ordered moments, introduce new anisotropy terms in the spin-wave Hamiltonian. The *dynamic* time-dependent modulations of the magnetic moments furthermore interfere with the lattice vibrations. We shall start with a discussion of the static effects, and then consider the magnon–phonon interaction. The magnetoelastic crystal-field Hamiltonian was introduced in Section 1.4, where the different contributions were classified according to the symmetry of the strain parameters. The two-ion coupling may also change with the strain, as exemplified by eqn (2.2.32). We shall continue considering the basal-plane ferromagnet and, in order to simplify the discussion, we shall only treat the low-rank magnetoelastic couplings of single-ion origin. In the ferromagnetic case, the magnetoelastic two-ion couplings do not introduce any effects which differ qualitatively from those due to the crystal-field interactions. Consequently, those interactions which are not included in the following discussion only influence the detailed dependence of the effective coupling parameters on the magnetization and, in the case of the dynamics, on the wave-vector.

5.4.1 Magnetoelastic effects on the energy gap

The static effects of the α-strains on the spin-wave energies may be included in a straightforward manner, by replacing the crystal-field parameters in (5.2.1) with effective strain-dependent values, i.e. $B_2^0 \rightarrow B_2^0 + B_{\alpha 1}^{(2)} \, \bar{\epsilon}_{\alpha 1} + B_{\alpha 2}^{(2)} \, \bar{\epsilon}_{\alpha 2}$, with α-strains proportional to $\langle Q_2^0 \rangle$. Equivalent contributions appear in the magnetic anisotropy, discussed in Section 2.2.2. This simplification is not possible with the γ- or the ϵ-strain contributions, because these, in contrast to the α-strains, change the symmetry of the lattice. When $\theta = \pi/2$, the ϵ-strains vanish, and the

γ-strain part of the magnetoelastic Hamiltonian is given by eqn (2.2.23):

$$\mathcal{H}_\gamma = \sum_i \left[\tfrac{1}{2} c_\gamma (\epsilon_{\gamma 1}^2 + \epsilon_{\gamma 2}^2) - B_{\gamma 2} \{ Q_2^2(\mathbf{J}_i) \epsilon_{\gamma 1} + Q_2^{-2}(\mathbf{J}_i) \epsilon_{\gamma 2} \} \right.$$
$$\left. - B_{\gamma 4} \{ Q_4^4(\mathbf{J}_i) \epsilon_{\gamma 1} - Q_4^{-4}(\mathbf{J}_i) \epsilon_{\gamma 2} \} \right]. \tag{5.4.1}$$

The equilibrium condition, $\partial F / \partial \epsilon_\gamma = 0$, leads to eqn (2.2.25) for the static strains $\overline{\epsilon}_\gamma$. The static-strain variables are distinguished by a bar from the dynamical contributions $\epsilon_\gamma - \overline{\epsilon}_\gamma$. The expectation values of the Stevens operators may be calculated by the use of the RPA theory developed in the preceding section, and with $\theta = \pi/2$ we obtain, for instance,

$$\langle Q_2^2 \rangle = \langle \tfrac{1}{2}(O_2^0 + O_2^2) \cos 2\phi + 2 O_2^{-1} \sin 2\phi \rangle = J^{(2)} \hat{I}_{5/2}[\sigma] \eta_-^{-1} \cos 2\phi$$
$$\langle Q_2^{-2} \rangle = \langle \tfrac{1}{2}(O_2^0 + O_2^2) \sin 2\phi - 2 O_2^{-1} \cos 2\phi \rangle = J^{(2)} \hat{I}_{5/2}[\sigma] \eta_-^{-1} \sin 2\phi. \tag{5.4.2}$$

We note that $\langle O_2^{-1} \rangle$ vanishes only as long as $\mathcal{H}'$ in (5.2.12) can be neglected. Introducing the magnetostriction parameters C and A via eqn (2.2.26a), when $\theta = \pi/2$,

$$\overline{\epsilon}_{\gamma 1} = C \cos 2\phi - \tfrac{1}{2} A \cos 4\phi$$
$$\overline{\epsilon}_{\gamma 2} = C \sin 2\phi + \tfrac{1}{2} A \sin 4\phi, \tag{5.4.3}$$

and calculating $\langle Q_4^{\pm 4} \rangle$, we obtain

$$C = \frac{1}{c_\gamma} B_{\gamma 2} J^{(2)} \hat{I}_{5/2}[\sigma] \eta_-^{-1}$$
$$A = -\frac{2}{c_\gamma} B_{\gamma 4} J^{(4)} \hat{I}_{9/2}[\sigma] \eta_-^{-6}, \tag{5.4.4}$$

instead of eqn (2.2.26b), including the effects of the elliptical precession of the moments. The equilibrium conditions allow us to split the magnetoelastic Hamiltonian into two parts:

$$\mathcal{H}_\gamma(\text{sta}) = \sum_i \left[\tfrac{1}{2} c_\gamma (\overline{\epsilon}_{\gamma 1}^2 + \overline{\epsilon}_{\gamma 2}^2) - B_{\gamma 2} \{ Q_2^2(\mathbf{J}_i) \overline{\epsilon}_{\gamma 1} + Q_2^{-2}(\mathbf{J}_i) \overline{\epsilon}_{\gamma 2} \} \right.$$
$$\left. - B_{\gamma 4} \{ Q_4^4(\mathbf{J}_i) \overline{\epsilon}_{\gamma 1} - Q_4^{-4}(\mathbf{J}_i) \overline{\epsilon}_{\gamma 2} \} \right], \tag{5.4.5}$$

depending only on the static strains, and

$$\mathcal{H}_\gamma(\text{dyn}) = \sum_i \left[\tfrac{1}{2} c_\gamma \{ (\epsilon_{\gamma 1} - \overline{\epsilon}_{\gamma 1})^2 + (\epsilon_{\gamma 2} - \overline{\epsilon}_{\gamma 2})^2 \} \right.$$
$$- \big(B_{\gamma 2} \{ Q_2^2(\mathbf{J}_i) - \langle Q_2^2 \rangle \} + B_{\gamma 4} \{ Q_4^4(\mathbf{J}_i) - \langle Q_4^4 \rangle \} \big)(\epsilon_{\gamma 1} - \overline{\epsilon}_{\gamma 1})$$
$$\left. - \big(B_{\gamma 2} \{ Q_2^{-2}(\mathbf{J}_i) - \langle Q_2^{-2} \rangle \} - B_{\gamma 4} \{ Q_4^{-4}(\mathbf{J}_i) - \langle Q_4^{-4} \rangle \} \big)(\epsilon_{\gamma 2} - \overline{\epsilon}_{\gamma 2}) \right] \tag{5.4.6}$$

depending only on the dynamical part of the strains.

To leading order, the magnetoelastic energy is determined by the static part (5.4.5), corresponding to eqn (2.2.27). $\mathcal{H}_\gamma$ influences the equilibrium condition determining ϕ and, in the spin-wave approximation ($\mathcal{H}'$ is neglected), we have

$$\frac{1}{N}\frac{\partial F}{\partial \phi} = \frac{1}{N}\Big\langle \frac{\partial}{\partial \phi}\{\mathcal{H} + \mathcal{H}_\gamma\}\Big\rangle \simeq \frac{1}{N}\Big\langle \frac{\partial}{\partial \phi}\{\mathcal{H} + \mathcal{H}_\gamma(\text{sta})\}\Big\rangle$$

$$= -6B_6^6 J^{(6)}\hat{I}_{13/2}[\sigma]\eta_-^{-15}\sin 6\phi + g\mu_B H J\sigma \sin(\phi - \phi_H)$$

$$+2c_\gamma C(\overline{\epsilon}_{\gamma 1}\sin 2\phi - \overline{\epsilon}_{\gamma 2}\cos 2\phi) - 2c_\gamma A(\overline{\epsilon}_{\gamma 1}\sin 4\phi + \overline{\epsilon}_{\gamma 2}\cos 4\phi),$$

$$(5.4.7)$$

or, using the equilibrium values of $\overline{\epsilon}_{\gamma 1}$ and $\overline{\epsilon}_{\gamma 2}$,

$$\frac{1}{N}\frac{\partial F}{\partial \phi} = g\mu_B J\sigma\Big\{H\sin(\phi - \phi_H) - \tfrac{1}{6}\widetilde{H}_c\sin 6\phi\Big\}, \qquad (5.4.8a)$$

with the definition

$$g\mu_B\widetilde{H}_c = 36\kappa_6^6/(J\sigma) = 36\big\{B_6^6 J^{(6)}\hat{I}_{13/2}[\sigma]\eta_-^{-15} + \tfrac{1}{2}c_\gamma CA\big\}/(J\sigma).$$
$$(5.4.8b)$$

If $H = 0$, the equilibrium condition $\partial F/\partial \phi = 0$ determines the stable direction of magnetization to be along either a b-axis or an a-axis, depending on whether $\widetilde{H}_c$ is positive or negative respectively.

The additional anisotropy terms introduced by $\mathcal{H}_\gamma$ and proportional to the static strains, as for instance the term $-B_{\gamma 2}Q_2^2(\mathbf{J}_i)\overline{\epsilon}_{\gamma 1}$ in (5.4.5), contribute to the spin-wave energies. Proceeding as in Section 5.3, we find the additional contributions to $A_\mathbf{0}(T) \pm B_\mathbf{0}(T)$ in (5.3.22), proportional to the static γ-strains,

$$\Delta\{A_\mathbf{0}(T) + B_\mathbf{0}(T)\}$$
$$= \frac{c_\gamma}{J\sigma}\big\{2C^2 + A^2\eta_+^{-8}\eta_-^{-4} - CA(2 + \eta_+^{-8}\eta_-^{-4})\cos 6\phi\big\}\eta_+^{-1}\eta_-$$

$$\Delta\{A_\mathbf{0}(T) - B_\mathbf{0}(T)\} = \frac{c_\gamma}{J\sigma}\big\{4C^2 + 4A^2 - 10CA\cos 6\phi\big\}. \qquad (5.4.9)$$

The contribution to $A_\mathbf{0}(T) - B_\mathbf{0}(T)$ is expressible directly in terms of the strain-parameters, C and A, without the further correction factors necessary for $A_\mathbf{0}(T) + B_\mathbf{0}(T)$. By using $\widetilde{H}_c$ and the non-negative quantity

$$\Lambda_\gamma = \frac{4c_\gamma}{J\sigma}(C^2 + A^2 + 2CA\cos 6\phi), \qquad (5.4.10)$$

we can write the *total* spin-wave parameter

$$A_\mathbf{0}(T) - B_\mathbf{0}(T) = \Lambda_\gamma - g\mu_B\widetilde{H}_c\cos 6\phi + g\mu_B H\cos(\phi - \phi_H). \quad (5.4.11)$$

This parameter does not obey the relation (5.3.14) with the second derivative $F_{\phi\phi}$ of the free energy. A differentiation $\partial F/\partial\phi$, as given by (5.4.8), with respect to ϕ shows that (5.3.14) accounts for the last two terms in (5.4.11), but not for Λ_γ. A calculation from (5.4.7) of the second derivative of F, when the strains are kept constant, instead of under the constant (zero) stress-condition assumed above, yields

$$A_{\mathbf{0}}(T) - B_{\mathbf{0}}(T) = \frac{1}{NJ\sigma}\frac{\partial^2 F}{\partial\phi^2}\bigg|_{\epsilon=\bar{\epsilon}} = \Lambda_\gamma + \frac{1}{NJ\sigma}F_{\phi\phi}, \qquad (5.4.12)$$

which replaces (5.3.14). The relation (5.3.14), determining $A_{\mathbf{0}}(T) - B_{\mathbf{0}}(T)$, was based on a calculation of the frequency dependence of the bulk susceptibility and, as we shall see later, it is the influence of the lattice which invalidates this argument. The Λ_γ term was originally suggested by Turov and Shavrov (1965), who called it the 'frozen lattice' contribution because the dynamic strain-contributions were not considered. However, as we shall show in the next section, the magnon–phonon coupling does not change this result.

The modifications caused by the magnetoelastic γ-strain couplings are strongly accentuated at a second-order phase transition, at which $F_{\phi\phi}$ vanishes. Let us consider the case where $\widetilde{H}_c$ is positive, $\widetilde{H}_c = |\widetilde{H}_c| \equiv H_c$, i.e. the b-axis is the easy axis. If a field is applied along an a-axis, $\phi_H = 0$, then the magnetization is pulled towards this direction, as described by eqn (5.4.8):

$$H = H_c\frac{\sin 6\phi}{6\sin\phi} = H_c\big(1 - \tfrac{16}{3}\sin^2\phi + \tfrac{16}{3}\sin^4\phi\big)\cos\phi, \qquad (5.4.13)$$

as long as the field is smaller than H_c. At the critical field $H = H_c$, the moments are pulled into the hard direction, so that $\phi = 0$ and the second derivative of the free energy,

$$F_{\phi\phi} = Ng\mu_B\{H\cos\phi - H_c\cos 6\phi\}J\sigma, \qquad (5.4.14)$$

vanishes. So a second-order phase transition occurs at $H = H_c$, and the order parameter can be considered to be the component of the moments perpendicular to the a-axis, which is zero for $H \geq H_c$. An equally good choice for the order parameter is the strain $\bar{\epsilon}_{\gamma 2}$, and these two possibilities reflect the nature of the linearly coupled magnetic–structural phase transition. The free energy does not contain terms which are cubic in the order parameters, but the transition might be changed into one of first-order by terms proportional to $\cos 12\phi$, e.g. if σ or $\eta_\pm$, and thereby $\widetilde{H}_c$, depend sufficiently strongly on ϕ (Jensen 1975). At the transition, eqn (5.4.11) leads to

$$A_{\mathbf{0}}(T) - B_{\mathbf{0}}(T) = \Lambda_\gamma \qquad \text{at} \quad H = H_c, \qquad (5.4.15)$$

which shows the importance of the constant-strain contribution Λ_γ. It ensures that the spin-wave energy gap $E_{\mathbf{0}}(T)$, instead of going to zero as $|H - H_c|^{1/2}$, remains non-zero, as illustrated in Fig. 5.4, when the transition at $H = H_c$ is approached. Such a field just cancels the macroscopic hexagonal anisotropy, but energy is still required in the spin wave to precess the moments against the strain field of the lattice.

By symmetry, the γ-strains do not contain terms linear in $(\theta - \frac{\pi}{2})$, and the choice between constant-stress and constant-strain conditions therefore has no influence on their contribution to the second derivative of F with respect to θ, at $\theta = \pi/2$. Consequently, the γ-strains do not change the relation between $A_{\mathbf{0}}(T) + B_{\mathbf{0}}(T)$ and $F_{\theta\theta}$, given by eqn (5.3.14). The ε-strains vanish at $\theta = \pi/2$, but they enter linearly with $(\theta - \frac{\pi}{2})$. Therefore they have no effect on $A_{\mathbf{0}}(T) + B_{\mathbf{0}}(T)$, but they contribute to $F_{\theta\theta}$. To see this, we consider the ε-strain part of the Hamiltonian, eqn (2.2.29):

$$\mathcal{H}_\varepsilon = \sum_i \left[\tfrac{1}{2}c_\varepsilon(\epsilon_{\varepsilon 1}^2 + \epsilon_{\varepsilon 2}^2) - B_{\varepsilon 1}\{Q_2^1(\mathbf{J}_i)\epsilon_{\varepsilon 1} + Q_2^{-1}(\mathbf{J}_i)\epsilon_{\varepsilon 2}\}\right]. \quad (5.4.16)$$

The equilibrium condition is

$$\overline{\epsilon}_{\varepsilon 1} = \frac{1}{c_\varepsilon}B_{\varepsilon 1}\langle Q_2^1 \rangle = \tfrac{1}{4}H_\varepsilon \sin 2\theta \cos \phi,$$

in terms of the magnetostriction parameter H_ε. In the basal-plane ferromagnet, $\overline{\epsilon}_{\varepsilon 1}$ and $\overline{\epsilon}_{\varepsilon 2}$ both vanish. The transformation (5.2.2) leads to

$$Q_2^1 = \tfrac{1}{4}(O_2^0 - O_2^2)\sin 2\theta \cos \phi - O_2^1 \cos 2\theta \cos \phi + O_2^{-1} \cos \theta \sin \phi$$
$$+ \tfrac{1}{2}O_2^{-2} \sin \theta \sin \phi, \quad (5.4.17)$$

and Q_2^{-1} is given by the same expression, if ϕ is replaced by $\phi - \frac{\pi}{2}$. This implies that

$$H_\varepsilon = \frac{4}{c_\varepsilon}B_{\varepsilon 1}\langle \tfrac{1}{4}(O_2^0 - O_2^2)\rangle = \frac{2}{c_\varepsilon}B_{\varepsilon 1}J^{(2)}\hat{I}_{5/2}[\sigma]\eta_+^{-1}. \quad (5.4.18)$$

The static ε-strains are zero and do not contribute to the spin-wave parameters $A_{\mathbf{0}}(T) \pm B_{\mathbf{0}}(T)$, but they affect the second derivative of F, with respect to θ, under zero-stress conditions and, corresponding to (5.4.12), we have

$$A_{\mathbf{0}}(T) + B_{\mathbf{0}}(T) = \frac{1}{NJ\sigma}\frac{\partial^2 F}{\partial \theta^2}\bigg|_{\epsilon = \overline{\epsilon}} = \Lambda_\varepsilon + \frac{1}{NJ\sigma}F_{\theta\theta}, \quad (5.4.19)$$

with

$$\Lambda_\varepsilon = \frac{c_\varepsilon}{4J\sigma} H_\varepsilon^2, \tag{5.4.20}$$

where Λ_ε in (5.4.19) just cancels the ε-contribution to $F_{\theta\theta}/(NJ\sigma)$ determined from eqn (2.2.34).

The dependence of the magnon energy gap in Tb on magnetic field and temperature has been studied in great detail by Houmann $et\ al.$ (1975a). They expressed the axial- and hexagonal-anisotropy energies of eqn (5.2.44) in the form

$$A_0(T) \pm B_0(T) = P_0(\pm) - P_6(\pm)\cos 6\phi + g\mu_B H \cos(\phi - \phi_H) \tag{5.4.21}$$

and, by a least-squares fitting of their results, some of which are shown in Fig. 5.4, they were able to deduce the values of the four parameters $P_{0,6}(\pm)$, shown as a function of magnetization in Fig. 5.5. According to eqns (5.3.22) and (5.4.9), these parameters are given at low temperatures by:

$$P_0(+) = \left\{6B_2^0 J^{(2)} - 60B_4^0 J^{(4)} + 210B_6^0 J^{(6)} + c_\gamma(2C^2 + A^2)\right\}/J \quad (a)$$

$$P_6(+) = \left\{6B_6^6 J^{(6)} + 3c_\gamma CA\right\}/J \qquad\qquad (b)$$

$$P_0(-) = 4c_\gamma\left\{C^2 + A^2\right\}/J \qquad\qquad (c)$$

$$P_6(-) = \left\{36B_6^6 J^{(6)} + 10c_\gamma CA\right\}/J, \qquad\qquad (d)$$

$$\tag{5.4.22}$$

where, for convenience, we have set the renormalization parameters σ and $\eta_\pm$ to unity. These expressions for the parameters $P_{0,6}(\pm)$ are derived from a particular model. In general, additional contributions may appear due to other magnetoelastic interactions, and to anisotropic two-ion couplings. Nevertheless, within the RPA, the relations between the spin-wave energy parameters $A_0(T) \pm B_0(T)$ and the bulk anisotropy parameters, (5.4.12) and (5.4.19) combined with (5.3.7), should still be valid. The values of the anisotropy parameters, and their temperature dependences, determine the static magnetic and magnetoelastic properties, and can thus be obtained from bulk measurements on single crystals. A comparison between such static parameters and the dynamic values $P_{0,6}(\pm)$, derived from the field dependence of the spin-wave energy gap, can therefore elucidate the extent to which the spin-wave theory of the anisotropic ferromagnet is complete and correct.

Such a comparison has been made by Houmann $et\ al.$ (1975a). The axial-anisotropy parameter $P_0(+) + P_6(+)$, when the moments are along the easy axis, agrees with the values deduced from torque and magnetization experiments, to within the rather large uncertainties of the
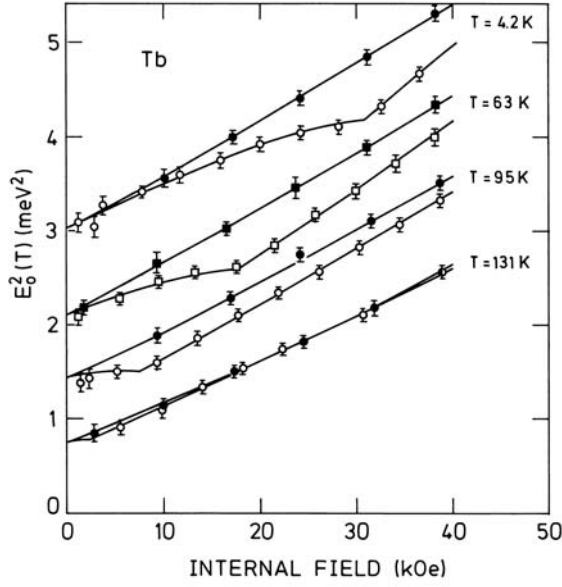
Fig. 5.4. The dependence of the square of the magnon energy gap in Tb on the internal magnetic field. Open symbols represent results for the field in the hard direction, and closed symbols are for the easy direction. The non-zero value of the gap at the critical field, which just turns the moments into the hard direction, is due to the constant-strain contribution Λ_γ. The full lines are least-squares fits of the theoretical expressions for the energy gap, given in the text, to the experimental results.

latter. The basal-plane anisotropies, as determined from the critical field H_c and the magnetoelastic γ-strain parameters, are well established by bulk measurements. Here $P_0(-)$ agrees, within the small combined uncertainties, with that derived from (5.4.22c) and (5.4.11), both in magnitude and temperature dependence. On the other hand, the small parameter $P_6(-)$ differs from the static value, so that

$$\delta_6(-) \equiv P_6(-) - g\mu_B \widetilde{H}_c + 8c_\gamma CA/(J\sigma) \qquad (5.4.23a)$$

is found to be non-zero. A part of this discrepancy may be explained by a twelve-fold anisotropy term, but this would also affect $P_0(-)$, and is expected to decrease more rapidly with increasing temperature than the experiments indicate. Within the accuracy of the experimental results, the non-zero value of $\delta_6(-)$ is the only indication of an additional renormalization of the spin-wave energy gap, compared with that derived from the second derivatives of the free energy.
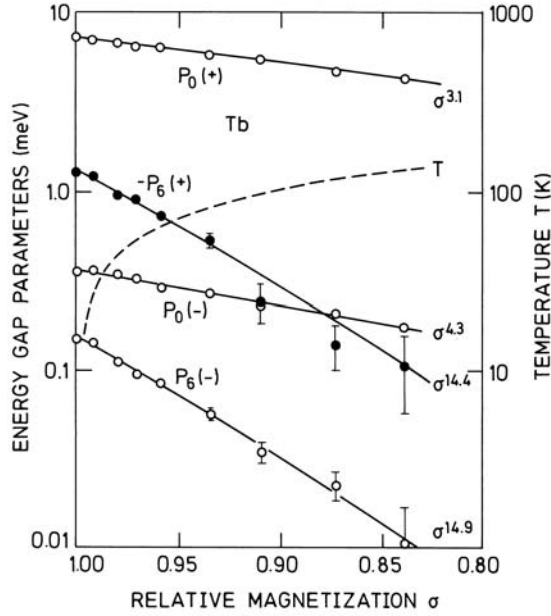
Fig. 5.5.   Anisotropy parameters in Tb as a function of the relative magnetization, deduced from results of the type illustrated in Fig. 5.4.

The σ^3-dependence of $P_0(+)$ on temperature is consistent with the σ^2-renormalization of the dominant two-fold term in (5.4.22a) predicted by the Callen–Callen theory, but a comparison with the studies of dilute Tb-alloys by Høg and Touborg (1975) suggests that a large part of the axial anisotropy may have its origin in the two-ion coupling. The effect of the two-ion anisotropy is directly apparent in that part of the axial anisotropy $P_6(+)$ which depends on the orientation of the moments in the basal plane. If only single-ion anisotropy of the type which we have considered is important, $P_6(+)$ in (5.4.22b) is directly related to the critical field necessary to turn the moments into the hard direction. However, the experimental value of $P_6(+)$ bears little relation to $g\mu_B\widetilde{H}_c/6$, even having the opposite sign. We can express this discrepancy by the parameter ΔM, defined by

$$\Delta M = P_6(+) - g\mu_B\widetilde{H}_c/6. \qquad (5.4.23b)$$

The influence of ΔM can be directly seen in the results of Fig. 5.4, since it is responsible for the difference between the slopes when the field is applied in the easy and hard directions. Although it could in principle be due to higher-rank γ-strain magnetoelastic terms, the large magnitude

of ΔM, compared to the contributions of C and A to the energy gap, effectively precludes this possibly. We must therefore ascribe it to two-ion anisotropy.

In the analysis of the field dependence of the magnon energy gap, the possible dependences of the renormalization parameters σ and $\eta_\pm$ on magnetic field and the orientation of the moments were neglected at zero temperature, but included at non-zero temperatures, assuming the different parameters effectively to be functions of σ only. In the case of Dy, the zero-temperature change of the renormalization as a function of ϕ is of some importance (Egami 1972; Jensen 1975; Egami and Flanders 1976), whereas in Tb we have estimated by various means that both approximations are justified. There are some indications that there might be a systematic error involved in the determination of the ϕ-dependent energy-gap parameters $P_6(\pm)$, possibly arising from the influence of the classical dipole forces on the inelastic neutron-scattering at long wavelength, discussed in Section 5.5.1. An extrapolation of the results found at non-zero wave-vectors to $\mathbf{q} = \mathbf{0}$ suggests that both $P_6(+)$ and $P_6(-)$ may be about a factor of two smaller than shown in Fig. 5.5. If this were the case, ΔM would still be too large to be explained by the γ-strain couplings, but $\delta_6(-)$ would be reduced almost to the level of the experimental uncertainties. Otherwise a non-zero value of $\delta_6(-)$ can only be explained by theories beyond the RPA, e.g. by effects, proportional to the frequency, due to the interaction between the spin-waves and the electron-hole pair-excitations of the conduction electrons.

5.4.2 The magnon–phonon interaction

The displacement of the ith ion from its equilibrium position, $\delta\mathbf{R}_i = \mathbf{u}(\mathbf{R}_i)$, can be expanded in normal phonon coordinates in the usual way:

$$\mathbf{u}(\mathbf{R}_i) = \sum_{\nu\mathbf{k}} \mathbf{F}_{\mathbf{k}}^\nu (\beta_{\nu\mathbf{k}} + \beta_{\nu-\mathbf{k}}^+) e^{i\mathbf{k}\cdot\mathbf{R}_i}, \qquad (5.4.24a)$$

with

$$F_{\mathbf{k},\alpha}^\nu = \left[\frac{\hbar}{2NM\omega_{\nu\mathbf{k}}} \right]^{\frac{1}{2}} f_{\mathbf{k},\alpha}^\nu. \qquad (5.4.24b)$$

M is the mass of the ions and $f_{\mathbf{k},\alpha}^\nu$ is the α-component of the phonon-polarization vector. $\beta_{\nu\mathbf{k}}$ is the phonon-annihilation operator and $\omega_{\nu\mathbf{k}}$ the corresponding phonon frequency, where ν denotes one of the three (acoustic) branches. The polarization vectors are normalized and are mutually orthogonal:

$$\sum_\alpha (f_{\mathbf{k},\alpha}^\nu)^* f_{\mathbf{k},\alpha}^{\nu'} = \delta_{\nu\nu'}. \qquad (5.4.24c)$$

For simplicity, we assume that there is only one ion per unit cell, but the results we shall derive are also applicable to the hcp lattice, at least for the acoustic modes at long wavelengths. In this limit $\mathcal{H}_\gamma(\mathrm{dyn})$, eqn (5.4.6), augmented by the kinetic energy of the ions, is adequate for discussing dynamical effects due to the γ-strains, if $\epsilon_{\alpha\beta}$ are replaced by their local values

$$\epsilon_{\alpha\beta}(i) = \overline{\epsilon}_{\alpha\beta} + \frac{i}{2}\sum_{\nu\mathbf{k}}(k_\alpha F^\nu_{\mathbf{k},\beta} + k_\beta F^\nu_{\mathbf{k},\alpha})(\beta_{\nu\mathbf{k}} + \beta^+_{\nu-\mathbf{k}})e^{i\mathbf{k}\cdot\mathbf{R}_i}. \quad (5.4.25)$$

We shall initially concentrate on the most important dynamical effects, and consider only the inhomogeneous-strain terms involving Stevens operators with odd m. Assuming for the moment that $\phi = p\frac{\pi}{2}$, we obtain the contribution $-B_{\gamma 2}\{-2O_2^{-1}(\mathbf{J}_i)\cos 2\phi\}(\epsilon_{\gamma 2}(i)-\overline{\epsilon}_{\gamma 2})$ from eqn (5.4.6), and a corresponding term in $B_{\gamma 4}$. Introducing the spin-deviation operators through (5.2.8) and (5.2.9), we obtain, to leading order in m and b,

$$\begin{aligned}
B_{\gamma 2}O_2^{-1}(\mathbf{J}_i) &= J^{(2)}B_{\gamma 2}\frac{i}{\sqrt{2J}}\Big\{a_i^+ - a_i - \frac{5}{4J}(a_i^+ a_i^+ a_i - a_i^+ a_i a_i)\Big\} \\
&= J^{(2)}B_{\gamma 2}\frac{i}{\sqrt{2J}}\big(1 - \tfrac{5}{2}m + \tfrac{5}{4}b\big)(a_i^+ - a_i) \\
&= c_\gamma C\frac{i}{\sqrt{2J}}\big(1 + \tfrac{1}{2}m + \tfrac{1}{4}b\big)(a_i^+ - a_i) \\
&= ic_\gamma C\sum_{\mathbf{q}}\left[\frac{A_{\mathbf{q}}(T) + B_{\mathbf{q}}(T)}{2NJ\sigma E_{\mathbf{q}}(T)}\right]^{\frac{1}{2}}(\alpha_{\mathbf{q}}^+ - \alpha_{-\mathbf{q}})\,e^{-i\mathbf{q}\cdot\mathbf{R}_i},
\end{aligned}$$

$$(5.4.26)$$

utilizing the RPA decoupling (5.2.29) and introducing the (renormalized) magnon operators $\alpha_{\mathbf{q}}^+$ and $\alpha_{-\mathbf{q}}$, analogously with (5.2.39) and (5.2.40). The $B_{\gamma 4}$-term is treated in the same way, and introducing the phonon-operator expansion of the strains (5.4.25) into (5.4.6), we find that $\mathcal{H} + \mathcal{H}_\gamma$ leads to the following Hamiltonian for the system of magnons and phonons:

$$\mathcal{H}_{\mathrm{mp}} = \sum_{\mathbf{k}}E_{\mathbf{k}}(T)\alpha_{\mathbf{k}}^+\alpha_{\mathbf{k}} + \sum_{\nu\mathbf{k}}\big\{\hbar\omega_{\nu\mathbf{k}}\beta_{\nu\mathbf{k}}^+\beta_{\nu\mathbf{k}} + W_{\mathbf{k}}^\nu(\alpha_{\mathbf{k}}^+ - \alpha_{-\mathbf{k}})(\beta_{\nu\mathbf{k}} + \beta_{\nu-\mathbf{k}}^+)\big\}$$

$$(5.4.27)$$

with a *magnon–phonon interaction* given by

$$W_{\mathbf{k}}^\nu = -c_\gamma\sqrt{N}(k_1 F_{\mathbf{k},2}^\nu + k_2 F_{\mathbf{k},1}^\nu)\left[\frac{A_{\mathbf{k}}(T) + B_{\mathbf{k}}(T)}{2J\sigma E_{\mathbf{k}}(T)}\right]^{\frac{1}{2}}(C\cos 2\phi + A\cos 4\phi).$$

$$(5.4.28)$$

This Hamiltonian includes the part of $\mathcal{H}_\gamma$ which is linear in the magnon operators when $\phi = p\frac{\pi}{2}$. The effects of the static deformations are

included in $E_{\mathbf{k}}(T)$ through (5.4.11). In general, $W_{\mathbf{k}}^{\nu}$ couples all three phonon modes with the magnons. A simplification occurs when $\mathbf{k}$ is along the 1- or 2-axis, i.e. when $\mathbf{k}$ is either parallel or perpendicular to the magnetization vector. In this case, $W_{\mathbf{k}}^{\nu}$ is only different from zero when ν specifies the mode as a transverse phonon with its polarization vector parallel to the basal plane. In order to analyse this situation, we introduce the four Green functions:

$$G_1(\mathbf{k}, \omega) = \langle\langle \alpha_{\mathbf{k}} \, ; \, \alpha_{\mathbf{k}}^+ - \alpha_{-\mathbf{k}} \rangle\rangle \qquad G_2(\mathbf{k}, \omega) = \langle\langle \alpha_{-\mathbf{k}}^+ \, ; \, \alpha_{\mathbf{k}}^+ - \alpha_{-\mathbf{k}} \rangle\rangle$$

$$G_3(\mathbf{k}, \omega) = \langle\langle \beta_{\mathbf{k}} \, ; \, \alpha_{\mathbf{k}}^+ - \alpha_{-\mathbf{k}} \rangle\rangle \qquad G_4(\mathbf{k}, \omega) = \langle\langle \beta_{-\mathbf{k}}^+ \, ; \, \alpha_{\mathbf{k}}^+ - \alpha_{-\mathbf{k}} \rangle\rangle,$$

$$\text{(5.4.29)}$$

where the phonon mode is as specified above (the index ν is suppressed). $\mathcal{H}_{\mathrm{mp}}$ then leads to the following coupled equations of motion for these Green functions:

$$\{\hbar\omega - E_{\mathbf{k}}(T)\}G_1(\mathbf{k}, \omega) - W_{\mathbf{k}}\{G_3(\mathbf{k}, \omega) + G_4(\mathbf{k}, \omega)\} = 1$$

$$\{\hbar\omega + E_{\mathbf{k}}(T)\}G_2(\mathbf{k}, \omega) - W_{\mathbf{k}}\{G_3(\mathbf{k}, \omega) + G_4(\mathbf{k}, \omega)\} = 1$$

$$\{\hbar\omega - \hbar\omega_{\mathbf{k}}\}G_3(\mathbf{k}, \omega) + W_{-\mathbf{k}}\{G_1(\mathbf{k}, \omega) - G_2(\mathbf{k}, \omega)\} = 0$$

$$\{\hbar\omega + \hbar\omega_{\mathbf{k}}\}G_4(\mathbf{k}, \omega) - W_{-\mathbf{k}}\{G_1(\mathbf{k}, \omega) - G_2(\mathbf{k}, \omega)\} = 0.$$

$$\text{(5.4.30)}$$

These four equations may be solved straightforwardly and, using $W_{-\mathbf{k}} = -W_{\mathbf{k}}$, we obtain, for instance,

$$\langle\langle \alpha_{\mathbf{k}} - \alpha_{-\mathbf{k}}^+ \, ; \, \alpha_{\mathbf{k}}^+ - \alpha_{-\mathbf{k}} \rangle\rangle = G_1(\mathbf{k}, \omega) - G_2(\mathbf{k}, \omega)$$

$$= 2E_{\mathbf{k}}(T)\{(\hbar\omega)^2 - (\hbar\omega_{\mathbf{k}})^2\}/\mathcal{D}(\mathbf{k}, \omega),$$

$$\text{(5.4.31)}$$

where the denominator is

$$\mathcal{D}(\mathbf{k}, \omega) = \{(\hbar\omega)^2 - E_{\mathbf{k}}^2(T)\}\{(\hbar\omega)^2 - (\hbar\omega_{\mathbf{k}})^2\} - 4W_{\mathbf{k}}^2\hbar\omega_{\mathbf{k}}E_{\mathbf{k}}(T). \quad \text{(5.4.32)}$$

In a similar way, introducing the appropriate Green functions, we find

$$\langle\langle \alpha_{\mathbf{k}} + \alpha_{-\mathbf{k}}^+ \, ; \, \alpha_{\mathbf{k}}^+ + \alpha_{-\mathbf{k}} \rangle\rangle = \left[2E_{\mathbf{k}}(T)\{(\hbar\omega)^2 - (\hbar\omega_{\mathbf{k}})^2\} + 8W_{\mathbf{k}}^2\hbar\omega_{\mathbf{k}} \right]/\mathcal{D}(\mathbf{k}, \omega).$$

$$\text{(5.4.33)}$$

In this situation, the polarization factor is $(k_1 f_{\mathbf{k},2} + k_2 f_{\mathbf{k},1}) = \pm k$, with $k = |\mathbf{k}|$. At long wavelengths, the velocity $v = \omega_{\mathbf{k}}/k$ of the transverse sound waves is related to the elastic constant $c_{66} = \rho v^2$, and hence

$$c_\gamma = 4c_{66}V/N = 4M\omega_{\mathbf{k}}^2/k^2, \qquad \text{(5.4.34)}$$

and the coupling term in $\mathcal{D}(\mathbf{k}, \omega)$ can be written

$$4W_{\mathbf{k}}^2\hbar\omega_{\mathbf{k}}E_{\mathbf{k}}(T) = \{A_{\mathbf{k}}(T) + B_{\mathbf{k}}(T)\}(\hbar\omega_{\mathbf{k}})^2\Lambda_\gamma, \qquad \text{(5.4.35)}$$

where the parameter Λ_γ is given by (5.4.10). The magnetic susceptibilities can be expressed in terms of the Green functions calculated above, using (5.2.39) and (5.2.40), and we finally arrive at

$$\chi_{xx}(\mathbf{q}, \omega) = J\sigma\big[\{A_{\mathbf{q}}(T) - B_{\mathbf{q}}(T)\}\{(\hbar\omega_{\mathbf{q}})^2 - (\hbar\omega)^2\} - \Lambda_\gamma(\hbar\omega_{\mathbf{q}})^2\big]/\mathcal{D}(\mathbf{q}, \omega) \tag{5.4.36a}$$

and

$$\chi_{yy}(\mathbf{q}, \omega) = J\sigma\{A_{\mathbf{q}}(T) + B_{\mathbf{q}}(T)\}\{(\hbar\omega_{\mathbf{q}})^2 - (\hbar\omega)^2\}/\mathcal{D}(\mathbf{q}, \omega). \tag{5.4.36b}$$

Because $\omega_{\mathbf{q}} \propto q$ and $E_{\mathbf{0}}(T) > 0$, it is possible to satisfy the inequality $E_{\mathbf{q}}(T) \gg \hbar\omega_{\mathbf{q}}$ by choosing a sufficiently small q. As mentioned earlier, $E_{\mathbf{0}}(T)$ is always greater than zero, if the magnetoelastic coupling is non-zero, on account of the constant-strain term Λ_γ. Under these circumstances the elementary-excitation energies, determined by the poles of the susceptibilities or by $\mathcal{D}(\mathbf{q}, \omega) = 0$, are found to be

$$(\hbar\omega)^2 = \begin{cases} E_{\mathbf{q}}^2(T) + 4W_{\mathbf{q}}^2 \hbar\omega_{\mathbf{q}}/E_{\mathbf{q}}(T) \\ (\hbar\omega_{\mathbf{q}})^2 - 4W_{\mathbf{q}}^2 \hbar\omega_{\mathbf{q}}/E_{\mathbf{q}}(T), \end{cases} \tag{5.4.37}$$

to leading order in $\hbar\omega_{\mathbf{q}}/E_{\mathbf{q}}(T)$. The different excitations have become mixed magnetoelastic modes, which mutually repel due to the magnetoelastic coupling, and their squared energies are shifted up or down by an equal amount. When $E_{\mathbf{q}}(T) \gg \hbar\omega_{\mathbf{q}}$, the change in energy of the upper, predominantly magnon-like branch can be neglected, whereas the frequency of the lower phonon-like mode, as obtained from (5.4.37), using the relation (5.4.35),

$$\omega^2 = \omega_{\mathbf{q}}^2 \left(1 - \frac{\Lambda_\gamma}{A_{\mathbf{0}}(T) - B_{\mathbf{0}}(T)}\right) + \mathcal{O}\big(\{\hbar\omega_{\mathbf{q}}/E_{\mathbf{q}}(T)\}^4\big), \tag{5.4.38a}$$

may be modified appreciably relative to the unperturbed phonon frequency. This relation implies that the elastic constant, relative to the unperturbed value, as determined by the velocity of these magneto-acoustic sound waves, is

$$\frac{c_{66}^*}{c_{66}} = 1 - \frac{\Lambda_\gamma}{A_{\mathbf{0}}(T) - B_{\mathbf{0}}(T)} \qquad ; \quad \mathbf{q} \parallel \text{ or } \perp \langle\mathbf{J}\rangle. \tag{5.4.38b}$$

At $\mathbf{q} = \mathbf{0}$, the dynamic coupling vanishes identically and the spin-wave energy gap is still found at $\hbar\omega = E_{\mathbf{0}}(T) = \{A_{\mathbf{0}}^2(T) - B_{\mathbf{0}}^2(T)\}^{1/2}$, with the static-strain contributions included in $A_{\mathbf{0}}(T) \pm B_{\mathbf{0}}(T)$. Due to the vanishing of the eigenfrequencies of the elastic waves at zero wave-vector, the lattice cannot respond to a uniform precession of the magnetic moments

at a non-zero frequency. Therefore the spin-wave mode at $\mathbf{q} = \mathbf{0}$ perceives the lattice as being completely static or 'frozen'. This is clearly consistent with the result (5.4.12), that the spin-wave energy gap is proportional to the second derivative of the free energy under constant-strain, rather than constant-stress, conditions.

If the lattice is able to adapt itself to the applied constant-stress condition, in the static limit $\omega \ll \omega_{\mathbf{q}}$, then, according to (5.4.36b),

$$\chi_{yy}(\mathbf{q} \to \mathbf{0}, 0) = \chi_{yy}(\mathbf{q} \equiv \mathbf{0}, 0) = \frac{J\sigma}{A_{\mathbf{0}}(T) - B_{\mathbf{0}}(T) - \Lambda_\gamma} = N\frac{(J\sigma)^2}{F_{\phi\phi}},$$
(5.4.39)

in agreement with (5.3.7). However, the first equality is not generally valid. The susceptibility depends on the direction from which $\mathbf{q}$ approaches $\mathbf{0}$. If the direction of $\mathbf{q}$ is specified by the spherical coordinates $(\theta_{\mathbf{q}}, \phi_{\mathbf{q}})$, then eqn (5.4.39) is valid only in the configuration considered, i.e. for $\theta_{\mathbf{q}} = \frac{\pi}{2}$ and $\phi_{\mathbf{q}} = 0$ or $\frac{\pi}{2}$. If we assume elastically isotropic conditions ($c_{11} = c_{33}$, $c_{44} = c_{66}$, and $c_{12} = c_{13}$), which is a reasonable approximation in Tb and Dy, we find that (5.4.39) is replaced by the more general result

$$\chi_{yy}(\mathbf{q} \to \mathbf{0}, 0) =$$
$$\frac{J\sigma}{A_{\mathbf{0}}(T) - B_{\mathbf{0}}(T) - \Lambda_\gamma \sin^2 \theta_{\mathbf{q}}\{1 - (1-\xi)\sin^2 \theta_{\mathbf{q}} \sin^2 2\phi_{\mathbf{q}}\}},$$
(5.4.40)

when $\phi = 0$ or $\frac{\pi}{2}$, and $\xi = c_{66}/c_{11}$ ($\simeq 0.3$ in Tb or Dy). The reason for this modification is that discussed in Section 2.2.2; the ability of the lattice to adapt to various static-strain configurations is limited if these strains are spatially modulated. If $\mathbf{q}$ is along the c-axis ($\theta_{\mathbf{q}} = 0$), the γ-strains are 'clamped', remaining constant throughout the crystal, so that the susceptibilities at both zero and finite frequencies are determined by the uniform γ-strain contributions alone. We note that, according to (5.4.28), $W_{\mathbf{k}}^\nu$ vanishes if $\mathbf{k}$ is parallel to the c-axis ($k_1 = k_2 = 0$). The opposite extreme occurs when $\theta_{\mathbf{q}} = \frac{\pi}{2}$ and $\phi_{\mathbf{q}} = 0$ or $\frac{\pi}{2}$. The relevant strain-mode is determined by the equilibrium conditions (5.4.3) at zero constant stress, but generalized to the non-uniform case where the y-component of the moments has a small modulation, with the wave-vector $\mathbf{q}$ along the x-direction. This strain mode ($\bar{\epsilon}_{\gamma2}(i) + \bar{\omega}_{21}(i) \propto \cos(\mathbf{q}\cdot\mathbf{R}_i + \varphi)$) coincides with a phonon eigenstate, the transverse phonon at $\mathbf{q}$ with its polarization vector in the basal plane. This coincidence makes the equilibrium strain-mode viable, which then explains the constant-stress result (5.4.39) obtained for χ_{yy} in this situation.

We shall now return to the discussion of the second-order transition occurring at $H = H_c$, when the field is applied along a hard direction

in the basal plane. From (5.4.36a), we see that $\chi_{xx}(\mathbf{q} \to \mathbf{0}, 0)$ does not show an anomaly at the transition. The critical behaviour is confined to the yy-component of the static susceptibility. At the transition, $A_{\mathbf{0}}(T) - B_{\mathbf{0}}(T) = \Lambda_{\gamma}$, according to eqn (5.4.15), and (5.4.40) then predicts a very rapid variation of $\chi_{yy}(\mathbf{q} \to \mathbf{0}, 0)$ with the direction of $\mathbf{q}$, with a divergent susceptibility in the long wavelength limit in the two cases where $\mathbf{q}$ is along the z- or the y-axis, both lying in the basal plane, parallel or perpendicular to the magnetic moments. These divergences reflect a softening of two modes in the system, the transverse phonons propagating parallel to either of the two axes ($\theta_{\mathbf{q}} = \frac{\pi}{2}$ and $\phi_{\mathbf{q}} = p\frac{\pi}{2}$), with their polarization vectors in the basal plane. Equation (5.4.38) predicts that the velocity of these modes is zero, or $c_{66}^{*} = 0$, at $H = H_c$, at which field the dispersion is quadratic in q instead of being linear. The softening of these modes was clearly observed in the ultrasonic measurements of Jensen and Palmer (1979). Although the ultrasonic velocity could not be measured as a function of magnetic field all the way to H_c, because of the concomitant increase in the attenuation of the sound waves, the mode with $\mathbf{q}$ parallel to the magnetization could be observed softening according to (5.4.38b), until the elastic constant was roughly halved. On the other hand, as discussed in the next section, the dipolar interaction prevents the velocity of the mode in which the ionic motion is along the magnetization from falling to zero, and (5.4.38b) is replaced by (5.5.13). When they took this effect into account, Jensen and Palmer (1979) could fit their results over a wide range of fields and temperatures with the RPA theory, without adjustable parameters or corrections for critical phenomena, using the bulk values of the three basal-plane anisotropy parameters C, A, and $\widetilde{H}_c$,

The absence of such corrections may be explained by the behaviour of the *critical fluctuations*, which is the same as that found in a pure structural phase-transition in an orthorhombic crystal, where c_{66} is again the soft elastic constant (Cowley 1976; Folk *et al.* 1979). The strong bounds set by the geometry on the soft modes in reciprocal space constrain the transition to exhibit mean-field behaviour. The *marginal dimensionality d^**, as estimated for example by Als-Nielsen and Birgeneau (1977), using a real space version of the Ginzburg criterion, is $d^* = 2$ in this kind of system. Whenever the dimensionality d of the system is larger than d^*, as in this case, Wilson's *renormalization group* theory predicts no corrections to Landau's mean-field theory. The transition at $H = H_c$ is thus profoundly influenced by the magnetoelastic effects. Without them, i.e. with $C = A = 0$, the spin-wave energy gap would vanish at the transition, and the critical fluctuations, the long-wavelength magnons, would not be limited to certain directions in $\mathbf{q}$-space. Under such circumstances, the system would behave analogously to a three-

dimensional Ising model, $d^* = 4$, with pronounced modifications induced by the critical fluctuations. The original treatment by Turov and Shavrov (1965) of the γ-strain contributions, which prevent the uniform magnon mode from going soft at the critical field, included only the static-strain components. The more complete analyses, including the phonon dynamics, were later given by Jensen (1971a,b), Liu (1972b), and Chow and Keffer (1973).

When the wave-vector is in the c-direction, the γ-strain couplings vanish, but instead the ε-strains become important. The O_2^1-term in Q_2^1, given by eqn (5.4.17), leads to a linear coupling between the magnons and the phonons, and proceeding as in eqns (5.4.26–27), we find the additional contribution to $\mathcal{H}_{\mathrm{mp}}$

$$\Delta \mathcal{H}_{\mathrm{mp}} = \sum_{\mathbf{k}} i W_{\mathbf{k}}^{\nu}(\varepsilon)(\alpha_{\mathbf{k}}^{+} + \alpha_{-\mathbf{k}})(\beta_{\nu \mathbf{k}} + \beta_{\nu -\mathbf{k}}^{+}), \qquad (5.4.41a)$$

with

$$W_{\mathbf{k}}^{\nu}(\varepsilon) = -\tfrac{1}{4} c_{\varepsilon} \sqrt{N} \big\{ (k_1 F_{\mathbf{k},3}^{\nu} + k_3 F_{\mathbf{k},1}^{\nu}) \cos \phi + (k_2 F_{\mathbf{k},3}^{\nu} + k_3 F_{\mathbf{k},2}^{\nu}) \sin \phi \big\}$$
$$\times \left[\frac{A_{\mathbf{k}}(T) - B_{\mathbf{k}}(T)}{2 J \sigma E_{\mathbf{k}}(T)} \right]^{\frac{1}{2}} H_{\varepsilon}, \qquad (5.4.41b)$$

in the long-wavelength limit. When $\mathbf{k}$ is parallel to the c-axis, (5.4.28) and (5.4.41) predicts that only the transverse phonons with their polarization vectors parallel to the magnetization are coupled to the magnons. The calculation of the velocity of this coupled mode leads, by analogy to (5.4.38), to an elastic constant

$$\frac{c_{44}^{*}}{c_{44}} = 1 - \frac{\Lambda_{\varepsilon}}{A_{\mathbf{0}}(T) + B_{\mathbf{0}}(T)} \qquad \text{when} \quad \mathbf{f}_{\mathbf{k}}^{\nu} \parallel \langle \mathbf{J} \rangle. \qquad (5.4.42)$$

The same result is obtained for the transverse-phonon mode propagating in the direction of the ordered moments, with the polarization vector parallel to the c-axis. These are the two modes which go soft in the case of a second-order transition to a phase with a non-zero c-axis moment.

We have so far only considered the dynamics in the long-wavelength limit. At shorter wavelengths, where the phonon and spin-wave energies may be comparable, the magnon–phonon interaction leads to a strong hybridization of the normal modes, with energy gaps at points in the Brillouin zone where the unperturbed magnon and phonon dispersion relations cross each other, as illustrated in Fig. 5.6. The interaction amplitudes (5.4.28) and (5.4.41b) are correct only for small wave-vectors. At shorter wavelengths, we must consider explicitly the relative positions

of neighbouring ions, instead of the local strains. Evenson and Liu (1969) have devised a simple procedure for replacing the local-strain variables in the magnetoelastic Hamiltonian with the relative displacements of the neighbouring ions. Using their procedure, and assuming the nearest-neighbour interactions to be dominant, we find that eqn (5.4.41b) is replaced by

$$W_{\mathbf{k}}^{\nu}(\varepsilon) = -\tfrac{1}{4}c_{\varepsilon}\sqrt{N}\left(\frac{2}{c}\sin\left(kc/2\right)\right)F_{\mathbf{k},\parallel}^{\nu}\left[\frac{A_{\mathbf{k}}(T) - B_{\mathbf{k}}(T)}{2J\sigma E_{\mathbf{k}}(T)}\right]^{\frac{1}{2}}H_{\varepsilon}, \quad (5.4.43)$$

when $\mathbf{k}$ is along the c-axis. c is the lattice constant and $F_{\mathbf{k},\parallel}^{\nu}$ is the component of $\mathbf{F}_{\mathbf{k}}^{\nu}$ parallel to the magnetization vector, which is only non-zero for one of the transverse-phonon modes. This interaction does not distinguish between the two sublattices in the hcp crystal. This means that $W_{\mathbf{k}}^{\nu}(\varepsilon)$ only couples the magnons with the phonons at a certain $\mathbf{k}$ if the modes are either both acoustic or both optical, consistent with the double-zone representation in the c-direction. Except for the replacement of (5.4.41b) by (5.4.43), the interaction Hamiltonian (5.4.41a) is unchanged. From the equations of motion of the Green functions, we may derive the susceptibilities, when $\mathbf{k}$ is along the c-direction, in the same way as before, eqns (5.4.29–36), and the results are found to be:

$$\chi_{xx}(\mathbf{k},\omega) = J\sigma\{A_{\mathbf{k}}(T) - B\mathbf{k}(T)\}\{(\hbar\omega_{t\mathbf{k}})^2 - (\hbar\omega)^2\}/\mathcal{D}_{\varepsilon}(\mathbf{k},\omega)$$

$$\chi_{yy}(\mathbf{k},\omega) = J\sigma\{A_{\mathbf{k}}(T) + B_{\mathbf{k}}(T)\}$$
$$\times\left\{(\hbar\omega_{t\mathbf{k}})^2 - (\hbar\omega)^2 - 4W_{\mathbf{k}}^2(\varepsilon)\hbar\omega_{t\mathbf{k}}/E_{\mathbf{k}}(T)\right\}/\mathcal{D}_{\varepsilon}(\mathbf{k},\omega),$$
$$(5.4.44)$$

with

$$\mathcal{D}_{\varepsilon}(\mathbf{k},\omega) = \{E_{\mathbf{k}}^2(T) - (\hbar\omega)^2\}\{(\hbar\omega_{t\mathbf{k}})^2 - (\hbar\omega)^2\} - 4W_{\mathbf{k}}^2(\varepsilon)\hbar\omega_{t\mathbf{k}}E_{\mathbf{k}}(T),$$
$$(5.4.45)$$

where $\omega_{t\mathbf{k}}$ is the angular frequency of the transverse phonon mode at $\mathbf{k}$. Introducing the parameter

$$\Upsilon_{\mathbf{k}} = \left[1 + \frac{16\hbar\omega_{t\mathbf{k}}E_{\mathbf{k}}(T)W_{\mathbf{k}}^2(\varepsilon)}{\{E_{\mathbf{k}}^2(T) - (\hbar\omega_{t\mathbf{k}})^2\}^2}\right]^{\frac{1}{2}}, \quad (5.4.46)$$

we find the poles in the susceptibilities at

$$\hbar\omega = \pm E_{\mathbf{k}}^{\pm} = \pm\left[\tfrac{1}{2}\{E_{\mathbf{k}}^2(T) + (\hbar\omega_{t\mathbf{k}})^2\} \pm \tfrac{1}{2}\{E_{\mathbf{k}}^2(T) - (\hbar\omega_{t\mathbf{k}})^2\}\Upsilon_{\mathbf{k}}\right]^{\frac{1}{2}},$$
$$(5.4.47a)$$

corresponding to

$$\mathcal{D}_{\varepsilon}(\mathbf{k},\omega) = \{(E_{\mathbf{k}}^+)^2 - (\hbar\omega)^2\}\{(E_{\mathbf{k}}^-)^2 - (\hbar\omega)^2\}. \quad (5.4.47b)$$

By a straightforward manipulation of these expressions, we obtain

$$\chi_{yy}''(\mathbf{k}, \omega) = \mathrm{Im}\big[\chi_{yy}(\mathbf{k}, \omega)\big] = \pi J \sigma \frac{A_{\mathbf{k}}(T) + B_{\mathbf{k}}(T)}{2E_{\mathbf{k}}(T)}$$

$$\times \Big[\frac{E_{\mathbf{k}}^+}{E_{\mathbf{k}}(T)} \frac{\Upsilon_{\mathbf{k}} + 1}{2\Upsilon_{\mathbf{k}}} \big\{ \delta(E_{\mathbf{k}}^+ - \hbar\omega) - \delta(E_{\mathbf{k}}^+ + \hbar\omega) \big\}$$

$$+ \frac{E_{\mathbf{k}}^-}{E_{\mathbf{k}}(T)} \frac{\Upsilon_{\mathbf{k}} - 1}{2\Upsilon_{\mathbf{k}}} \big\{ \delta(E_{\mathbf{k}}^- - \hbar\omega) - \delta(E_{\mathbf{k}}^- + \hbar\omega) \big\} \Big].$$

$$(5.4.48)$$

Almost the same expression is obtained for $\chi_{xx}''(\mathbf{k}, \omega)$; the sign before $B_{\mathbf{k}}(T)$ is reversed and the factors $E_{\mathbf{k}}^{\pm}/E_{\mathbf{k}}(T)$ are replaced by their reciprocals. If $W_{\mathbf{k}}(\varepsilon) = 0$, then $\Upsilon_{\mathbf{k}} = 1$ and $E_{\mathbf{k}}^+ = E_{\mathbf{k}}(T)$, and (5.4.48) is equivalent to eqn (5.2.40b). When $W_{\mathbf{k}}(\varepsilon)$ is non-zero, $\Upsilon_{\mathbf{k}} > 1$ and there are two poles in the magnetic susceptibilities, one at $E_{\mathbf{k}}^+$ closest to $E_{\mathbf{k}}(T)$, and the other at $E_{\mathbf{k}}^-$ closest to the energy of the transverse-phonon mode. Both poles lie outside the energy interval between $E_{\mathbf{k}}(T)$ and $\hbar\omega_{t\mathbf{k}}$. The two normal modes at $\mathbf{k}$, the magnons and the transverse phonons polarized parallel to the magnetization, are transformed into two magnetoelastic modes, both of which give rise to a magnetic scattering of neutrons. The cross-section for neutrons scattered by a pure phonon-mode is proportional to $(\boldsymbol{\kappa} \cdot \mathbf{f}_{\mathbf{k}}^\nu)^2$. If the scattering vector $\boldsymbol{\kappa}$ is along the c-axis, the transverse phonons in this direction do not therefore scatter neutrons, unless they are coupled to the magnons. With $\boldsymbol{\kappa}$ parallel to the c-axis, the (magnetic) scattering amplitude is proportional to $\chi_{yy}''(\mathbf{k}, \omega)$ and, in this situation, eqn (5.4.48), combined with (4.2.2) and (4.2.3), determines the total scattered intensity due to the coupled magnon and transverse-phonon modes. If the energy difference between the two uncoupled modes at some $\mathbf{k}$ is large, $\Upsilon_{\mathbf{k}}$ is only slightly greater than 1, and the coupling induces only a small repulsion of the mode energies. The pole at energy $E_{\mathbf{k}}^+$, close to the unperturbed magnons, then dominates the magnetic scattering cross-section. The strongest modification occurs at the $\mathbf{k}$-vector where $E_{\mathbf{k}}(T) = \hbar\omega_{t\mathbf{k}}$, at which $\Upsilon_{\mathbf{k}} \to \infty$ and eqn (5.4.48) predicts nearly equal scattering intensities of the two modes at energies determined by

$$(\hbar\omega)^2 = E_{\mathbf{k}}^2(T) \pm 2E_{\mathbf{k}}(T)|W_{\mathbf{k}}(\varepsilon)| \qquad ; \qquad E_{\mathbf{k}}(T) = \hbar\omega_{t\mathbf{k}}, \qquad (5.4.49a)$$

corresponding to an energy splitting, or energy gap, between the two modes of magnitude

$$\Delta \simeq 2|W_{\mathbf{k}}(\varepsilon)|, \qquad (5.4.49b)$$

to leading order. These *resonance* or *hybridization* phenomena, the redistribution of the scattered intensity and the creation of an energy gap,

are observed whenever two normal modes are coupled linearly with each other, and the value of the energy gap at the **k**-point where the two coupled modes are closest in energy, or where their scattering intensities are equal, gives a direct measure of the coupling amplitude at that particular **k**-vector. The effect of the magnon–phonon interaction on the excitation spectrum in Tb is illustrated in Fig. 5.6.
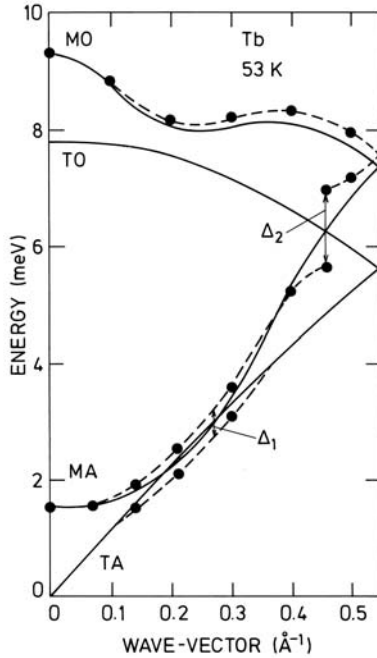
Fig. 5.6. The dispersion relations for the magnons and phonons propagating in the c-direction of Tb at 53 K, illustrating the magnon–phonon interaction. The calculated unperturbed modes are depicted by the full curves. The normal modes are mixed magnon–phonon states, and energy gaps appear at the crossing points of the unperturbed dispersion relations. The acoustic magnons interact both with the acoustic and the optical phonons.

The method described above, based on the magnetoelastic Hamiltonian, is not sufficiently general to enable a prediction of all possible couplings allowed by symmetry, i.e. the *selection rules*. To accomplish this, it is necessary either to use group-theoretical arguments, or to derive a general version of the magnon–phonon Hamiltonian based exclusively on symmetry considerations. These two methods have been applied to this system by respectively Cracknell (1974) and Jensen and Houmann (1975). Their analyses show that, when **k** is along the c-direction, a further mixing is allowed in addition to that considered above. This requires the single-zone representation in the c-direction, since it couples an acoustic mode to an optical mode at the same **k**-vector. The phonon modes in question are once more transverse, but their coupling to the magnons depends on the polarization relative to the direction of magnetization. In an a-axis magnet, the polarization vector should be parallel

to the magnetization, as is assumed in eqn (5.4.43), whereas in a b-axis magnet, the acoustic–optical coupling involves the transverse phonons polarized perpendicular to the magnetization (i.e. still along an a-axis). The symmetry arguments show that this coupling must be quadratic in k in the long wavelength limit, instead of linear as is $W_{\mathbf{k}}(\varepsilon)$. It therefore has no influence on the uniform strains or the elastic constants, and accordingly no counterpart in the magnetoelastic Hamiltonian. Liu (1972a) has discussed the possible origin of such an acoustic–optical interaction, and he concludes that it cannot be a crystalline-field effect, but must be mediated indirectly via the conduction electrons and be proportional to the spin–orbit coupling forces. As is illustrated in Fig. 5.6, the acoustic–optical magnon–phonon interaction is clearly observed in Tb, where it leads to the energy gap Δ_2, the strongest hybridization effect seen in the metal. However, a closer examination (Jensen and Houmann 1975) shows that the transverse phonon modes involved are those polarized parallel to the magnetization, in spite of the fact that Tb has its magnetization vector in the b-direction. Hence this interaction violates the selection rules deduced from the general symmetry arguments, leading to the conclusion that the ground-state of Tb cannot be a simple b-axis ferromagnet as assumed. The $4f$ moments are undoubtedly along an easy b-axis, but the spins of the conduction electrons are not necessarily polarized collinearly with the angular momenta of the core electrons, because of their spin–orbit coupling. If the ground-state spin-density wave of the conduction electrons in Tb has a polarization which varies in space within a single unit cell, a coupling mediated by this spin-density wave may violate the selection rules based on the symmetry properties of the simple ferromagnet. The presence of the 'symmetry-breaking' acoustic–optical interaction in Tb demonstrates that the conduction electrons play a more active role than passively transmitting the indirect-exchange interaction. This magnon–phonon coupling is directly dependent on spin–orbit effects in the band electrons, in accordance with Liu's explanation, and its appearance demonstrates that the polarization of the conduction-electron spins must have a component perpendicular to the angular momenta.

To complete this section, we shall briefly discuss the additional magnon–phonon interaction terms which are linear in the phonon operators, but quadratic in the magnon operators:

$$\mathcal{H}_{\mathrm{mp}}^{(2)} = \sum_{\mathbf{qk}\nu} \big[U_\nu(\mathbf{k},\mathbf{q}) \alpha_{\mathbf{q+k}}^+ \alpha_{\mathbf{q}} + \tfrac{1}{2} V_\nu(\mathbf{k},\mathbf{q}) \alpha_{\mathbf{q+k}}^+ \alpha_{-\mathbf{q}}^+$$
$$+ \tfrac{1}{2} V_\nu^*(-\mathbf{k},-\mathbf{q}) \alpha_{\mathbf{q}} \alpha_{-\mathbf{q-k}} \big] (\beta_{\nu\mathbf{k}} + \beta_{\nu-\mathbf{k}}^+). \quad (5.4.50)$$

Referring back to the magnetoelastic Hamiltonian, we find that such an

interaction may originate from, for instance, the term

$$-B_{\gamma 2}\{(O_2^0 + O_2^2) - \langle O_2^0 + O_2^2 \rangle\}\tfrac{1}{2}\cos 2\phi(\epsilon_{\gamma 1} - \overline{\epsilon}_{\gamma 1})$$

in (5.4.6), or the corresponding terms in (5.4.16). In contrast to the linear couplings considered above, the symmetry-preserving α-strain part of the magnetoelastic Hamiltonian makes a contribution to the quadratic interaction terms. Using the procedure of Evenson and Liu (1969), it is straightforward, if somewhat tedious, to relate the interaction amplitudes in eqn (5.4.50) to the magnetoelastic coupling parameters. We shall not perform this analysis here, but refer instead to the detailed calculations of Jensen (1971a,b). The interactions in eqn (5.4.50) have the consequence that the equations of motion of the magnon Green function $\langle\langle \alpha_{\mathbf{q}} ; \alpha_{\mathbf{q}}^+ \rangle\rangle$ involve new, higher-order mixed Green functions like $\langle\langle \alpha_{\mathbf{q-k}} \beta_{\mathbf{k}} ; \alpha_{\mathbf{q}}^+ \rangle\rangle$. Performing an RPA or Hartree–Fock decoupling, as in (5.2.29), of the three-operator products which occur in the equations of motion of the new Green functions, we obtain a closed expression for the magnon Green function, which may be written

$$\langle\langle \alpha_{\mathbf{q}} ; \alpha_{\mathbf{q}}^+ \rangle\rangle = \frac{1}{\hbar\omega - E_{\mathbf{q}}(T) - \Sigma(\mathbf{q},\omega)}, \qquad (5.4.51)$$

where $\Sigma(\mathbf{q},\omega)$ is the *self-energy*, due to the interactions in (5.4.50), of the magnons of wave-vector $\mathbf{q}$. Neglecting $V_\nu(\mathbf{q},\mathbf{k})$, we find that the self-energy at $T = 0$ is

$$\Sigma(\mathbf{q},\omega) = \lim_{\epsilon\to 0^+} \sum_{\mathbf{k}\nu} \frac{|U_\nu(\mathbf{k},\mathbf{q})|^2}{\hbar\omega + i\hbar\epsilon - E_{\mathbf{q+k}}(0) - \hbar\omega_{\nu\mathbf{k}}} . \qquad (5.4.52)$$

These interactions are not diagonal in reciprocal space and the magnons are therefore affected by all the phonons. Whenever $\mathbf{k}$ has a value such that $E_{\mathbf{q}}(0) \simeq E_{\mathbf{q+k}}(0) + \hbar\omega_{\nu\mathbf{k}}$, the real part of the denominator in (5.4.52) vanishes close to the magnon pole at $\mathbf{q}$, as determined by (5.4.51). This implies a negative imaginary contribution to $\Sigma(\mathbf{q},\omega)$, when $\hbar\omega \simeq E_{\mathbf{q}}(0)$, and hence a reduction in the lifetime of the magnons. The energy of the magnons at $\mathbf{q}$ is approximately given by $E_{\mathbf{q}}(0) + \mathrm{Re}\big[\Sigma(\mathbf{q},\omega)\big]$, with $\hbar\omega \simeq E_{\mathbf{q}}(0)$. At non-zero temperatures, the self-energy terms increase in proportion to the Bose population-factors of the magnons and phonons involved. These interactions, quadratic in the magnon operators, do not lead to the kind of hybridization effects produced by the linear couplings, but rather give rise to a (small) renormalization of the normal-mode energies and to a finite lifetime of the excitations. These effects are entirely similar to those due to the magnon–magnon interactions appearing in the spin-wave theory in the third order

of $1/J$. Equation (5.4.52) shows that the 'zero-point' motion of the ions, at $T = 0$, has a slight effect on the magnons. A similar effect occurs due to the magnon–magnon interactions, but only in an anisotropic ferromagnet where B is non-zero, as we discussed in the previous section. In most cases, the contributions due to the magnon–magnon interactions are expected to predominate, because the magnon–phonon coupling parameters are usually quite small, in comparison with the spin-wave interactions. Although the interactions in (5.4.50) may not be important for the magnons, they may have observable effects on the phonons at finite temperatures. For instance, they affect the velocity of the transverse sound waves propagating in the c-direction and polarized perpendicular to the magnetization, but not those polarized parallel to the magnetization, which are modified by the linear couplings as discussed above. Deriving the perturbed phonon Green functions in the same way as the magnon Green function, and taking the long-wavelength limit, we find (Jensen 1971a,b)

$$\frac{c_{44}^*}{c_{44}} = 1 - \Lambda_\varepsilon \frac{1}{NJ} \sum_{\mathbf{q}} \frac{n_{\mathbf{q}}}{E_{\mathbf{q}}(T)} \qquad \text{when} \quad \mathbf{f}_{\mathbf{k}}^\nu \perp \langle \mathbf{J} \rangle. \qquad (5.4.53)$$

We note that this result is of higher order in $1/J$ than the effect due to the linear coupling, given in (5.4.42). However, the extra factor $1/J$ may be compensated by the magnon population-factor $n_{\mathbf{q}}$ in the sum over $\mathbf{q}$, at elevated temperatures.

Modifications of the results obtained above may occur, due to anharmonic terms of third order in the strains, or magnetoelastic terms quadratic in the strains. These higher-order contributions may possibly be of some importance for the temperature dependence of the elastic constants and the spin-wave parameters. However, they should be of minor significance under the nearly constant-strain conditions which obtain, for instance, when the magnetic-field dependence of the elastic constants is considered.

5.5 Two-ion anisotropy

In this section, we discuss the components of the two-ion coupling which cannot be included in the *isotropic* Heisenberg Hamiltonian considered hitherto, i.e. the two-ion term in eqn (5.2.1). We first consider the classical magnetic *dipole–dipole interaction* in some detail, and show how it may affect the spin-wave energies and ultrasonic velocities. Thereafter we discuss some of the complexities resulting from the presence of *general two-ion couplings*, which are consistent with the symmetry properties of the magnetic phase. The experimental manifestations of such interactions, which either have been observed in the excitation spectrum of Tb, or could in principle be observed, are finally summarized.

5.5.1 The dipole–dipole interaction

A general two-ion Hamiltonian involving only the dipolar moments of the $4f$ electrons is

$$\mathcal{H}_{\mathrm{dd}} = -\frac{1}{2} \sum_{ij} \sum_{\alpha\beta} \mathcal{J}_{\alpha\beta}(ij) J_{i\alpha} J_{j\beta}. \tag{5.5.1}$$

The Heisenberg interaction, when expressed in this way, is diagonal, with the form $\mathcal{J}(ij)\delta_{\alpha\beta}$. The most familiar example of an *anisotropic* two-ion coupling is the classical magnetic dipole–dipole interaction, which gives a contribution

$$\Delta\mathcal{J}_{\alpha\beta}(ij) = \frac{N}{V}(g\mu_B)^2 D_{\alpha\beta}(ij), \tag{5.5.2a}$$

where $D_{\alpha\beta}(ij)$ is the dimensionless coupling parameter

$$D_{\alpha\beta}(ij) = \frac{V}{N} \frac{3(R_{i\alpha} - R_{j\alpha})(R_{i\beta} - R_{j\beta}) - \delta_{\alpha\beta}|\mathbf{R}_i - \mathbf{R}_j|^2}{|\mathbf{R}_i - \mathbf{R}_j|^5}, \tag{5.5.2b}$$

recalling that the magnetic moment of the ith ion is $g\mu_B\mathbf{J}_i$. This coupling is weak, being typically one or two orders of magnitude smaller than the indirect exchange between near neighbours, but it is extremely long-range and anisotropic and may therefore have important consequences for the magnetic properties, as we shall discuss in the following. We wish to calculate the spatial Fourier transform

$$D_{\alpha\beta}(\mathbf{q}) = \frac{1}{N} \sum_i \sum_j D_{\alpha\beta}(ij)\, e^{-i\mathbf{q}\cdot(\mathbf{R}_i - \mathbf{R}_j)}. \tag{5.5.3}$$

If $\mathbf{q}$ is along the c-axis, which is a three-fold axis of the hcp lattice, the symmetry dictates that the only non-zero elements of $\mathcal{J}_{\alpha\beta}(\mathbf{q})$ are $\mathcal{J}_{\xi\xi}(\mathbf{q}) = \mathcal{J}_{\eta\eta}(\mathbf{q})$ and $\mathcal{J}_{\zeta\zeta}(\mathbf{q})$. In addition, the condition $\sum_\alpha D_{\alpha\alpha}(\mathbf{q}) = 0$ implies that

$$D_{\zeta\zeta}(\mathbf{q}) = -2D_{\xi\xi}(\mathbf{q}) = -2D_{\eta\eta}(\mathbf{q}) \qquad ; \quad \mathbf{q} \parallel c - \text{axis}, \tag{5.5.4}$$

with the extra stipulation that $\mathbf{q} \neq \mathbf{0}$, in which case the surface of the sample does not contribute. In the limit of long wavelengths, the shape of the sample becomes important, and for convenience we assume it to be an ellipsoid, with the principal axes along the symmetry ξ-, η-, and ζ-axes. We consider first the limit $\mathbf{q} = \mathbf{0}$ where, because the sample is an ellipsoid, the summation over j in (5.5.3) leads to a result independent of i, since an ellipsoid placed in a constant magnetic field has a uniform magnetization throughout its interior. Furthermore, when $\mathbf{r} = \mathbf{R}_i - \mathbf{R}_j$ becomes large, it may be replaced by a continuous variable, and the sum

over j may be split into a sum over the lattice points lying within a large sphere plus an integral over the rest of the sample:

$$\sum_j \cdots = \sum_{j\in\text{sphere}} \cdots + \frac{N}{V} \int_{\text{sphere}}^{\text{sample}} \cdots d\mathbf{r}.$$

The value of the integral for the zz-component is

$$\int \frac{1}{r^3}\Big(\frac{3z^2}{r^2} - 1\Big) d\mathbf{r} = -\int \nabla \cdot \Big(\frac{\mathbf{z}}{r^3}\Big) d\mathbf{r} = \int_{\text{sphere}} \frac{\mathbf{z}\cdot d\mathbf{S}}{r^3} - \int_{\text{sample}} \frac{\mathbf{z}\cdot d\mathbf{S}}{r^3}$$
$$= \frac{4\pi}{3} - N_z,$$

where $d\mathbf{S}$ is a vectorial surface element of the sphere/sample, and N_ξ is the *demagnetization factor*

$$N_\xi = \int_{\text{sample}} \left(\frac{\hat{\boldsymbol{\xi}}\cdot\mathbf{r}}{r^3}\right) \hat{\boldsymbol{\xi}} \cdot d\mathbf{S}, \qquad (5.5.5)$$

where $\hat{\boldsymbol{\xi}}$ is a unit vector along the ξ-axis. It is easily seen that $N_\xi + N_\eta + N_\zeta = 4\pi$. Hence we obtain

$$D_{\xi\xi}(\mathbf{0}) = \frac{4\pi}{3} + \big[D_{\xi\xi}(\mathbf{0})\big]_L - N_\xi, \qquad (5.5.6)$$

plus equivalent results for the other diagonal components. The first term is the *Lorentz factor*, and $\big[D_{\xi\xi}(\mathbf{0})\big]_L$ is the value of the lattice sum over the sphere, satisfying the relations $\big[D_{\zeta\zeta}(\mathbf{0})\big]_L = -2\big[D_{\xi\xi}(\mathbf{0})\big]_L = -2\big[D_{\eta\eta}(\mathbf{0})\big]_L$. In the case of a cubic lattice, the lattice sums vanish by symmetry. This is nearly also true for an hcp lattice with an ideal c/a-ratio, because of the close relationship between the fcc lattice and the ideal hcp lattice. The hcp lattice of the heavy rare earths is slightly distorted, as may be seen from Table 1.2, in which case the lattice sums become non-zero, approximately proportionally to the deviation from the ideal c/a-ratio; $\big[D_{\xi\xi}(\mathbf{0})\big]_L = -0.0024 + 1.50\big(c/a - \sqrt{8/3}\big)$. Brooks and Goodings (1968) overestimate the anisotropy in the free energy due to the dipole interaction by a factor of two.

When considering the lattice sum determining $D_{\alpha\beta}(\mathbf{q}) - D_{\alpha\beta}(\mathbf{0})$, we may immediately apply the continuum approximation in the long-wavelength limit $2\pi/q \gg a$, and replace the sum with the corresponding integral. In the calculation above at $\mathbf{q} = \mathbf{0}$, this approximation is not directly applicable, because the corresponding integral contains a divergence at the origin, which is however removed in the difference

$D_{\alpha\beta}(\mathbf{q}) - D_{\alpha\beta}(\mathbf{0})$. In addition to the condition $q \ll 2\pi/a$, we shall assume that $q \gg 2\pi/L$, or more specifically $q \geq 10/L$ (Keffer 1966), where L is a length dimension of the crystal, in which case the effects of the boundaries on $D_{\alpha\beta}(\mathbf{q})$ are averaged out because of the relatively rapid variation of the exponential factor on the surface. Using these two conditions, we find

$$
D_{\alpha\beta}(\mathbf{q}) = D_{\alpha\beta}(\mathbf{0}) + \int \frac{3(\hat{\boldsymbol{\alpha}}\cdot\mathbf{r})(\hat{\boldsymbol{\beta}}\cdot\mathbf{r}) - \delta_{\alpha\beta}\, r^2}{r^5}\big(e^{i\mathbf{q}\cdot\mathbf{r}} - 1\big)d\mathbf{r}
$$

$$
= \big[D_{\alpha\beta}(\mathbf{0})\big]_L +
$$

$$
\iint \frac{3(\hat{\boldsymbol{\alpha}}\cdot\mathbf{r})(\hat{\boldsymbol{\beta}}\cdot\mathbf{r}) - \delta_{\alpha\beta}r^2}{r^5}\Big[\sum_{l=0}^{\infty}[4\pi(2l+1)]^{1/2}\,i^l\,j_l(qr)Y_{l0}(\theta,\phi)\Big]r^2 dr d\Omega.
$$

The $\mathbf{q}$-independent term in the first integral leads to the same result as in (5.5.6), but without the lattice-sum contribution, and adding $D_{\alpha\beta}(\mathbf{0})$, we are left with the term $\big[D_{\alpha\beta}(\mathbf{0})\big]_L$. The $\mathbf{q}$-dependent exponential is expanded in terms of the spherical Bessel functions, as in (4.1.8), with the polar axis chosen to be parallel to $\mathbf{q}$. The dipole factor in the resulting integral may be written as a linear combination of the spherical harmonics of second rank $Y_{2m}(\theta,\phi)$, multiplied by r^{-3}, ensuring that only the term with $l = 2$ in the sum over l survives the integration over solid angles. Further, if $\hat{\boldsymbol{\alpha}}$ and $\hat{\boldsymbol{\beta}}$ are either parallel or perpendicular to $\mathbf{q}$, only the diagonal components may differ from zero. With $\hat{\boldsymbol{\alpha}}$ and $\hat{\boldsymbol{\beta}}$ both parallel to $\mathbf{q}$, the longitudinal component is

$$
D_{\|}(\mathbf{q}) - \big[D_{\|}(\mathbf{0})\big]_L
$$

$$
= \iint [16\pi/5]^{1/2}Y_{20}(\theta,\phi)r^{-3}[4\pi\cdot 5]^{1/2}(-1)j_2(qr)Y_{20}(\theta,\phi)r^2 dr d\Omega
$$

$$
= -8\pi \int_0^\infty \frac{1}{\rho}j_2(\rho)d\rho = -8\pi\Big[-\frac{j_1(\rho)}{\rho}\Big]_0^\infty = -\frac{8\pi}{3},
$$

recalling that $j_1(\rho)/\rho \to \frac{1}{3}$ or 0, for respectively $\rho \to 0$ or ∞. This result implies that the two transverse components are

$$
D_\perp(\mathbf{q}) - \big[D_\perp(\mathbf{0})\big]_L = -\tfrac{1}{2}\big\{D_{\|}(\mathbf{q}) - \big[D_{\|}(\mathbf{0})\big]_L\big\} = \frac{4\pi}{3}; \qquad (5.5.7)
$$

$$
\text{when} \quad 2\pi/L \ll q \ll 2\pi/a.
$$

The dipole-coupling components change from the values given by (5.5.6) to those above within a very narrow range of q, i.e. when q goes from zero to about $10/L$, as shown by the detailed analysis of Keffer (1966). At larger wave-vectors, the variation of $D_{\alpha\beta}(\mathbf{q})$ is smooth and gradual,

and it may be described by a few interplanar coupling parameters of the type used for other two-ion interactions. Cohen and Keffer (1955) have calculated the **q**-dependence for the three cubic Bravais lattices, and their results also determine approximately $D_{\alpha\beta}(\mathbf{q})$, with **q** along the c-axis, in the hcp lattice with the ideal c/a-ratio, since this is equivalent to **q** along a (111)-direction in the fcc crystal. In the distorted case, with $c/a = 0.963\sqrt{8/3}$ (corresponding to Ho), a numerical calculation gives

$$D_{\xi\xi}(\mathbf{q}) + 0.0221\frac{4\pi}{3} = \big\{0.9190 + 0.0816\cos{(qc/2)} - 0.0006\cos{(qc)}\big\}\frac{4\pi}{3}$$

when $\mathbf{q} \parallel c$-axis and $q \geq 10/L$, so that the **q**-dependence in the c-direction is very weak, except for the jump at small **q**, which is illustrated for the example of Ho in Fig. 5.7.

In a uniform ferromagnet, the demagnetization factor leads to a positive contribution to the internal energy. Without any external applied
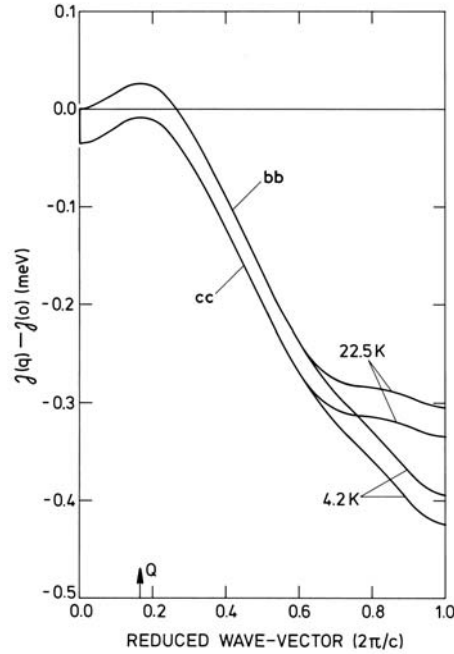

Fig. 5.7. Parallel and perpendicular components of the Fourier transform, for **q** along the c-direction, of the two-ion coupling in Ho, deduced from the spin-wave energies. The coupling is assumed to comprise an isotropic indirect-exchange contribution and the classical dipole–dipole interaction, which gives rise to the discontinuity at $\mathbf{q} = \mathbf{0}$ in the parallel component, and stabilizes the cone structure at low temperatures.

field, it is therefore energetically favourable for the system to split up in *domains*, in which the magnetization vector points in different directions, so that the magnetization almost vanishes at the surface. The greater the number of domains, the more effectively the demagnetization contribution may be eliminated, but this tendency is opposed by the cost in energy of the *domain-walls*. It is only the contribution due to the demagnetization factor (as determined by the magnetization at the surface) which is affected by the creation of domains, and in a simple model in which the energy of the domain-walls is neglected, the internal energy per unit volume, due to the dipole coupling and including the Zeeman energy, is

$$U_D + U_Z \simeq -\tfrac{1}{2} D_{zz}^{\text{eff}}(\mathbf{0}) M^2 + \tfrac{1}{2} N_z \langle M \rangle^2 - H_A \langle M \rangle.$$

The demagnetization factor is considered separately, so that $D_{zz}^{\text{eff}}(\mathbf{0}) = 4\pi/3 + \left[D_{zz}(\mathbf{0}) \right]_L$, and H_A is the field applied in the z-direction. M is the magnetization,

$$M = \frac{N}{V} g \mu_B \langle J_z \rangle \tag{5.5.8}$$

in each domain, whereas $\langle M \rangle$ is the magnetization averaged over the whole crystal. If the *internal field H_I* and the *demagnetization field H_D* are defined by

$$H_I = H_A - H_D \qquad ; \qquad H_D = N_z \langle M \rangle, \tag{5.5.9}$$

the energy is minimized by the conditions; $H_I = 0$ when $\langle M \rangle < M$, and $\langle M \rangle = M$ when $H_I > 0$. As a function of H_I, the magnetization jumps from zero to its 'saturation' value at $H_I = 0$.

The strong $\mathbf{q}$-dependence of the dipole coupling at small $\mathbf{q}$ is reflected in the energies of the magnetic excitations. In the case of the anisotropic ferromagnet, it is straightforward to deduce that the two-ion coupling of eqn (5.5.1) leads to spin-wave energies determined by

$$
\begin{aligned}
E_T^2(\mathbf{q}) = & \left[A_{\mathbf{0}}(T) + B_{\mathbf{0}}(T) + \langle J_z \rangle \{ \mathcal{J}_{\xi\xi}(\mathbf{0}) - \mathcal{J}_{\zeta\zeta}(\mathbf{q}) \} \right] \\
& \times \left[A_{\mathbf{0}}(T) - B_{\mathbf{0}}(T) + \langle J_z \rangle \{ \mathcal{J}_{\xi\xi}(\mathbf{0}) - \mathcal{J}_{\eta\eta}(\mathbf{q}) \} \right] - \left[\langle J_z \rangle \mathcal{J}_{\eta\zeta}(\mathbf{q}) \right]^2,
\end{aligned}
\tag{5.5.10}
$$

assuming that the magnetization vector in the basal plane is parallel to the ξ-axis, and that $\mathcal{J}_{\eta\zeta}(\mathbf{q}) = \mathcal{J}_{\zeta\eta}(\mathbf{q})$. This result may be obtained by an extension of the procedure used in Section 5.2, most easily from the MF susceptibility (5.2.42). Introducing the above results into this expression, we find, at $\mathbf{q} \equiv \mathbf{0}$,

$$E_T^2(\mathbf{0}) = \left[A_{\mathbf{0}}'(T) + B_{\mathbf{0}}'(T) + g\mu_B \langle M \rangle N_\zeta \right] \left[A_{\mathbf{0}}(T) - B_{\mathbf{0}}(T) + g\mu_B \langle M \rangle N_\eta \right], \tag{5.5.11a}$$

where the H appearing in $A_{\mathbf{0}}(T)$ in (5.2.37) or (5.3.22) is the internal field H_I, and

$$A_{\mathbf{0}}'(T) + B_{\mathbf{0}}'(T) = A_{\mathbf{0}}(T) + B_{\mathbf{0}}(T) + g\mu_B M \big(\big[D_{\xi\xi}(\mathbf{0}) \big]_L - \big[D_{\zeta\zeta}(\mathbf{0}) \big]_L \big).$$
$$(5.5.11b)$$

In comparison with the other anisotropy terms, the lattice-sum contribution to $A_{\mathbf{0}}'(T) + B_{\mathbf{0}}'(T)$ is very small (except in Gd) and may be neglected. Equation (5.5.11) demonstrates that the energy gap at $\mathbf{q} = \mathbf{0}$ depends on the shape of the sample, as was first pointed out by Kittel (1948). The same is the case with all other spin-wave modes in the *magnetostatic region* $q \leq 10/L$, which are the observable states in ferromagnetic resonance experiments. In a neutron-scattering experiment, the volume in reciprocal space enclosed by the resolution function is normally several orders of magnitude larger than the volume of the magnetostatic region. The spin-waves in the long-wavelength limit, detected by inelastic neutron-scattering, therefore emanate from the much larger region where $q \geq 10/L$, but is still much smaller than $2\pi/a$, so that any two-ion coupling, except for the dipole coupling, is the same as that at $\mathbf{q} = \mathbf{0}$. The spin-wave energies in this regime are determined by eqn (5.5.10), when the dipole-coupling tensor in (5.5.7) is transformed to the $(\xi\eta\zeta)$-coordinate system, and are

$$E_T^2(\mathbf{q} \approx \mathbf{0}) = E_T^2(\widetilde{\mathbf{0}}) + 4\pi g\mu_B M \big[\{A_{\mathbf{0}}(T) - B_{\mathbf{0}}(T)\} \cos^2\theta_{\mathbf{q}}$$
$$+ \{A_{\mathbf{0}}'(T) + B_{\mathbf{0}}'(T)\} \sin^2\theta_{\mathbf{q}} \sin^2\phi_{\mathbf{q}} \big], \quad (5.5.12a)$$

where $(\theta_{\mathbf{q}}, \phi_{\mathbf{q}})$ are the polar angles of $\mathbf{q}$ with respect to the c-axis or ζ-axis, and

$$E_T^2(\widetilde{\mathbf{0}}) = \big[A_{\mathbf{0}}'(T) + B_{\mathbf{0}}'(T) \big]\big[A_{\mathbf{0}}(T) - B_{\mathbf{0}}(T) \big]. \qquad (5.5.12b)$$

As long as the magnetization is in the basal-plane, this result is generally valid if $\phi_{\mathbf{q}}$ is redefined to be the angle between the magnetization vector and the projection of $\mathbf{q}$ on the basal-plane. $E_T(\widetilde{\mathbf{0}})$ is the minimum excitation energy, and the corresponding spin waves propagate parallel to the magnetization vector. If $A_{\mathbf{0}}'(T) + B_{\mathbf{0}}'(T)$ is significantly larger than $A_{\mathbf{0}}(T) - B_{\mathbf{0}}(T)$ (in Tb it is an order of magnitude greater at $T = 0$), the maximum value of $E_T(\mathbf{q} \approx \mathbf{0})$ occurs when $\mathbf{q}$ lies in the basal plane perpendicular to the magnetic moments, whereas the spin waves propagating in the c-direction only have an energy slightly greater than $E_T(\widetilde{\mathbf{0}})$. An inelastic neutron-scattering experiment, with the mean value of the scattering vector equal to a reciprocal lattice vector, will sample a whole spectrum of spin waves with energies between the two extremes. The shape of the scattering peak will be dependent on the

form of the resolution function. With a spherical resolution, the scattering will be quite sharply peaked at the intermediate energy of the spin waves propagating in the c-direction, as illustrated in the case of Tb in Fig. 5.8. The calculated sharp peak at about 1.8 meV and the high-energy shoulder are clearly apparent in the experimental measurements of Houmann *et al.* (1975a). In the measurements of Bjerrum Møller and Mackintosh (1979), on the other hand, the resolution function was such that the modes propagating in the basal plane perpendicular to the magnetization were most heavily weighted, so that the predominant peak occurs at about 2.0 meV. In Ho, the effect of the dipole interaction on the long-wavelength spin waves is even more pronounced. This is an example of the opposite extreme, where $A'_{\mathbf{0}}(T) + B'_{\mathbf{0}}(T)$ is much smaller than $A_{\mathbf{0}}(T) - B_{\mathbf{0}}(T)$, so that the maximum value of $E_T(\mathbf{q} \approx \mathbf{0})$ occurs when $\mathbf{q}$ lies along the c-direction. As illustrated in Fig. 5.9, the dipolar splitting in this case is sufficiently great that the neutron scattering at $\mathbf{q} \approx \mathbf{0}$ can be resolved into two peaks.

Another consequence of the strong directional dependence of the dipolar contributions to the spin-wave energies is found in the behaviour of the coupled magneto-acoustic sound waves, discussed in the previous section. The region in $\mathbf{q}$-space sampled in ultrasonic measurements (with frequencies in the MHz regime) is just that in which eqn (5.5.12)
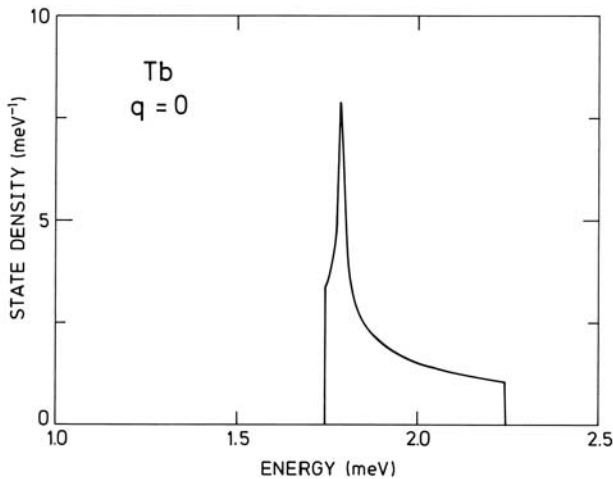

Fig. 5.8.   The state density of the long-wavelength spin-wave mode $E_T(\mathbf{q} \approx \mathbf{0})$ in Tb at 4 K, calculated from eqn (5.5.12), taking into account the splitting of the dispersion relations by the dipole–dipole interaction. The sharp peak is due to the branch in the c-direction.

applies. If **q** is parallel to the magnetization, the spin-wave energies
are unchanged from the values deduced in Sections 5.2–4, provided that
the lattice-sum contribution is included in the axial anisotropy term
(5.5.11b), and eqn (5.4.38) is still valid. On the other hand, when **q** is
in the basal-plane and perpendicular to the magnetization, the ultrasonic

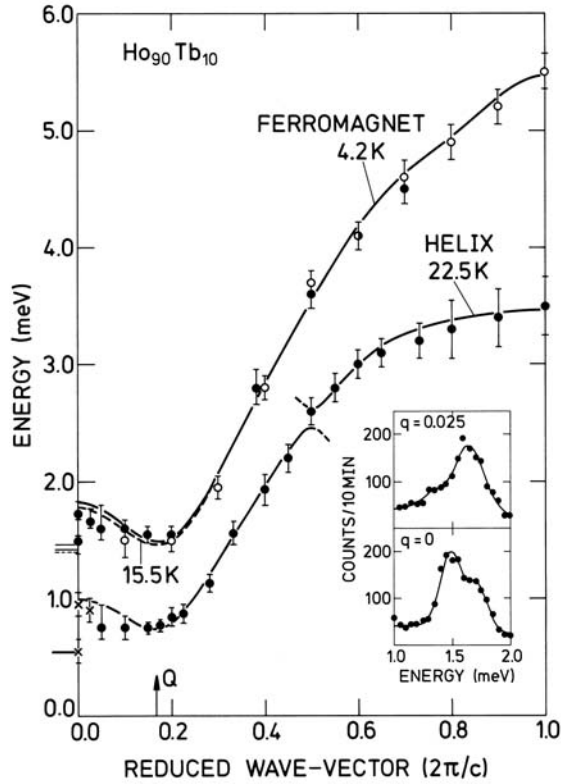**Fig. 5.9.** Dispersion relations, in the double-zone representation, for
magnetic excitations propagating in the c-direction of $Ho_{90}Tb_{10}$ in the
ferromagnetic phase (upper branch), and the bunched helical structure
(lower branch). The full and dashed lines for the ferromagnetic phase
show the theoretical dispersion relations at 4 K and 16 K respectively, and
the open and filled symbols are the corresponding experimental results.
The calculated long-wavelength energies in the basal plane are shown to
the left of the ordinate axis and the discontinuity, which is due to the
dipole–dipole interaction, is clearly manifested in the neutron-scattering
spectra in the inset. This discontinuity also appears in the helical phase,
and the bunching causes an energy gap on the ALH face of the Brillouin
zone, which is not resolved in these measurements.

velocities are determined by

$$\frac{c_{cc}^*}{c_{66}} = 1 - \frac{\Lambda_\gamma}{A_{\mathbf{0}}(T) - B_{\mathbf{0}}(T) + 4\pi g\mu_B M} \quad ; \quad \mathbf{q} \perp \langle \mathbf{J} \rangle. \qquad (5.5.13)$$

This modification means that only the velocity of those magneto-acoustic modes which propagate parallel to the magnetization vanishes at the critical field $H_I = H_c$ where, according to (5.4.15), $A_{\mathbf{0}}(T) - B_{\mathbf{0}}(T) = \Lambda_\gamma$, whereas the velocity of the modes propagating in the basal-plane perpendicular to the field remains non-zero. This difference in the velocities of the ultrasonic modes was very clearly manifested in the ultrasonic experiment on Tb discussed in Section 5.4 (Jensen and Palmer 1979). This example shows that the dipolar coupling is able to lift the degeneracy in the velocities of two transverse sound-waves which are related to each other by an interchange of the directions of the wave-vector and the polarization vector. The same effect may be produced by the torque exerted on the moments when the local magnetic anisotropy axes are rotated by the transverse phonons relative to the direction of an external magnetic field. As discussed by Melcher (1972) and Dohm and Fulde (1975) the influence of this mechanism on the sound velocities may be derived from the principle that the total system has to be *rotationally invariant*. Their theory has been extended by Jensen (1988b), who finds that the dipolar-coupling contribution strongly dominates in a ferromagnet, but that the importance of the two mechanisms may be comparable in paramagnets.

5.5.2 General two-ion interactions

The two-ion couplings described by eqn (5.5.1) only involve the dipolar moments of the $4f$ electrons. A more general two-ion Hamiltonian is

$$\begin{aligned}
\mathcal{H}_{\mathrm{JJ}} = -\frac{1}{2} \sum_{ij} \sum_{l+l': \mathrm{even}} \sum_{mm'} &\big[K_{ll'}^{mm'}(ij) \widetilde{O}_{lm}(\mathbf{J}_i) \widetilde{O}_{l'm'}(\mathbf{J}_j) \\
&+ (-1)^{m+m'} \{ K_{ll'}^{mm'}(ij) \}^* \widetilde{O}_{l\,-m}(\mathbf{J}_i) \widetilde{O}_{l'\,-m'}(\mathbf{J}_j) \big],
\end{aligned}$$

$$(5.5.14)$$

expressed in terms of the *Racah operators* or *tensor operators* $\widetilde{O}_{lm}(\mathbf{J}_i)$ introduced in Section 1.4, rather than the Stevens operators. Tables of these operators and a discussion of their properties may be found in Buckmaster *et al.* (1972) and in Lindgård and Danielsen (1974). Here we neglect the possible effects of the *polar* tensors, which vanish for the isolated ions. In principle, these polar tensors may be non-zero in the hcp metals, because the surroundings lack inversion symmetry, but they occur only because of odd-parity configuration-mixing of the $4f$ wavefunctions, which should be insignificant for the ground-state multiplet.

This leaves only the *axial* tensors, i.e. magnetic multipoles of odd rank and electric multipoles of even rank. Time reversal of these tensors effects the transformation $c\widetilde{O}_{lm} \to c^*(-1)^{l+m}\widetilde{O}_{l\,-m}$, whereas Hermitian conjugation gives $(c\widetilde{O}_{lm})^\dagger = c^*(-1)^m\widetilde{O}_{l\,-m}$. The requirement that $\mathcal{H}_{\mathrm{JJ}}$ should be invariant under both transformations allows only those terms in eqn (5.5.14) for which $l + l'$ is even. The violation of time-reversal symmetry which occurs when the system is magnetically ordered implies that $\mathcal{H}_{\mathrm{JJ}}$ should be supplemented by interactions proportional to $\langle\widetilde{O}_{\lambda\mu}\rangle\widetilde{O}_{lm}(\mathbf{J}_i)\widetilde{O}_{l'm'}(\mathbf{J}_j)$, satisfying the condition that $\lambda + l + l'$ is even. An obvious example is magnetoelastic contributions to the Hamiltonian such as eqn (5.4.5). The tensor operators in (5.5.14) emanate from localized $4f$ wavefunctions with the orbital quantum number $l_{\mathrm{f}} = 3$, which puts the further restriction on the phenomenological expansion of $\mathcal{H}_{\mathrm{JJ}}$ that l and l' cannot be larger than $2l_{\mathrm{f}}+1 = 7$, as the operator-equivalents of higher rank than this vanish identically.

In the rare earth metals, several different mechanisms may give rise to such anisotropic two-ion couplings, and these have been listed by, for instance, Wolf (1971) and Jensen *et al.* (1975). We have already considered the magnetostatic coupling of lowest rank in the magnetic multipole expansion, namely the classical magnetic dipole–dipole interaction. This is of importance only because of its long range. The higher order magnetostatic couplings are of shorter range ($\propto (1/r)^{l+l'+1}$) and have negligible effects. The electrostatic Coulomb interaction gives rise to terms in (5.5.14) in which both l and l' are even. The single-ion contributions ($l' = 0$) are of decisive importance, when $L \neq 0$, but even the lowest-order electrostatic two-ion term, which contributes to the quadrupole–quadrupole interactions, is so small that it may be neglected.

The overlap between the $4f$ wavefunctions of neighbouring ions is so weak that it cannot generate any two-ion coupling of significance. The dominant terms in the two-ion Hamiltonian $\mathcal{H}_{\mathrm{JJ}}$ therefore arise indirectly via the propagation of the conduction electrons. We have already mentioned in Section 1.4 the most important of these, due to the exchange interaction between the band electrons and the $4f$ electrons, and it will be discussed in more detail in Section 5.7. In the simplest approximation, the indirect exchange is invariant with respect to a uniform rotation of the angular momenta, i.e. this RKKY interaction is *isotropic*. However, the neglect of the contribution of the orbital moment in the scattering process is not generally justified. If L is non-zero, the orbital state of the $4f$ electrons may change in an exchange-scattering process, if the conduction electron is scattered into a state with a different orbital momentum relative to the ion. The leading-order corrections to the isotropic RKKY interaction due to such processes have been

considered by Kaplan and Lyons (1963) and Kasuya and Lyons (1966). In order to obtain an estimate of the importance of the corrections, they assumed plane-wave states for the conduction electrons, expanded in a series of spherical Bessel functions centred at the ion. These calculations indicated anisotropic two-ion couplings with a magnitude of the order of 10% of the isotropic coupling, or greater (Specht 1967). As discussed in Section 1.3, the free-electron model does not provide a very satisfactory description of the conduction electrons in the rare earths. It is particularly inadequate when orbital effects are involved, since the expansion of the plane-wave states clearly underestimates the ($l = 2$)-character of the d-like band-electrons, which dominates the exchange interaction in the ($L = 0$)-case of Gd (Lindgård *et al.* 1975). When L is non-zero, the *Kaplan–Lyons* terms may be of comparable importance to the RKKY interaction in the rare earth metals. The relativistic modification of the band states, due to the spin–orbit coupling, may enhance the orbital effects and also lead to anisotropic interactions in Gd. In addition to the exchange, the direct Coulomb interaction between the $4f$ and the band electrons may contribute to eqn (5.5.14), with terms in which l and l' are both even. This coupling mechanism, via the conduction electrons, is probably more important for this kind of term than the direct electrostatic contribution mentioned above.

The RKKY interaction is derived on the assumption that the $4f$ electrons are localized in the core, and that their mixing with the conduction electrons is exclusively due to the exchange. However, the Coulomb interaction may lead to a slight hybridization of the localized $4f$ states with the band states. In recent years, Cooper and his co-workers (Cooper *et al.* 1985; Wills and Cooper 1987) have analysed the consequences of a weak hybridization between an ion with one or two f electrons and the band electrons, with special reference to the magnetic behaviour of Ce compounds and the actinides. They find that the magnetic two-ion coupling becomes highly anisotropic in the Ce compounds. Although Ce is the rare earth element in which the strongest hybridization effects would be expected to occur, these results and the analysis of Kaplan and Lyons (1963) suggest that the presence of anisotropic two-ion couplings should be a common feature in rare earth metals with orbital angular momentum on the ion.

As is clear from the above discussion, an analysis from first principles cannot at present give a reliable estimate of the relative magnitude of the Heisenberg exchange interaction and the various possible anisotropic two-ion couplings in the rare earth metals. We cannot a priori exclude any terms of the form given by eqn (5.5.14). In order to arrive at such an estimate, it is necessary to calculate the consequences of the anisotropic two-ion terms and compare the predictions with exper-

imental observations. In the case of the nearly saturated ferromagnet, it is straightforward to take into account the effects of $\mathcal{H}_{JJ}$ on the ground-state properties and the spin-waves. The Racah operators, defined with reference to the (ξ, η, ζ)-coordinate system, may be expanded in terms of the spin deviation operators. When the moments in the basal-plane $(\theta = \pi/2)$ are close to their saturation value $(\langle J_z \rangle \simeq J)$,

$$\langle \widetilde{O}_{lm} \rangle \simeq \left(\frac{4\pi}{2l+1} \right)^{1/2} J^{(l)} Y_{lm}(\theta = \frac{\pi}{2}, \phi) = J^{(l)} \Gamma_{lm} \, e^{im\phi}, \qquad (5.5.15a)$$

where

$$\Gamma_{lm} = \begin{cases} (-1)^{(l+m)/2} \dfrac{[(l+m)!(l-m)!]^{1/2}}{(l+m)!!(l-m)!!} & , \; l+m \text{ even} \\[2mm] \qquad\qquad 0 \qquad , \qquad l+m \text{ odd.} \end{cases} \qquad (5.5.15b)$$

Utilizing the equivalence between the Racah operators and the spherical harmonics, and the connection between the spin-wave energies and the angular derivatives of the expectation values (which leads to the relation (5.3.14)), we have to first order in $1/J$ (Jensen *et al.* 1975):

$$\widetilde{O}_{lm}(\mathbf{J}_i) =$$
$$\left(1 - \frac{m}{\sqrt{2J}}(a_i^+ - a_i) - \frac{l(l+1)}{2J} a_i^+ a_i - \frac{l(l+1) - 2m^2}{4J}(a_i^+ a_i^+ + a_i a_i) \right)$$
$$\times J^{(l)} \Gamma_{lm} e^{im\phi}, \qquad (5.5.16a)$$

if $l + m$ is even, and if $l + m$ is odd

$$\widetilde{O}_{lm}(\mathbf{J}_i) =$$
$$[(l+1)^2 - m^2]^{1/2} \left(\frac{1}{\sqrt{2J}}(a_i^+ + a_i) - \frac{m}{2J}(a_i^+ a_i^+ - a_i a_i) \right) J^{(l)} \Gamma_{l+1\,m} e^{im\phi}.$$
$$(5.5.16b)$$

Introducing these expressions into the two-ion Hamiltonian, we may derive the spin-wave energies, to leading order in $1/J$. The number of terms in eqn (5.5.14) which contribute to the excitation energies, in this order, may be reduced by the symmetry elements of the lattice which leave the **q**-vector unchanged. In the simplest case, where **q** is along the c-axis, the three-fold symmetry about this axis plus the mirror-plane perpendicular to the ξ-axis (i.e. the a-axis) ensure that only terms with $m + m' = 3p$, where p is an integer, contribute, and that their contribution is proportional to $\cos(3p\phi)$. The terms in which p is an odd integer couple the acoustic and optical magnons, but they do not

lift the degeneracy of the modes at A on the Brillouin-zone boundary of Fig 1.4. When $\mathbf{q}$ is parallel to the c-axis, a direct calculation of the spin-wave energies (Jensen *et al.* 1975) shows that the two-ion terms in $\mathcal{H}_{\mathrm{JJ}}$ lead to the following modifications of the earlier results (5.2.38) and (5.3.22):

(i) The two-ion anisotropy may contribute to the parameters $A_{\mathbf{q}}(T) \pm B_{\mathbf{q}}(T)$ at zero wave-vector.

(ii) $B_{\mathbf{q}}(T)$ becomes dependent on $\mathbf{q}$ to leading order in $1/J$.

(iii) The $\mathbf{q}$-dependent parts of $A_{\mathbf{q}}(T) \pm B_{\mathbf{q}}(T)$ may change when the direction of magnetization is changed.

There are no direct ways of separating the single- and two-ion contributions to the energy gap at zero wave-vector. However, a strong $\mathbf{q}$-dependence of $B_{\mathbf{q}}(T)$ is only possible if the two-ion Hamiltonian is anisotropic. One way to determine $B_{\mathbf{q}}(T)$ is to utilize the dependence of the neutron cross-section on this parameter, given by eqn (5.2.41). This method requires accurate intensity measurements and is not straightforward. The other possibility is to measure the field dependence of the spin-wave energies since, from (5.2.38) or (5.3.22),

$$\alpha_{\mathbf{q}}(T) \equiv \partial E_{\mathbf{q}}^2(T)/\partial(g\mu_B H) \simeq 2A_{\mathbf{q}}(T), \qquad (5.5.17)$$

when the field is parallel to the magnetization. This relation is only true to first order in $1/J$, and corrections have to be made for the influence of any field-dependent changes of the correlation functions σ and $\eta_{\pm}$. Both $A_{\mathbf{q}}(T)$ and $B_{\mathbf{q}}(T)$ may be determined from the energies and initial slopes, since

$$A_{\mathbf{q}}(T) \pm B_{\mathbf{q}}(T) \simeq \tfrac{1}{2}\alpha_{\mathbf{q}}(T) \pm \tfrac{1}{2}[\alpha_{\mathbf{q}}^2(T) - 4E_{\mathbf{q}}^2(T)]^{\frac{1}{2}}. \qquad (5.5.18)$$

This method was used by Jensen *et al.* (1975) for a comprehensive study ot the two-ion anisotropy in Tb. The values of $A_{\mathbf{q}}(T)$ and $B_{\mathbf{q}}(T)$, deduced from eqn (5.5.18), were parametrized in various ways, and clearly the best least-squares fit was obtained with expressions of the form

$$
\begin{aligned}
(A_{\mathbf{q}} + B_{\mathbf{q}}) - (A_{\mathbf{0}} + B_{\mathbf{0}}) &= \mathcal{I}(\mathbf{q}) + \mathcal{K}(\mathbf{q}) - \mathcal{C}(\mathbf{q})\cos 6\phi \\
(A_{\mathbf{q}} - B_{\mathbf{q}}) - (A_{\mathbf{0}} - B_{\mathbf{0}}) &= \mathcal{I}(\mathbf{q}) - \mathcal{K}(\mathbf{q}) - \mathcal{D}(\mathbf{q})\cos 6\phi,
\end{aligned}
\qquad (5.5.19)
$$

where $A_{\mathbf{0}} \pm B_{\mathbf{0}}$ were taken from the simultaneous measurements of the magnetic anisotropy at $\mathbf{q} = \mathbf{0}$, discussed in the previous section. The low-temperature isotropic coupling $\mathcal{I}(\mathbf{q})$, which in the absence of anisotropy would just be $J[\mathcal{J}(\mathbf{0}) - \mathcal{J}(\mathbf{q})]$, and the ϕ-independent two-ion anisotropy $\mathcal{K}(\mathbf{q})$ are shown in Fig. 5.10. The ϕ-dependent axial
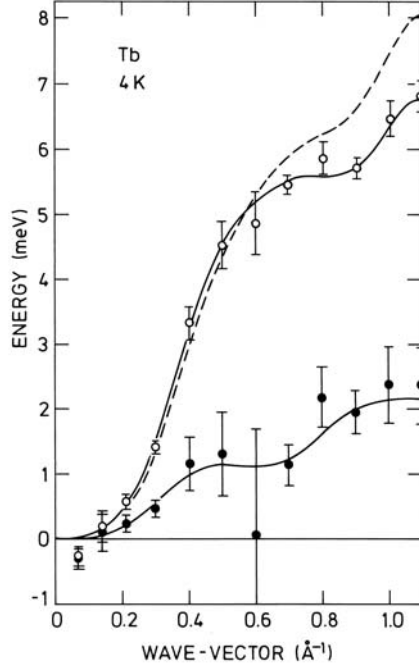
Fig. 5.10. Isotropic and anisotropic two-ion coupling parameters $\mathcal{I}(\mathbf{q})$ (upper curve) and $\mathcal{K}(\mathbf{q})$ (lower curve) for Tb at 4 K, deduced from the field dependence of the spin-wave energies. The former is closely related to $J[\mathcal{J}(\mathbf{0}) - \mathcal{J}(\mathbf{q})]$, an estimate of which is indicated by the dashed line. The magnon–phonon interaction causes relatively large uncertainties at intermediate wave-vectors.

anisotropy $\mathcal{C}(\mathbf{q})$ is about the same magnitude as $\mathcal{K}(\mathbf{q})$, while $\mathcal{D}(\mathbf{q})$ is very small. The ϕ-dependent anisotropy is detected very clearly in the experiments, since it gives rise to a change in the dispersion $E_{\mathbf{q}}(T)$, when the moments are rotated from the the easy to the hard planar direction. $\mathcal{C}(\mathbf{q})$ is the $\mathbf{q}$-dependent generalization of the ϕ-dependent anisotropy ΔM in $A_{\mathbf{0}} + B_{\mathbf{0}}$, introduced in the previous section, and $\Delta M \approx -\langle \mathcal{C}(\mathbf{q}) \rangle_{\mathbf{q}}$.

As mentioned in Section 5.4.1, the corrections to the field dependence of the magnon energies in (5.5.17) were included in an effective fashion, neglecting changes due to the rotation of the moments and assuming $\eta_- \simeq 1/\eta_+ \simeq \{1-b(T=0)\}\sigma^{-k}$, where k may be estimated to be about 0.3. The renormalization effects are thus taken as proportional to σ raised to a power which depends on the term considered. We estimate that the effects neglected in this approach only introduce corrections of the order of the experimental uncertainties. The two-ion coupling

parameters decrease with increasing temperature or decreasing mag-
netization. The three anisotropy component all decrease very rapidly,
roughly proportionally to σ^{15} (like ΔM), which means that they are only
important at low temperatures and may be neglected above about $150\,\mathrm{K}$.
The strong temperature dependence of the anisotropic components indi-
cates, according to the Callen–Callen theory, that higher-rank couplings
make the dominant contribution. The lowest-order term in eqn (5.5.14)
which contributes to $\mathcal{C}(\mathbf{q})$ involves K_{44}^{33}, and it should renormalize ap-
proximately as σ^{19}. The renormalization is observed to be $\mathbf{q}$-dependent
for all the parameters, being slower at larger wave-vectors, and it lies in
the range σ^2-$\sigma^{0.1}$ for $\mathcal{I}(\mathbf{q})$. In Tb, $\mathcal{I}(\mathbf{q})$ may include higher-rank con-
tributions besides the RKKY-exchange term, but the way in which it
renormalizes resembles quite closely the behaviour observed in Gd and
shown in Fig. 5.1. A $\mathbf{q}$-dependent renormalization may partially be ac-
counted for, in the self-consistent RPA theory, by the $\mathbf{k}$-sum terms in
(5.2.38).

When $\mathbf{q}$ is not along the c-axis, there are other ways in which the
presence of two-ion anisotropy may be detected in the ferromagnetic
excitation spectrum:

    (iv) Spin-wave energy gaps may appear at the boundaries of
           the Brillouin zone.

The isotropic two-ion coupling alone does not lead to energy gaps at
these boundaries, whereas anisotropic two-ion couplings may lift those
degeneracies which are not dictated by symmetry. In fact, the first in-
dication of the presence of two-ion anisotropy in the rare earth metals,
other than the classical magnetic-dipolar interaction, was the splitting
shown in Fig. 5.2 along the KH edge of the Brillouin zone in the ferro-
magnetic phase of Tb (Lindgård and Houmann 1971). Finally, we have
the related effect:

    (v) The spin-wave energies, at a particular $\mathbf{q}$, in domains with
         different angles between the $\mathbf{q}$-vector and the magnetiza-
         tion vectors, need not be equal if two-ion anisotropy is
         important.

In a single domain, the two-ion anisotropy forces may lift the 'accidental'
degeneracies between spin waves at $\mathbf{q}$-vectors which are equivalent in the
paramagnetic phase, but which are no longer equivalent in the Brillouin
zone of the ferromagnet. This manifestation of the two-ion anisotropy
has not yet been subjected to experimental investigation, but it may
provide a useful supplement to studies of the $\mathbf{q}$-dependence of $B_{\mathbf{q}}(T)$.

As we have seen, the expectation values $\langle \widetilde{O}_{lm} \rangle$ are approximately
proportional to $\sigma^{l(l+1)/2}$, if the extra modification due to the elliptical
polarization of the spin-waves is neglected. This means that the impor-
tance of the higher-rank couplings declines relatively rapidly with tem-

perature. The effects of these interactions on the ground state and the spin waves are therefore most pronounced in the low-temperature limit, whereas the behaviour of the system at high temperatures which, in the heavy rare earths, includes the critical region around the phase transition between the ordered and paramagnetic phases, is dominated by the coupling between the dipolar moments, and the single-ion quadrupole interaction, i.e. by the terms in eqn (5.5.14) with $l + l' = 2$.

5.6 Binary rare earth alloys

The great similarity in the chemical properties of the different rare earth metals allows almost complete mutual solubility. It is therefore possible to fabricate rare earth alloys with nearly uniform electronic properties, but containing ions with disparate magnetic properties, distributed randomly on a single lattice. By a judicious choice of the constituents, the macroscopic magnetic properties, such as the ordering temperatures and the anisotropy parameters, may be continuously adjusted as desired. From a macroscopic viewpoint, such an alloy resembles a uniform and homogeneous crystal, with magnetic properties reflecting the characteristics and concentrations of the constituents. The spectrum of magnetic excitations also displays such average behaviour (Larsen *et al.* 1986), but in addition, there are effects which depend explicitly on the disparity between the different sites.

We restrict ourselves to binary alloys, which are described by the Hamiltonian,

$$\mathcal{H} = \sum_i \left\{ c_i \mathcal{H}_1(\mathbf{J}_{1i}) + (1 - c_i)\mathcal{H}_2(\mathbf{J}_{2i}) \right\}$$

$$- \frac{1}{2} \sum_{i \neq j} \mathcal{J}(ij) \left\{ c_i \mathbf{J}_{1i} + \gamma(ij)(1 - c_i)\mathbf{J}_{2i} \right\} \cdot \left\{ (c_j \mathbf{J}_{1j} + \gamma(ij)(1 - c_j)\mathbf{J}_{2j} \right\},$$

$$(5.6.1)$$

where c_i is a variable which is 1 if the ion on site i is of type 1, and 0 if the ith ion is of type 2. The configurational average of c_i is the atomic concentration of the type-1 ions, $\langle c_i \rangle_{\mathrm{cf}} = c$. In addition to the simplifications made earlier in the Hamiltonian, we shall assume that $\gamma(ij)$ is a constant γ, independent of i and j. This approximation is consistent with a model in which the indirect exchange is assumed to dominate the two-ion coupling, in which case

$$\gamma(ij) = \gamma = (g_2 - 1)/(g_1 - 1), \qquad (5.6.2)$$

where the indices 1 and 2 refer to the two types of ions with angular momenta J_1 and J_2.

In order to derive the excitation spectrum of the alloy system, we first make the assumption that the surroundings of each ion are

so close to the average that individual variations can be neglected. Thus we replace the actual MF Hamiltonian of the ith ion with the configurationally-averaged MF Hamiltonian and, considering a type 1 ion ($c_i = 1$), obtain

$$\mathcal{H}_{\mathrm{MF}}(i) \simeq \langle \mathcal{H}_{\mathrm{MF}}(i) \rangle_{\mathrm{cf}} =$$
$$\mathcal{H}_1(\mathbf{J}_{1i}) - (\mathbf{J}_{1i} - \tfrac{1}{2}\langle \mathbf{J}_{1i} \rangle) \cdot \sum_j \mathcal{J}(ij)\{c\langle \mathbf{J}_{1j} \rangle + (1-c)\,\gamma\langle \mathbf{J}_{2j} \rangle\}. \quad (5.6.3)$$

From this equation, and the similar one for $c_i = 0$, we may determine the MF values of the two moments $\langle \mathbf{J}_1 \rangle$ and $\langle \mathbf{J}_2 \rangle$, and the corresponding susceptibilities $\overline{\overline{\chi}}_1^o(\omega)$ and $\overline{\overline{\chi}}_2^o(\omega)$. For a paramagnetic or ferromagnetic system these quantities are all site-independent, in the present approximation. We note that (5.6.3) is correct in the case of a paramagnet, as possible environmental variations on the individual ions are already neglected in the starting Hamiltonian. The next step is the introduction of a 2×2 matrix of susceptibility tensors $\overline{\overline{\chi}}_{rs}(ij,\omega)$, where the elements with $r = 1$ or 2 are defined in terms of $c_i\mathbf{J}_{1i}$ or $(1-c_i)\mathbf{J}_{2i}$ respectively, and $s = 1$ or 2 similarly specifies the other component. We may then write the RPA equation (3.5.7):

$$\overline{\overline{\chi}}_{rs}(ij,\omega) = \overline{\overline{\chi}}_r(i,\omega)\Big(\delta_{rs}\delta_{ij} + \sum_{j'}\sum_{s'} \gamma_{rs'}\mathcal{J}(ij')\overline{\overline{\chi}}_{s's}(j'j,\omega)\Big), \quad (5.6.4a)$$

where

$$\overline{\overline{\chi}}_1(i,\omega) = c_i\overline{\overline{\chi}}_1^o(\omega) \qquad ; \qquad \overline{\overline{\chi}}_2(i,\omega) = (1-c_i)\overline{\overline{\chi}}_2^o(\omega), \qquad (5.6.4b)$$

recalling that $c_i^2 = c_i$ (= 0 or 1), and defining $\mathcal{J}_{rs}(ij) = \gamma_{rs}\mathcal{J}(ij)$, with

$$\gamma_{11} = 1 \qquad ; \qquad \gamma_{12} = \gamma_{21} = \gamma \qquad ; \qquad \gamma_{22} = \gamma^2. \qquad (5.6.4c)$$

In spite of the great simplification introduced through the random-phase approximation, the RPA equation for the alloy is still very complicated, because $\overline{\overline{\chi}}_r(i,\omega)$ depends on the randomness, and it cannot be solved without making quite drastic approximations. The simplest result is obtained by neglecting completely the site-dependence of $\overline{\overline{\chi}}_r(i,\omega)$, and consequently replacing c_i in (5.6.4b) by its average value c. This procedure corresponds to the replacement of each individual angular momentum $\mathbf{J}_{ri}$ by the average $c\mathbf{J}_{1i} + (1-c)\mathbf{J}_{2i}$, and it is known as the *virtual crystal approximation* (VCA). In this approximation, (5.6.4) may be solved straightforwardly after a Fourier transformation, and defining the *T-matrices* according to

$$\overline{\overline{\chi}}_{rs}(\mathbf{q},\omega) = \overline{\overline{\chi}}_r(\omega)\delta_{rs} + \overline{\overline{\chi}}_r(\omega)\overline{\overline{T}}_{rs}(\mathbf{q},\omega)\overline{\overline{\chi}}_s(\omega), \qquad (5.6.5a)$$

where

$$\overline{\overline{\chi}}_1(\omega) = c\overline{\overline{\chi}}_1^{\,o}(\omega) \quad \text{and} \quad \overline{\overline{\chi}}_2(\omega) = (1-c)\overline{\overline{\chi}}_2^{\,o}(\omega), \qquad (5.6.5b)$$

we find that these T-matrices are given by

$$\overline{\overline{T}}_{rs}(\mathbf{q},\omega) = \gamma_{rs}\mathcal{J}(\mathbf{q})\,\overline{\overline{D}}(\mathbf{q},\omega)^{-1}, \qquad (5.6.6a)$$

with

$$\overline{\overline{D}}(\mathbf{q},\omega) = 1 - \left\{ c\overline{\overline{\chi}}_1^{\,o}(\omega) + (1-c)\,\gamma^2\,\overline{\overline{\chi}}_2^{\,o}(\omega) \right\} \mathcal{J}(\mathbf{q}). \qquad (5.6.6b)$$

This result is simplified by the assumption, (5.6.2) or (5.6.4c), that $\mathcal{J}_{12}(\mathbf{q})$ is the geometric mean of $\mathcal{J}_{11}(\mathbf{q})$ and $\mathcal{J}_{22}(\mathbf{q})$. In this and in more complex cases, the introduction of the T-matrices in (5.6.5) makes it somewhat easier to handle the RPA equations. The configurationally-averaged susceptibility is $\overline{\overline{\chi}}(\mathbf{q},\omega) = \sum_{rs} \overline{\overline{\chi}}_{rs}(\mathbf{q},\omega)$, but this does not directly determine the inelastic neutron-scattering cross-section. We must take into account the difference in the form factor $\{\frac{1}{2}gF(\boldsymbol{\kappa})\}$ for the two kinds of ions, in the differential cross-section (4.2.1). At small scattering vectors, $F(\boldsymbol{\kappa})$ is generally close to one and the most important variation is due to the g-factor. In this case, the inelastic scattering is proportional to the susceptibility:

$$g^2\overline{\overline{\chi}}(\mathbf{q},\omega) \equiv \sum_{rs} g_r g_s \overline{\overline{\chi}}_{rs}(\mathbf{q},\omega)$$
$$= g_1^2 c\,\overline{\overline{\chi}}_1^{\,o}(\omega) + g_2^2(1-c)\,\overline{\overline{\chi}}_2^{\,o}(\omega) + \overline{\overline{\chi}}_3(\omega)\mathcal{J}(\mathbf{q})\,\overline{\overline{D}}(\mathbf{q},\omega)^{-1}\overline{\overline{\chi}}_3(\omega), \qquad (5.6.7a)$$

with

$$\overline{\overline{\chi}}_3(\omega) = g_1 c\,\overline{\overline{\chi}}_1^{\,o}(\omega) + g_2(1-c)\,\gamma\,\overline{\overline{\chi}}_2^{\,o}(\omega). \qquad (5.6.7b)$$

If $\overline{\overline{\chi}}_r(i,\omega)$ only depends on c_i, as assumed in (5.6.4b), the RPA equation (5.6.4a) is equivalent to that describing the phonons in a crystal with *diagonal disorder*, in the harmonic approximation. The possible variation of the molecular field (or other external fields) from site to site, which is neglected in (5.6.3), introduces *off-diagonal disorder*. If such off-diagonal disorder is neglected, the main effects of the randomness, in 3-dimensional systems, are very well described in the *coherent potential approximation* (CPA) (Taylor 1967; Soven 1967; Elliott *et al.* 1974; Lage and Stinchcombe 1977; Whitelaw 1981). In the CPA, the different types of ion are treated separately, but they are assumed to interact with a common surrounding medium. This configurationally-averaged medium, i.e. the *effective medium*, is established in a self-consistent fashion. The method may be described in a relatively simple manner, following the

approach of Jensen (1984). We first consider the case where $\overline{\overline{\chi}}_2^o(\omega)$ vanishes identically, corresponding to the presence of non-magnetic impurities with a concentration $1 - c$. The RPA equation (5.6.4a) may then be solved formally by iteration:

$$
\overline{\overline{\chi}}(ij, \omega) = c_i \overline{\overline{\chi}}^o(\omega) \delta_{ij} + c_i \overline{\overline{\chi}}^o(\omega) \mathcal{J}(ij) c_j \overline{\overline{\chi}}^o(\omega)
$$
$$
+ \sum_{j'} c_i \overline{\overline{\chi}}^o(\omega) \mathcal{J}(ij') c_{j'} \overline{\overline{\chi}}^o(\omega) \mathcal{J}(j'j) c_j \overline{\overline{\chi}}^o(\omega) + \cdots .
$$
$$
(5.6.8)
$$

The VCA result is obtained by assuming $\langle c_{j'}^n \rangle_{\mathrm{cf}} = c^n$, which is incorrect since $\langle c_{j'}^n \rangle_{\mathrm{cf}} = \langle c_{j'} \rangle_{\mathrm{cf}} = c$. Consequently, the VCA leads to errors already in the fourth term in this expansion, or in the third term if $i = j$, even though $\mathcal{J}(ii)$ is zero. In order to ameliorate these deficiencies, we first consider the series for $\overline{\overline{\chi}}(ii, \omega)$, where $i = j$. The different terms in this series may be collected in groups according to how many times the ith site appears, which allows us to write

$$
\overline{\overline{\chi}}(ii, \omega) = c_i \Big[\overline{\overline{\chi}}^o(\omega) + \overline{\overline{\chi}}^o(\omega) \overline{\overline{K}}(i, \omega) \overline{\overline{\chi}}^o(\omega)
$$
$$
+ \overline{\overline{\chi}}^o(\omega) \overline{\overline{K}}(i, \omega) \overline{\overline{\chi}}^o(\omega) \overline{\overline{K}}(i, \omega) \overline{\overline{\chi}}^o(\omega) + \cdots \Big]
$$
$$
= c_i \big\{ 1 - \overline{\overline{\chi}}^o(\omega) \overline{\overline{K}}(i, \omega) \big\}^{-1} \overline{\overline{\chi}}^o(\omega), \qquad (5.6.9)
$$

where $\overline{\overline{K}}(i, \omega)$ is the infinite sum of all the 'interaction chains' involving the ith site only at the ends, but nowhere in between. A similar rearrangement of the terms in the general RPA series leads to

$$
\overline{\overline{\chi}}(ij, \omega) = \overline{\overline{\chi}}(ii, \omega) \delta_{ij} + \overline{\overline{\chi}}(ii, \omega) \overline{\overline{T}}(ij, \omega) \overline{\overline{\chi}}(jj, \omega), \qquad (5.6.10)
$$

where $\overline{\overline{T}}(ij, \omega)$ is only non-zero if $i \neq j$ and, by exclusion, is the sum of all the interaction chains in which the ith site appears only at the beginning, and the jth site only at the end of the chains. Introducing this expression in the RPA equation (5.6.4), we may write it

$$
\overline{\overline{\chi}}(ij, \omega) =
$$
$$
c_i \overline{\overline{\chi}}^o(\omega) \Big[\delta_{ij} + \mathcal{J}(ij) \overline{\overline{\chi}}(jj, \omega) + \sum_{j'} \mathcal{J}(ij') \overline{\overline{\chi}}(j'j', \omega) \overline{\overline{T}}(j'j, \omega) \overline{\overline{\chi}}(jj, \omega) \Big].
$$

From (5.6.9), we have $\overline{\overline{\chi}}^o(\omega)^{-1} \overline{\overline{\chi}}(ii, \omega) = c_i \{ 1 + \overline{\overline{K}}(i, \omega) \overline{\overline{\chi}}(ii, \omega) \}$, and a comparison of this equation for $\overline{\overline{\chi}}(ij, \omega)$ with (5.6.10), leads to the result:

$$
\delta_{ij} + \mathcal{J}(ij) \overline{\overline{\chi}}(jj, \omega) + \sum_{j'} \mathcal{J}(ij') \overline{\overline{\chi}}(j'j', \omega) \overline{\overline{T}}(j'j, \omega) \overline{\overline{\chi}}(jj, \omega)
$$
$$
= \{ 1 + \overline{\overline{K}}(i, \omega) \overline{\overline{\chi}}(ii, \omega) \} \{ \delta_{ij} + \overline{\overline{T}}(ij, \omega) \overline{\overline{\chi}}(jj, \omega) \}, \quad (5.6.11)
$$

leaving out the common factor c_i. Although this means that $\overline{\overline{K}}(i,\omega)$ and $\overline{\overline{T}}(ij,\omega)$ may be non-zero even when c_i is zero, this has no consequences in eqn (5.6.10). In order to derive the configurational average of this equation, we make the assumption that each site is surrounded by the same effective medium. Hence $\overline{\overline{K}}(i,\omega) \simeq \overline{\overline{K}}(\omega)$ is considered to be independent of the site considered, and therefore we have, from (5.6.9),

$$\overline{\overline{\chi}}(ii,\omega) = c_i\overline{\overline{\chi}}(\omega) \quad ; \quad \overline{\overline{\chi}}(\omega) = \left\{1 - \overline{\overline{\chi}}^{o}(\omega)\overline{\overline{K}}(\omega)\right\}^{-1}\overline{\overline{\chi}}^{o}(\omega). \quad (5.6.12)$$

With this replacement, the configurational average of eqn (5.6.11) may be derived straightforwardly, as we can take advantage of the condition that, for instance, $c_{j'}$ only occurs once in the sum over j'. It is important here that the common factor c_i was cancelled, because $\overline{\overline{T}}(j'j,\omega)$ involves the site i, making the averaging of $c_i\overline{\overline{T}}(j'j,\omega)$ more complicated. Introducing the notation $\overline{\overline{T}}_{\mathrm{E}}(ij,\omega) = \left\langle\overline{\overline{T}}(ij,\omega)\right\rangle_{\mathrm{cf}}$, we get from (5.6.11) the CPA equation

$$\delta_{ij} + c\mathcal{J}(ij)\overline{\overline{\chi}}(\omega) + \sum_{j'} c^2\,\mathcal{J}(ij')\overline{\overline{\chi}}(\omega)\overline{\overline{T}}_{\mathrm{E}}(j'j,\omega)\overline{\overline{\chi}}(\omega)$$

$$= \{1 + c\overline{\overline{K}}(\omega)\overline{\overline{\chi}}(\omega)\}\{\delta_{ij} + c\overline{\overline{T}}_{\mathrm{E}}(ij,\omega)\overline{\overline{\chi}}(\omega)\} \quad (5.6.13)$$

for the effective medium, which may be diagonalized by a Fourier transformation. Introducing the effective coupling parameter

$$\overline{\overline{\mathcal{J}}}_{\mathrm{E}}(\mathbf{q}) = \mathcal{J}(\mathbf{q}) - \overline{\overline{K}}(\omega), \quad (5.6.14)$$

where the scalar appearing in a matrix equation is, as usual, multiplied by the unit matrix, we get

$$\overline{\overline{T}}_{\mathrm{E}}(\mathbf{q},\omega) = \overline{\overline{\mathcal{J}}}_{\mathrm{E}}(\mathbf{q})\overline{\overline{D}}_{\mathrm{E}}(\mathbf{q},\omega)^{-1} \quad ; \quad \overline{\overline{D}}_{\mathrm{E}}(\mathbf{q},\omega) = 1 - c\overline{\overline{\chi}}(\omega)\overline{\overline{\mathcal{J}}}_{\mathrm{E}}(\mathbf{q})$$
$$(5.6.15)$$

and, from (5.6.10),

$$\overline{\overline{\chi}}(\mathbf{q},\omega) = c\overline{\overline{\chi}}(\omega) + c^2\overline{\overline{\chi}}(\omega)\overline{\overline{T}}_{\mathrm{E}}(\mathbf{q},\omega)\overline{\overline{\chi}}(\omega) = \overline{\overline{D}}_{\mathrm{E}}(\mathbf{q},\omega)^{-1}c\overline{\overline{\chi}}(\omega). \quad (5.6.16)$$

Hence the result is similar to that obtained in the VCA, except that the parameters are replaced by the effective quantities introduced by eqns (5.6.12) and (5.6.14). These effective values are determined from the 'bare' parameters in terms of $\overline{\overline{K}}(\omega)$. It is easily seen that we retain the VCA result, i.e. $\overline{\overline{K}}(\omega)$ cancels out of (5.6.15), if (5.6.12) is replaced by the corresponding VCA equation $\overline{\overline{\chi}}(\omega) \simeq \left\{1 - c\overline{\overline{\chi}}^{o}(\omega)\overline{\overline{K}}(\omega)\right\}^{-1}\overline{\overline{\chi}}^{o}(\omega).$

In the case $c = 1$, both the VCA and the CPA results coincide with the usual RPA result. $K(\omega)$ is itself determined by the effective parameters, and (5.6.13), with $i = j$, leads to the following self-consistent equation

$$\overline{\overline{K}}(\omega) = \frac{1}{N} \sum_{\mathbf{q}} c\,\mathcal{J}(\mathbf{q})\overline{\overline{\chi}}(\omega)\overline{\overline{T}}_{\mathrm{E}}(\mathbf{q}, \omega). \qquad (5.6.17a)$$

This result may be written

$$\overline{\overline{K}}(\omega) = \frac{1}{N} \sum_{\mathbf{q}} \mathcal{J}(\mathbf{q})\overline{\overline{D}}_{\mathrm{E}}(\mathbf{q}, \omega)^{-1} = \sum_{\mathbf{q}} \mathcal{J}(\mathbf{q})\overline{\overline{\chi}}(\mathbf{q}, \omega) \Big/ \sum_{\mathbf{q}} \overline{\overline{\chi}}(\mathbf{q}, \omega),$$

$$(5.6.17b)$$

corresponding to the condition that the *effective* T-matrix vanishes when summed over $\mathbf{q}$, $\sum_{\mathbf{q}} \overline{\overline{T}}_{\mathrm{E}}(\mathbf{q}, \omega) = 0$, in accordance with our starting assumption, (5.6.10).

In order to derive the effective medium result (5.6.13), $\overline{\overline{\chi}}(j'j', \omega)$ in (5.6.11) was replaced by $c_{j'}\overline{\overline{\chi}}(\omega)$, which is an approximation, as this response depends on the actual surroundings, including the sites i and j. The CPA incorporates the same type of mistake as in the VCA, but it is clear that the frequency of such errors is substantially reduced. The dependence of $\overline{\overline{\chi}}(j'j', \omega)$ on c_i and c_j, corresponding to a site dependence of $\overline{K}(j', \omega)$, becomes relatively unimportant if the configuration number Z is large, since i or j may only be one of the Z neighbours of the site j'.

The effective medium procedure is straightforwardly generalized to the case where $\overline{\overline{\chi}}_2(i, \omega)$ is non-zero (Jensen 1984). Again the CPA result may be expressed in the same way as the VCA result, (5.6.5–6), except that all the quantities are replaced by their effective CPA counterparts; $\mathcal{J}(\mathbf{q})$ becomes $\overline{\overline{\mathcal{J}}}_{\mathrm{E}}(\mathbf{q})$, given by (5.6.14), and $\overline{\overline{\chi}}_r^o(\omega)$ in (5.6.6) is replaced by

$$\overline{\overline{\chi}}_r(\omega) = \left\{ 1 - \gamma_{rr}\overline{\overline{\chi}}_r^o(\omega)\overline{\overline{K}}(\omega) \right\}^{-1} \overline{\overline{\chi}}_r^o(\omega), \qquad (5.6.18)$$

where the effective-medium parameter $\overline{\overline{K}}(\omega)$ is determined by the same self-consistent equation (5.6.17) as above. To a first approximation, $\overline{\overline{D}}_{\mathrm{E}}(\mathbf{q}, \omega)^{-1}$ in this equation may be replaced by the simpler virtual-crystal result. Because of the poles in $\overline{\overline{D}}(\mathbf{q}, \omega)^{-1}$, both the real and imaginary parts of $\overline{\overline{K}}(\omega)$ are usually non-zero, and the imaginary contribution then predicts a finite lifetime for the excitations, due to the static disorder. This leading-order result may serve as the starting point in an iterative calculation of $\overline{\overline{K}}(\omega)$, and thus of a more accurate CPA result.

It is much more complicated to include the effects of off-diagonal disorder. They have been considered in the papers referred to above, but

only in relatively simple models like the dilute Heisenberg ferromagnet with nearest-neighbour interactions. This model may be considered as the extreme example of off-diagonal disorder, and the CPA concept of an effective medium loses its meaning completely below the *percolation* concentration, where all clusters of interacting spins are of finite size, precluding any long-range order. If the molecular field is independent of the site considered, i.e. $\mathcal{H}_{\mathrm{MF}}(i) = \langle\mathcal{H}_{\mathrm{MF}}(i)\rangle_{\mathrm{cf}}$ in (5.6.3), as happens in the paramagnetic case or if $\langle\mathbf{J}_1\rangle = \gamma\langle\mathbf{J}_2\rangle$, then the CPA result above should apply. However, except in a pure boson or fermion system, the 'dynamical' disorder due to thermal fluctuations introduces corrections to the RPA equation (5.6.4), with consequences of the same order of magnitude as $\overline{\overline{K}}(\omega)$ in (5.6.16), at least at elevated temperatures. In most magnetic systems, the two kinds of disorder may lead to damping effects of the same magnitude, and furthermore the use of the CPA result (5.6.16), without taking into account the dynamic renormalization of the RPA, occasionally leads to misleading results, as discussed for instance by Jensen (1984).

The excitations of binary heavy-rare-earth alloys have been studied much less extensively than their magnetic structures. However, the effect of 10% of Y, Dy, Ho, and Tm on the spin-wave spectrum of Tb has been examined, and the characteristic influence of the different solutes observed. The results of Larsen *et al.* (1986) for the Y and Dy alloys could be interpreted in terms of a simple average-crystal model, in which all sites are considered as equivalent, and the effect of the solute atoms is to modify the average exchange and the effective single-ion anisotropy. Thus Dy reduces the effective hexagonal anisotropy, and the spin-wave energy gap therefore decreases. On the other hand, Y dilutes the two-ion coupling, and therefore decreases T_N and the spin-wave energies, although the relative magnitude of the peak in $\mathcal{J}(\mathbf{q})$ increases, extending the temperature range over which the helical structure is stable. The first excited state of the Ho ion in the Tb host lies in the spin-wave energy band, and the dispersion relation is consequently strongly perturbed (Mackintosh and Bjerrum Møller 1972).

However, the most pronounced effects were observed by Larsen *et al.* (1988) in $\mathrm{Tb}_{90}\mathrm{Tm}_{10}$, where the Tm ions, with a spin $S = 1$, are relatively weakly coupled to the surrounding Tb moments, with $S = 3$. Furthermore, the axial anisotropy of the Tm ions is large and of opposite sign to that of Tb. As a result, well-defined quasi-localized states may be excited on the Tm sites, as shown in Fig. 5.11. These rather complex results were interpreted by means of a VCA calculation, in which the crystal-field parameters for the Tm ions were deduced from the dilute-alloy experiments of Touborg (1977), while the single-ion anisotropy and the two-ion coupling between the Tb ions were taken from the analysis
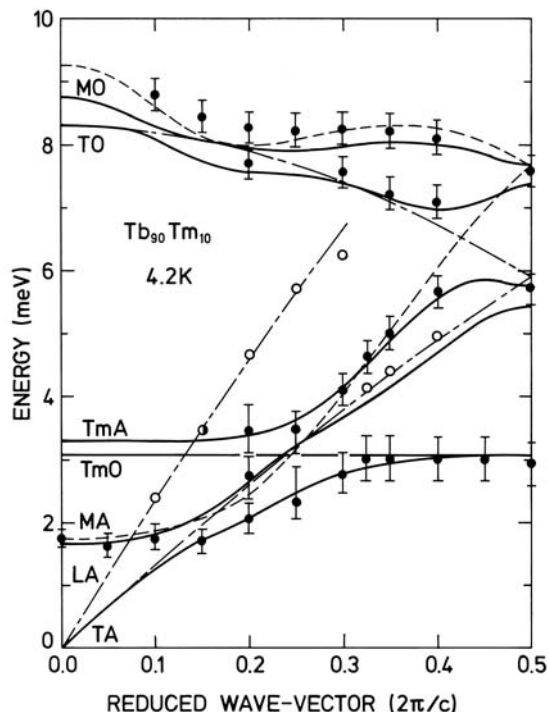
Fig. 5.11.   Excitations in the *c*-direction of $Tb_{90}Tm_{10}$ at 4 K. The Tb magnon modes, the crystal-field excitations on the Tm ions, and the transverse phonons polarized parallel to the magnetization mutually interfere to produce the calculated dispersion relations shown by the thick lines. The dashed lines indicate the unperturbed Tb magnons, and the short and long dashes the phonons. A and O signify acoustic and optical respectively.

of Jensen *et al.* (1975) of the magnon dispersion relations. The magnon–phonon interaction, which plays an important role in determining the dispersion relations, was incorporated in the calculations by the method which will be presented in Section 7.3.1, which leads to results consistent with those derived in Section 5.4.2. The effective exchange between the moments on the different ions was scaled as in eqn (5.6.1–2), but γ was given the value 0.24, instead of the 0.33 which (5.6.2) yields, in order to fix correctly the energy of the first excited state on the Tm ions. Such a departure from the simple de Gennes scaling is not particularly surprising for ions with very different orbital angular momenta. In the system $Pr_{95}Er_5$, for example, Rainford *et al.* (1988b) found that
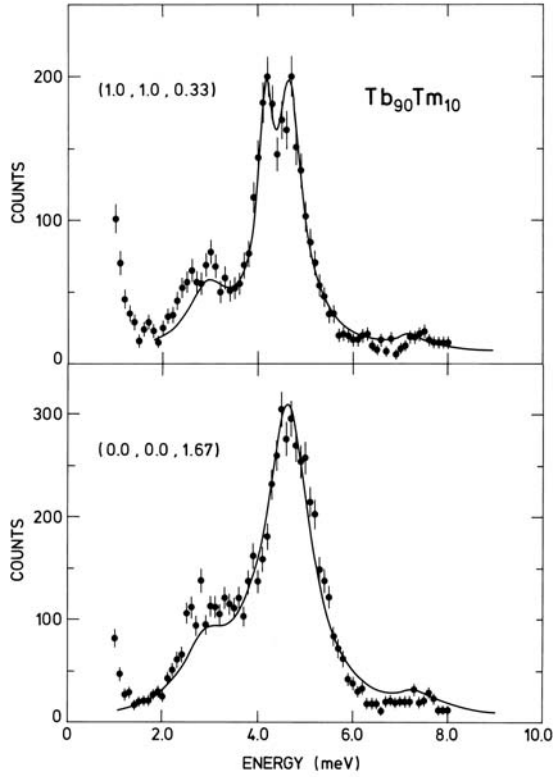
Fig. 5.12.   Experimental and calculated neutron-scattering spectra in $Tb_{90}Tm_{10}$ for the indicated scattering vectors, which correspond to a reduced wave-vector of 0.33 in Fig. 5.11. In the lower curve, the scattering vector is in the *c*-direction, while it is close to the hexagonal plane in the upper, where an unperturbed transverse phonon is observed. The ratio of the impurity intensity to the magnon peak is roughly doubled when the scattering vector moves from the *c*-direction to the plane, showing that the magnetic fluctuations in the impurity mode are predominantly along the *c*-axis.

the Er ions modify the two-ion coupling of the host substantially.

The theoretical results give a good account both of the excitation energies and of the observed neutron-scattering spectra, as illustrated in Fig. 5.12. They reveal that the difference between the interactions of the Tb and Tm ions in this alloy has a profound influence on the magnetic behaviour at the two types of site. The exchange forces the Tm moment to lie in the plane at low concentrations but, according to the calculations, the crystal fields reduce it from the saturation value of

$7\,\mu_B$ to about $5.9\,\mu_B$, whereas the Tb moment is very close to saturation. Furthermore, the first excited-state on the Tm ions is at a relatively low energy, and the associated magnetic fluctuations are predominantly in the c-direction, reflecting an incipient realignment of the moments, which actually occurs at higher concentrations (Hansen and Lebech 1976). The Tb fluctuations, on the other hand, are largely confined to the plane, with the result that the neutron-scattering intensity stemming from the c-axis fluctuations is comparable for the two types of site, even though only 10% of the ions are Tm.

The CPA theory has not yet been applied to heavy rare earth-alloys. The extra linewidth-effects due to the randomness are not expected to be very pronounced in the 10% alloys. At low temperatures, they are of the order of the contribution of the scattering against the electron-hole pair excitations of the conduction electrons, and they become decreasingly important compared with intrinsic effects at higher temperatures. The CPA theory has been applied to the light rare earth-alloy $\mathrm{Pr}_{95}\mathrm{Nd}_5$ (Jensen 1979a) in the paramagnetic phase, where the linewidth effects predicted by the CPA at $9\,\mathrm{K}$ are found to be of the same order as the intrinsic effects due to thermal disorder.

5.7 Conduction-electron interactions

As we have already discussed in Section 1.4, the conduction electrons in the rare earth metals act as the medium through which the coupling is established between the $4f$ electrons localized on the ions. In this section, we shall investigate this *RKKY* coupling in more detail, and consider its influence on both the *spin waves* in the ferromagnetic phase, and also on the *conduction electrons* themselves. The indirect-exchange interaction is first derived, and its effects in limiting the *lifetimes* of the spin waves and in *polarizing* the conduction electrons are deduced. The enhancement of the *effective mass* of the conduction electrons by the dynamical magnetic fluctuations is then calculated. Finally, the modification of the *electrical resistivity* by the exchange interaction is discussed, including the *scattering* of the conduction electrons by the spin-wave excitations, and the influence of the magnetic ordering on the conduction-electron band structure. For completeness, we include the effect of *magnetic superzones* in periodic structures in this section.

5.7.1 The indirect-exchange interaction

The starting point for our consideration of the indirect exchange, or RKKY coupling, of the localized moments is the Heisenberg–Dirac exchange between the $4f$ electrons and the conduction electrons. The $4f$-core electrons of the ion at site i are assumed to be described to a good approximation by non-overlapping atomic wavefunctions $\phi_{4f}(\mathbf{r} - \mathbf{R}_i)$.

We shall neglect the spin–orbit coupling of the conduction electrons, and assume their wavefunctions to be the Bloch functions

$$\psi_{n\mathbf{k}}(\mathbf{r}) = u_{n\mathbf{k}}(\mathbf{r})\, e^{i\mathbf{k}\cdot\mathbf{r}} = \psi_{n\mathbf{k}}(\mathbf{r} - \mathbf{R}_i)\, e^{i\mathbf{k}\cdot\mathbf{R}_i}, \qquad (5.7.1)$$

independent of the spin state σ. $u_{n\mathbf{k}}(\mathbf{r}) = u_{n\mathbf{k}}(\mathbf{r} - \mathbf{R}_i)$ has the periodicity of the lattice, and n is the band index. The Hamiltonian of the conduction electrons in *second quantization* is

$$\mathcal{H}_s = \sum_{n\mathbf{k}\sigma} \varepsilon_{n\mathbf{k}} c^+_{n\mathbf{k}\sigma} c_{n\mathbf{k}\sigma}, \qquad (5.7.2)$$

where the index s is conventionally used for the conduction electrons even though, as we saw in Section 1.3, they have predominantly d character. $c^+_{n\mathbf{k}\uparrow}$ creates and $c_{n\mathbf{k}\uparrow}$ annihilates a spin-up electron in the band-state $(n\mathbf{k})$, and they are Fermi-operators which satisfy the *anticommutation relations*

$$\{c_{n\mathbf{k}\sigma}, c^+_{n'\mathbf{k}'\sigma'}\} \equiv c_{n\mathbf{k}\sigma} c^+_{n'\mathbf{k}'\sigma'} + c^+_{n'\mathbf{k}'\sigma'} c_{n\mathbf{k}\sigma} = \delta_{nn'}\delta_{\mathbf{k}\mathbf{k}'}\delta_{\sigma\sigma'}$$
$$\{c^+_{n\mathbf{k}\sigma}, c^+_{n'\mathbf{k}'\sigma'}\} = \{c_{n\mathbf{k}\sigma}, c_{n'\mathbf{k}'\sigma'}\} = 0. \qquad (5.7.3)$$

An exposition of second quantization may be found, for example, in White (1983). The exchange interaction between a pair of electrons is $-2I\mathbf{s}_1 \cdot \mathbf{s}_2$, where I is the exchange integral. If $\mathbf{s}_1$ is the spin of a $4f$ electron at site i, then the sum over all the $4f$ electrons at this site gives

$$\sum_{4f\ el.} -2I\mathbf{s}_1 \cdot \mathbf{s}_2 = -2I\,\mathbf{S}_i \cdot \mathbf{s}_2 = -2I(g-1)\mathbf{J}_i \cdot \mathbf{s}_2,$$

where I is an average value of the exchange integral for the $4f$ electrons, and states other than those in the ground-state J-multiplet are neglected. The spin-density of the conduction electrons at $\mathbf{r}$ may be expressed in second-quantized form so that, for instance,

$$s_{2z}(\mathbf{r}) = \sum_{nn'}\sum_{\mathbf{k}\mathbf{k}'} \psi^*_{n'\mathbf{k}'}(\mathbf{r})\psi_{n\mathbf{k}}(\mathbf{r})\tfrac{1}{2}\left(c^+_{n'\mathbf{k}'\uparrow} c_{n\mathbf{k}\uparrow} - c^+_{n'\mathbf{k}'\downarrow} c_{n\mathbf{k}\downarrow}\right). \qquad (5.7.4)$$

The *sf-exchange interaction* is determined by the following exchange integral:

$$\int d\mathbf{r}_1 d\mathbf{r}_2 \psi^*_{n'\mathbf{k}'}(\mathbf{r}_1)\phi^*_{4f}(\mathbf{r}_2 - \mathbf{R}_i)\frac{e^2}{|\mathbf{r}_1 - \mathbf{r}_2|}\psi_{n\mathbf{k}}(\mathbf{r}_2)\phi_{4f}(\mathbf{r}_1 - \mathbf{R}_i)$$
$$= \frac{1}{N}I(n'\mathbf{k}', n\mathbf{k})e^{-i(\mathbf{k}'-\mathbf{k})\cdot\mathbf{R}_i},$$

with

$$I(n'\mathbf{k}', n\mathbf{k}) = N \int d\mathbf{r}_1 d\mathbf{r}_2 \psi^*_{n'\mathbf{k}'}(\mathbf{r}_1)\phi^*_{4f}(\mathbf{r}_2)\frac{e^2}{|\mathbf{r}_1 - \mathbf{r}_2|}\psi_{n\mathbf{k}}(\mathbf{r}_2)\phi_{4f}(\mathbf{r}_1),$$
$$(5.7.5)$$

where N is the number of rare earth ions. If there are several $4f$ electrons per ion, $I(n'\mathbf{k}', n\mathbf{k})$ should again be averaged over their wavefunctions. The Hamiltonian $\mathcal{H}_{sf}$, describing the exchange interaction between the conduction electrons and the $4f$ electrons, is then found to be

$$\mathcal{H}_{sf} = -\frac{1}{N}\sum_i \sum_{nn'} \sum_{\mathbf{k}\mathbf{k}'}(g-1)I(n'\mathbf{k}', n\mathbf{k})e^{-i(\mathbf{k}'-\mathbf{k})\cdot\mathbf{R}_i}$$
$$\times \left[(c^+_{n'\mathbf{k}'\uparrow}c_{n\mathbf{k}\uparrow} - c^+_{n'\mathbf{k}'\downarrow}c_{n\mathbf{k}\downarrow})J_{iz} + c^+_{n'\mathbf{k}'\uparrow}c_{n\mathbf{k}\downarrow}J_i^- + c^+_{n'\mathbf{k}'\downarrow}c_{n\mathbf{k}\uparrow}J_i^+\right],$$
$$(5.7.6)$$

in second quantization.

In the ordered ferromagnetic phase, we may use the MF approximation, in which case

$$\mathcal{H}_{sf}(\mathrm{MF}) = -\sum_{nn'}\sum_{\mathbf{k}}(g-1)I(n'\mathbf{k}, n\mathbf{k})(c^+_{n'\mathbf{k}\uparrow}c_{n\mathbf{k}\uparrow} - c^+_{n'\mathbf{k}\downarrow}c_{n\mathbf{k}\downarrow})\langle J_z\rangle.$$
$$(5.7.7)$$

This Hamiltonian gives rise to both diagonal and off-diagonal contributions to the energies of the conduction electrons. The diagonal energies are

$$\varepsilon_{n\mathbf{k}\uparrow} = \varepsilon_{n\mathbf{k}} - \langle J_z\rangle(g-1)I(n\mathbf{k}, n\mathbf{k})$$
$$\varepsilon_{n\mathbf{k}\downarrow} = \varepsilon_{n\mathbf{k}} + \langle J_z\rangle(g-1)I(n\mathbf{k}, n\mathbf{k}).$$
$$(5.7.8)$$

Second-order perturbation theory then gives the energies of the band electrons as

$$\widetilde{\varepsilon}_{n\mathbf{k}\sigma} = \varepsilon_{n\mathbf{k}\sigma} + \langle J_z\rangle^2(g-1)^2\sum_{n'\neq n}\frac{|I(n'\mathbf{k}, n\mathbf{k})|^2}{\varepsilon_{n\mathbf{k}} - \varepsilon_{n'\mathbf{k}}}. \qquad (5.7.9)$$

This dependence of the energies of the perturbed band-electrons on their state of polarization implies that the electron gas itself develops a non-zero magnetization. In order to calculate this moment, we first note that (5.7.9) corresponds to a replacement of $\mathcal{H}_s + \mathcal{H}_{sf}(\mathrm{MF})$ by an effective Hamiltonian for the band electron,

$$\widetilde{\mathcal{H}}_s = \sum_{n\mathbf{k}\sigma}\widetilde{\varepsilon}_{n\mathbf{k}\sigma}\widetilde{c}^+_{n\mathbf{k}\sigma}\widetilde{c}_{n\mathbf{k}\sigma}, \qquad (5.7.10)$$

where the new Fermi operators are determined in terms of the old by

$$c_{n\mathbf{k}\uparrow} = \widetilde{c}_{n\mathbf{k}\uparrow} + \sum_{n'}U_{\mathbf{k}}(n, n')\widetilde{c}_{n'\mathbf{k}\uparrow}$$
$$c_{n\mathbf{k}\downarrow} = \widetilde{c}_{n\mathbf{k}\downarrow} - \sum_{n'}U_{\mathbf{k}}(n, n')\widetilde{c}_{n'\mathbf{k}\downarrow},$$
$$(5.7.11a)$$

to leading order. $U_{\mathbf{k}}(n, n) = 0$ and, for $n' \neq n$,

$$U_{\mathbf{k}}(n, n') = (g - 1)\langle J_z\rangle\frac{I(n\mathbf{k}, n'\mathbf{k})}{\varepsilon_{n\mathbf{k}} - \varepsilon_{n'\mathbf{k}}}. \qquad (5.7.11b)$$

The (approximately) diagonal form of (5.7.9) implies that the thermal expectation values are

$$\langle\widetilde{c}^+_{n\mathbf{k}\sigma}\widetilde{c}_{n'\mathbf{k}'\sigma'}\rangle = \delta_{nn'}\delta_{\mathbf{k}\mathbf{k}'}\delta_{\sigma\sigma'}\,f_{n\mathbf{k}\sigma}, \qquad (5.7.12a)$$

where

$$f_{n\mathbf{k}\sigma} = \frac{1}{e^{\beta(\widetilde{\varepsilon}_{n\mathbf{k}\sigma} - \mu_F)} + 1} \qquad (5.7.12b)$$

is the *Fermi–Dirac distribution function* and μ_F is the chemical potential, equal to the Fermi energy $\widetilde{\varepsilon}_F$ in the temperature regime in which we shall be interested. The moment density is determined by (5.7.4), and introducing the new Fermi operators and using (5.7.12), we obtain

$$\langle\mu_z(\mathbf{r})\rangle_{\text{c.el.}} = \mu_B\sum_{nn'}\sum_{\mathbf{k}\mathbf{k},}\psi^*_{n'\mathbf{k}'}(\mathbf{r})\psi_{n\mathbf{k}}(\mathbf{r})\big(\langle c^+_{n'\mathbf{k}'\uparrow}c_{n\mathbf{k}\uparrow}\rangle - \langle c^+_{n'\mathbf{k}'\downarrow}c_{n\mathbf{k}\downarrow}\rangle\big)$$

$$= \mu_B\sum_{nn'}\sum_{\mathbf{k}}\psi^*_{n'\mathbf{k}}(\mathbf{r})\psi_{n\mathbf{k}}(\mathbf{r})\big[\{\delta_{nn'} + U^*_{\mathbf{k}}(n', n)\}(f_{n\mathbf{k}\uparrow} - f_{n\mathbf{k}\downarrow})$$

$$+ U_{\mathbf{k}}(n, n')(f_{n'\mathbf{k}\uparrow} - f_{n'\mathbf{k}\downarrow})\big]. \qquad (5.7.13)$$

The uniform, averaged part of this moment density can be obtained by an integration of eqn (5.7.13) over space, and remembering that the wavefunctions are orthogonal and normalized, we find the magnetic moment of the conduction electrons per ion to be

$$\langle\mu_z\rangle_{\text{c.el.}} = \mu_B\frac{1}{N}\sum_{n\mathbf{k}}\big(f_{n\mathbf{k}\uparrow} - f_{n\mathbf{k}\downarrow}\big). \qquad (5.7.14)$$

We note that, in addition to this uniform polarization of the conduction electrons, there is a spatially non-uniform component of the polarization density with the periodicity of the lattice. This non-uniform component reflects the variation in the electronic density, including the perturbative changes due to the *interband* contributions proportional to $U_{\mathbf{k}}(n, n')$. Furthermore, when the spin–orbit coupling of the conduction electrons is of importance, the interband coupling may induce a positional dependence in the direction of the spin polarization.

In order to obtain order-of-magnitude estimates of the exchange effects, we introduce a reasonable but somewhat crude approximation for the exchange integral, which is due to Overhauser (1963) and has

been discussed in detail by Freeman (1972). First we assume that the Coulomb interaction in eqn (5.7.5) is strongly shielded, so that it can be replaced by a δ-function. Next, using plane waves for the Bloch functions, we obtain

$$(g-1)I(n\mathbf{k}', n\mathbf{k}) \approx j(\mathbf{q} = \mathbf{k}' - \mathbf{k}) \propto \int d\mathbf{r} |\phi_{4f}(\mathbf{r})|^2 e^{-i\mathbf{q}\cdot\mathbf{r}}, \qquad (5.7.15)$$

which is the form factor of the $4f$-electron density, approximately the same as the local moment density (4.1.15). In this simplified model, where the conduction electrons are assumed to be free-electron-like, the interband exchange integrals, in which $n' \neq n$, are obtained by adding reciprocal-lattice vectors $\boldsymbol{\tau}$ to $\mathbf{q}$ in eqn (5.7.15). In this model, we obtain a rigid band-splitting, independent of $\mathbf{k}$, between the spin-down and spin-up bands, of magnitude

$$\Delta = \widetilde{\varepsilon}_{n\mathbf{k}\downarrow} - \widetilde{\varepsilon}_{n\mathbf{k}\uparrow} = 2\langle J_z \rangle j(\mathbf{0}). \qquad (5.7.16)$$

Since $j(\mathbf{0})$ has the same sign as $(g-1)$, it is positive in the heavy rare earth metals. If $\mathcal{N}(\varepsilon)$ is the density of electronic states per ion and per spin state in the paramagnetic phase, the shifts of the spin-up and spin-down bands lead to an excess number of spin-up electrons proportional to

$$\overline{\mathcal{N}}(\widetilde{\varepsilon}_F) = \frac{1}{\Delta} \int_{\widetilde{\varepsilon}_F - \frac{\Delta}{2}}^{\widetilde{\varepsilon}_F + \frac{\Delta}{2}} \mathcal{N}(\varepsilon) d\varepsilon, \qquad (5.7.17)$$

when the small modification of the density of states due to the interband coupling is neglected, so that $\widetilde{\varepsilon}_F$ is close to the Fermi energy ε_F of the non-magnetic system. In combination with eqn (5.7.14), this result predicts a (positive) augmentation of the ferromagnetic moment of the $4f$ electrons, due to the conduction electrons, of magnitude

$$\langle \mu_z \rangle_{\text{c.el.}} = \mu_B \overline{\mathcal{N}}(\widetilde{\varepsilon}_F)\Delta, \qquad (5.7.18)$$

when $k_B T \ll \widetilde{\varepsilon}_F$. The total moment per ion may then be expressed in terms of an effective g-factor:

$$\langle \mu_z \rangle = g\mu_B \langle J_z \rangle + \langle \mu_z \rangle_{\text{c.el.}} = (g + \Delta g)\mu_B \langle J_z \rangle, \qquad (5.7.19a)$$

where

$$\Delta g = 2j(\mathbf{0})\overline{\mathcal{N}}(\widetilde{\varepsilon}_F). \qquad (5.7.19b)$$

In the metals, the effective exchange integral $j(\mathbf{0})$ is $\sim (g-1) \times 0.1\,\text{eV}$, leading to an exchange splitting Δ which, in Gd for example, is nearly 1 eV. This relatively large splitting has the consequence that $\overline{\mathcal{N}}(\widetilde{\varepsilon}_F)$ may

differ somewhat from the value $\mathcal{N}(\varepsilon_F)$ in the paramagnetic phase. In the hcp metals, the band structure calculations discussed in Section 1.3 reveal that ε_F is near a peak in the density of states due to the d electrons, and that $\mathcal{N}(\varepsilon_F) \simeq 1\,\mathrm{eV}^{-1}$ per spin state per ion, corresponding to an electronic moment of the order of one-tenth of the local moment. In the example of Gd, for which $g = 2$, $\Delta g = 0.18$. The same value of $\Delta g/(g-1)$ accounts fairly well for the conduction-electron contribution to the moments of the other heavy rare earths in Table 1.6, bearing in mind the uncertainties in the experimental results, and the possible effects of the crystal fields in quenching the local moments.

The spin waves in the ferromagnetic phase are decisively influenced by the sf-exchange interaction. In order to consider such effects, we introduce the Bose operators acting on the angular-momentum states, as in eqns (5.2.6–8), and find, to first order in $1/J$,

$$
\mathcal{H}_{sf} \simeq \mathcal{H}_{sf}(\mathrm{MF}) - \frac{1}{N} \sum_{\mathbf{k}\mathbf{q}\tau} \sum_i j(\mathbf{q}+\boldsymbol{\tau})\, e^{-i\mathbf{q}\cdot\mathbf{R}_i} \Big[-\delta_{\mathbf{q}\mathbf{0}}(\langle c^+_{\mathbf{k}+\tau\uparrow}c_{\mathbf{k}\uparrow}\rangle
$$
$$
- \langle c^+_{\mathbf{k}+\tau\downarrow}c_{\mathbf{k}\downarrow}\rangle)a^+_i a_i + \sqrt{2J}c^+_{\mathbf{k}+\mathbf{q}+\tau\uparrow}c_{\mathbf{k}\downarrow}\, a^+_i + \sqrt{2J}c^+_{\mathbf{k}+\mathbf{q}+\tau\downarrow}c_{\mathbf{k}\uparrow}\, a_i \Big],
$$

using the simplified exchange of eqn (5.7.15), and neglecting effects of third or higher order in $j(\mathbf{q})$ due to $(c^+_{\mathbf{k}'\sigma}c_{\mathbf{k}\sigma} - \langle c^+_{\mathbf{k}'\sigma}c_{\mathbf{k}\sigma}\rangle)a^+_i a_i$. $\mathbf{q}$ is assumed to lie in the primitive Brillouin zone, but no such restriction is placed on $\mathbf{k}$. We note that $c^+_{\mathbf{k}}$ and $c^+_{\mathbf{k}+\tau}$, where $\boldsymbol{\tau}$ is a reciprocal lattice vector, create electrons in different bands in the free-electron model. Introducing the crystal-field Hamiltonian to first order in $1/J$ (eqn (5.2.14) with $\mathcal{J}(ij) = 0$), and the Fourier transforms of the Bose operators (5.2.16), we find that the total magnetic Hamiltonian becomes

$$
\mathcal{H} = \widetilde{\mathcal{H}}_s + \sum_{\mathbf{q}} \Big[\{A + J\widetilde{\mathcal{J}}(\mathbf{0},0)\}a^+_{\mathbf{q}}a_{\mathbf{q}} + B\tfrac{1}{2}(a_{\mathbf{q}}a_{-\mathbf{q}} + a^+_{\mathbf{q}}a^+_{-\mathbf{q}})\Big]
$$
$$
- \sqrt{2J/N} \sum_{\mathbf{k}\mathbf{q}\tau} j(\mathbf{q}+\boldsymbol{\tau})\big(c^+_{\mathbf{k}+\mathbf{q}+\tau\uparrow}c_{\mathbf{k}\downarrow}\, a^+_{-\mathbf{q}} + c^+_{\mathbf{k}+\mathbf{q}+\tau\downarrow}c_{\mathbf{k}\uparrow}\, a_{\mathbf{q}}\big),
$$
$$
(5.7.20)
$$

where

$$
\widetilde{\mathcal{J}}(\mathbf{0},0) = 2j^2(\mathbf{0})\overline{\mathcal{N}}(\widetilde{\epsilon}_F) + \frac{2}{N} \sum_{\mathbf{k},\tau\neq\mathbf{0}} |j(\boldsymbol{\tau})|^2 \frac{f_{\mathbf{k}\downarrow} - f_{\mathbf{k}+\tau\uparrow}}{\varepsilon_{\mathbf{k}+\tau} - \varepsilon_{\mathbf{k}}}, \qquad (5.7.21)
$$

including the 'interband' contributions as in (5.7.9). The spin-wave energies may be obtained from the poles in the Green function $\langle\langle a_{\mathbf{q}} ; a^+_{\mathbf{q}}\rangle\rangle$. The equation of motion (3.3.14) for this Green function is determined

from $\mathcal{H}$ to be

$$
\left\{\hbar\omega - A - J\widetilde{\mathcal{J}}(\mathbf{0},0)\right\}\langle\langle a_{\mathbf{q}}\,;\,a_{\mathbf{q}}^{+}\rangle\rangle - B\langle\langle a_{-\mathbf{q}}^{+}\,;\,a_{\mathbf{q}}^{+}\rangle\rangle
$$
$$
+ \sqrt{2J/N}\sum_{\mathbf{k}\tau}j(-\mathbf{q}-\boldsymbol{\tau})\langle\langle c_{\mathbf{k}-\mathbf{q}-\tau\uparrow}^{+}c_{\mathbf{k}\downarrow}\,;\,a_{\mathbf{q}}^{+}\rangle\rangle = 1. \quad (5.7.22)
$$

The equation of motion of the new Green function $\langle\langle c_{\mathbf{k}-\mathbf{q}-\tau\uparrow}^{+}c_{\mathbf{k}\downarrow}\,;\,a_{\mathbf{q}}^{+}\rangle\rangle$ involves the following commutator:

$$
[c_{\mathbf{k}-\mathbf{q}-\tau\uparrow}^{+}c_{\mathbf{k}\downarrow}\,,\mathcal{H}] = \left(\varepsilon_{\mathbf{k}\downarrow} - \varepsilon_{\mathbf{k}-\mathbf{q}-\tau\uparrow}\right)c_{\mathbf{k}-\mathbf{q}-\tau\uparrow}^{+}c_{\mathbf{k}\downarrow}
$$
$$
+ \sqrt{2J/N}\sum_{\mathbf{q}'}j(\mathbf{q}')\left(c_{\mathbf{k}-\mathbf{q}-\tau+\mathbf{q}'\downarrow}^{+}c_{\mathbf{k}\downarrow} - c_{\mathbf{k}-\mathbf{q}-\tau\uparrow}^{+}c_{\mathbf{k}-\mathbf{q}'\uparrow}\right)a_{\mathbf{q}'}
$$
$$
\simeq \left(\varepsilon_{\mathbf{k}\downarrow} - \varepsilon_{\mathbf{k}-\mathbf{q}-\tau\uparrow}\right)c_{\mathbf{k}-\mathbf{q}-\tau\uparrow}^{+}c_{\mathbf{k}\downarrow} + \sqrt{2J/N}\,j(\mathbf{q}+\boldsymbol{\tau})\left(f_{\mathbf{k}\downarrow} - f_{\mathbf{k}-\mathbf{q}-\tau\uparrow}\right)a_{\mathbf{q}}
$$
$$
(5.7.23)
$$

obtained by applying the anticommutator relations (5.7.3) and, in the second equation, an RPA decoupling of the operator products. It is not necessary here to differentiate between the new and the old Fermi operators, as the differences introduce corrections only in the third order of $|j(\mathbf{q})|$. Introducing this RPA result in the equation of motion for the Green function $\langle\langle c_{\mathbf{k}-\mathbf{q}-\tau\uparrow}^{+}c_{\mathbf{k}\downarrow}\,;\,a_{\mathbf{q}}^{+}\rangle\rangle$, we obtain

$$
\left(\hbar\omega - \varepsilon_{\mathbf{k}\downarrow} + \varepsilon_{\mathbf{k}-\mathbf{q}-\tau\uparrow}\right)\langle\langle c_{\mathbf{k}-\mathbf{q}-\tau\uparrow}^{+}c_{\mathbf{k}\downarrow}\,;\,a_{\mathbf{q}}^{+}\rangle\rangle
$$
$$
- \sqrt{2J/N}\,j(\mathbf{q}+\boldsymbol{\tau})\left(f_{\mathbf{k}\downarrow} - f_{\mathbf{k}-\mathbf{q}-\tau\uparrow}\right)\langle\langle a_{\mathbf{q}}\,;\,a_{\mathbf{q}}^{+}\rangle\rangle = 0, \quad (5.7.24)
$$

which, in combination with (5.7.22), leads to

$$
\left\{\hbar\omega - A - J\widetilde{\mathcal{J}}(\mathbf{0},0) + J\widetilde{\mathcal{J}}(\mathbf{q},\omega)\right\}\langle\langle a_{\mathbf{q}}\,;\,a_{\mathbf{q}}^{+}\rangle\rangle - B\langle\langle a_{-\mathbf{q}}^{+}\,;\,a_{\mathbf{q}}^{+}\rangle\rangle = 1, \quad (5.7.25)
$$

where

$$
\widetilde{\mathcal{J}}(\mathbf{q},\omega) = \lim_{\varepsilon\to 0^{+}}\frac{2}{N}\sum_{\tau}|j(\mathbf{q}+\boldsymbol{\tau})|^{2}\sum_{\mathbf{k}}\frac{f_{\mathbf{k}\downarrow} - f_{\mathbf{k}-\mathbf{q}-\tau\uparrow}}{\hbar\omega + i\hbar\varepsilon - \varepsilon_{\mathbf{k}\downarrow} + \varepsilon_{\mathbf{k}-\mathbf{q}-\tau\uparrow}}. \quad (5.7.26a)
$$

This result may be expressed in terms of the susceptibility of the conduction electrons. Introducing the spin susceptibility per ion, which is the usual magnetic susceptibility times $(2\mu_{B})^{-2}V/N$, so that

$$
\chi_{\mathrm{c.el.}}^{+-}(\mathbf{q},\omega) = -\frac{1}{N}\int d\mathbf{r}_{1}d\mathbf{r}_{2}\langle\langle s^{+}(\mathbf{r}_{1})\,;\,s^{-}(\mathbf{r}_{2})\rangle\rangle\,e^{-i\mathbf{q}\cdot(\mathbf{r}_{1}-\mathbf{r}_{2})}
$$
$$
= -\frac{1}{N}\sum_{\mathbf{k}'\mathbf{k}''}\langle\langle c_{\mathbf{k}'-\mathbf{q}\uparrow}^{+}c_{\mathbf{k}'\downarrow}\,;\,c_{\mathbf{k}''+\mathbf{q}\downarrow}^{+}c_{\mathbf{k}''\uparrow}\rangle\rangle \quad (5.7.26b)
$$
$$
= \lim_{\varepsilon\to 0^{+}}\frac{1}{N}\sum_{\mathbf{k}}\frac{f_{\mathbf{k}\downarrow} - f_{\mathbf{k}-\mathbf{q}\uparrow}}{\hbar\omega + i\hbar\varepsilon - \varepsilon_{\mathbf{k}\downarrow} + \varepsilon_{\mathbf{k}-\mathbf{q}\uparrow}},
$$

and neglecting the higher-order corrections to the spin-susceptibility, due to the coupling to the local moments, we can write the above result

$$\widetilde{\mathcal{J}}(\mathbf{q}, \omega) = 2 \sum_{\boldsymbol{\tau}} |j(\mathbf{q} + \boldsymbol{\tau})|^2 \chi_{\text{c.el.}}^{+-}(\mathbf{q} + \boldsymbol{\tau}, \omega), \qquad (5.7.26c)$$

where by the relation (3.2.15), $\chi_{\text{c.el.}}^{+-}(\mathbf{q}, \omega) = [\chi_{\text{c.el.}}^{-+}(-\mathbf{q}, -\omega)]^*$. In general, when the Coulomb interaction cannot be approximated by a δ-function, this factorization is not valid, and the indirect exchange is instead given by

$$\widetilde{\mathcal{J}}(\mathbf{q}, \omega) =$$
$$\lim_{\varepsilon \to 0^+} \frac{2}{N} \sum_{nn'} \sum_{\mathbf{k}} (g-1)^2 |I(n'\mathbf{k} - \mathbf{q}, n\mathbf{k})|^2 \frac{f_{n\mathbf{k}\downarrow} - f_{n'\mathbf{k}-\mathbf{q}\uparrow}}{\hbar\omega + i\hbar\varepsilon - \varepsilon_{n\mathbf{k}\downarrow} + \varepsilon_{n'\mathbf{k}-\mathbf{q}\uparrow}}, \tag{5.7.27}$$

where $\mathbf{k}$ is now confined to the primitive Brillouin zone.

In the frequency regime of the spin waves, where $|\hbar\omega|$ is much smaller than the Fermi energy or the exchange splitting Δ, the frequency dependence of $\widetilde{\mathcal{J}}(\mathbf{q}, \omega)$ can, to a good approximation, be neglected. The spins of the conduction electrons respond essentially instantaneously to any changes in the state of the local angular momenta, compared with the time-scale of these changes. For a Bravais-lattice, $\widetilde{\mathcal{J}}(\mathbf{q}, \omega) \simeq \widetilde{\mathcal{J}}(\mathbf{q}, 0) = \widetilde{\mathcal{J}}(-\mathbf{q}, 0)$. A comparison of eqn (5.7.25) with the $1/J$ spin-wave result (5.2.18) shows that $\widetilde{\mathcal{J}}(\mathbf{0}, 0) - \widetilde{\mathcal{J}}(\mathbf{q}, 0)$ replaces the contribution of the Heisenberg interaction considered in eqn (5.2.1). In this equation, $\mathcal{J}(ii) \equiv 0$ by definition and, since this is not the case for $\widetilde{\mathcal{J}}(ii) = (1/N) \sum_{\mathbf{q}} \widetilde{\mathcal{J}}(\mathbf{q}, 0)$, $\widetilde{\mathcal{J}}(\mathbf{q}, 0)$ cannot be associated directly with $\mathcal{J}(\mathbf{q})$. The instantaneous or frequency-independent part of the coupling of $\mathbf{J}_i$ with itself leads to a contribution $\frac{1}{2} N \widetilde{\mathcal{J}}(ii) \langle \mathbf{J}_i \cdot \mathbf{J}_i \rangle$ to the total energy, where $\langle \mathbf{J}_i \cdot \mathbf{J}_i \rangle = J(J+1)$, independently of the magnetic ordering or the temperature. This assertion may be verified (to first order in $1/J$) by a direct calculation of $\langle \mathcal{H} \rangle$ from (5.7.20). For this purpose $\langle c_{\mathbf{k}-\mathbf{q}-\boldsymbol{\tau}\uparrow}^+ c_{\mathbf{k}\downarrow} a_{\mathbf{q}}^+ \rangle$, for instance, is determined from eqn (5.7.24), but a *self-energy* correction of a factor $1/2$ must be included in its contribution to $\langle \mathcal{H} \rangle$. Taking this condition into account, we may finally write

$$\mathcal{J}(\mathbf{q}) = \widetilde{\mathcal{J}}(\mathbf{q}, 0) - \frac{1}{N} \sum_{\mathbf{q}'} \widetilde{\mathcal{J}}(\mathbf{q}', 0). \qquad (5.7.28)$$

The exchange interaction between the $4f$ electrons and the conduction electrons thus leads to an effective Heisenberg interaction between the local angular momenta, as given in (5.2.1). This is the RKKY interaction discussed earlier in Section 1.4.

The above calculation has been performed for a Bravais lattice, but the result (5.7.26) is readily generalized to a crystal with a basis of p ions, as the conduction electrons, in the approximation adopted, are not affected by the presence of the basis. If the couplings between the different sublattices are introduced in an equivalent manner to (5.1.1), then

$$\widetilde{\mathcal{J}}_{ss'}(\mathbf{q},\omega) = \frac{2}{p}\sum_{\boldsymbol{\tau}} |j(\mathbf{q}+\boldsymbol{\tau})|^2 \chi^{+-}_{\text{c.el.}}(\mathbf{q}+\boldsymbol{\tau},\omega)\exp(i\boldsymbol{\rho}_{ss'}\cdot\boldsymbol{\tau}) \quad (5.7.29)$$

replaces (5.7.26c), where $\boldsymbol{\rho}_{ss'}$ is the vector connecting the two sublattices s and s'.

The interaction between the localized moments is effectuated via virtual electron-hole pair-excitations of the conduction electrons. The transmission of any time-dependent event may be disturbed in two ways; either by the finite propagation-time of the pairs, or by a decay of the pair states into unbound electron and hole excitations, the so-called *Stoner* excitations. The second effect produces by far the most important correction to the instantaneous interaction, but we shall begin with a discussion of the frequency-dependence of the real part of $\widetilde{\mathcal{J}}(\mathbf{q},\omega)$, due to the finite transmission time. Returning to the simple model leading to (5.7.26), we find that the exchange coupling is proportional to the susceptibility function $\chi^{+-}_{\text{c.el.}}(\mathbf{q},\omega)$, which for unpolarized free electrons is the same as the *Lindhard function* (Lindhard 1954). If corrections of the order $k_B T/\varepsilon_F$ are neglected, the real part at zero wave-vector is

$$\begin{aligned}
\text{Re}\big[\chi^{+-}_{\text{c.el.}}(\mathbf{0},\omega)\big] &= \frac{1}{N}\sum_{\mathbf{k}} \frac{f_{\mathbf{k}\downarrow}-f_{\mathbf{k}\uparrow}}{\hbar\omega-\varepsilon_{\mathbf{k}\downarrow}+\varepsilon_{\mathbf{k}\uparrow}} \\
&= \frac{1}{N}\sum_{\mathbf{k}} \frac{f_{\mathbf{k}\uparrow}-f_{\mathbf{k}\downarrow}}{\Delta-\hbar\omega} = \overline{\mathcal{N}}(\widetilde{\epsilon}_F)\Big(1+\frac{\hbar\omega}{\Delta}\Big).
\end{aligned} \quad (5.7.30)$$

From this result, we find immediately that the intra-band contribution at zero frequency to $\widetilde{\mathcal{J}}(\mathbf{q}\to\mathbf{0},0)$ in eqn (5.7.26a) is $2j^2(\mathbf{0})\overline{\mathcal{N}}(\widetilde{\epsilon}_F)$, which is the same as in (5.7.21). On the other hand, the interband contributions differ in the two expressions, as the denominator in (5.7.26a) involves the exchange splitting Δ, whereas that in (5.7.21) does not. However, this difference can be neglected, as it is of the order $(\Delta/\varepsilon_F)^2$ times the intra-band contribution, which is beyond the order considered in these calculations. In fact, since the starting Hamiltonian (5.7.6) is invariant with respect to the choice of z-axis for the electronic spins and the angular momenta, the spin-wave frequency must vanish when $\mathbf{q}\to\mathbf{0}$ and $A=B=0$, according to the *Goldstone theorem*, which will be discussed in the next chapter. Therefore $\widetilde{\mathcal{J}}(\mathbf{q}\to\mathbf{0},0)=\widetilde{\mathcal{J}}(\mathbf{0},0)$,

and we simply assume that eqn (5.7.26a), with $(\mathbf{q}, \omega) = (\mathbf{0}, 0)$, replaces eqn (5.7.21). In the presence of an external field, Δ in eqn (5.7.16) is increased by an amount $2\mu_B H$, which leads to the extra contribution $\Delta g \mu_B H$ to $\widetilde{\mathcal{J}}(\mathbf{0}, 0)$ in (5.7.21), as the change with field of the interband terms may be neglected. To leading order, $\widetilde{\mathcal{J}}(\mathbf{q} \to \mathbf{0}, 0)$ is not affected by the applied field, so to this order the extra polarization of the conduction electrons, due to an external field, may simply be accounted for by replacing $g\mu_B H$ by $(g + \Delta g)\mu_B H$, both in the Zeeman energy (5.7.19a) and in the spin-wave energy parameters (in A). Writing the susceptibility in eqn (5.7.26b) as the sum of two terms, and replacing $\mathbf{k} - \mathbf{q}$ by $\mathbf{k}$ in the term involving $f_{\mathbf{k}-\mathbf{q}\uparrow}$, we obtain

$$
\mathrm{Re}\big[\chi_{\mathrm{c.el.}}^{+-}(\mathbf{q}, \omega)\big] =
$$
$$
\frac{V}{(2\pi)^3}\frac{2\pi}{N}\int_0^{k_{F\downarrow}} k^2 dk \int_{-1}^1 d\mu \Big[\hbar\omega - \Delta + \frac{(\hbar q)^2}{2m} - \frac{\hbar^2 kq}{m}\mu\Big]^{-1}
$$
$$
- \frac{V}{(2\pi)^3}\frac{2\pi}{N}\int_0^{k_{F\uparrow}} k^2 dk \int_{-1}^1 d\mu \Big[\hbar\omega - \Delta - \frac{(\hbar q)^2}{2m} - \frac{\hbar^2 kq}{m}\mu\Big]^{-1},
$$

or

$$
\mathrm{Re}\big[\chi_{\mathrm{c.el.}}^{+-}(\mathbf{q}, \omega)\big] =
$$
$$
\frac{V}{N}\frac{m}{(2\pi\hbar)^2}\Big\{k_{F\downarrow}(1-\eta)\mathcal{F}\Big(\frac{q}{2k_{F\downarrow}}(1-\eta)\Big) + k_{F\uparrow}(1+\eta)\mathcal{F}\Big(\frac{q}{2k_{F\uparrow}}(1+\eta)\Big)\Big\}
$$
$$
(5.7.31a)
$$

where we have introduced the function

$$
\mathcal{F}(x) = \frac{1}{2} + \frac{1-x^2}{4x}\ln\left|\frac{1+x}{1-x}\right| \tag{5.7.31b}
$$

and the parameter

$$
\eta = \frac{\Delta - \hbar\omega}{\varepsilon_F}\left(\frac{k_F}{q}\right)^2. \tag{5.7.31c}
$$

The Fermi energy is $\varepsilon_F = (\hbar k_F)^2/2m$, and the wave-vectors of the spin-up and the spin-down electrons at the Fermi surface are

$$
k_{F\uparrow} = k_F\Big(1 + \frac{\Delta}{2\varepsilon_F}\Big)^{\frac{1}{2}} \quad ; \quad k_{F\downarrow} = k_F\Big(1 - \frac{\Delta}{2\varepsilon_F}\Big)^{\frac{1}{2}}. \tag{5.7.31d}
$$

$\eta \to \infty$ in the limit $q \to 0$ and, using $\mathcal{F}(x) = 1/3x^2$ when $|x| \to \infty$, we may re-derive the result (5.7.30). At non-zero q, a numerical analysis shows that, to a good approximation,

$$
\mathrm{Re}\big[\chi_{\mathrm{c.el.}}^{+-}(\mathbf{q}, \omega)\big] = \overline{\mathcal{N}}(\widetilde{\epsilon}_F)\Big\{\mathcal{F}\Big(\frac{q}{2k_F}\Big) + \xi_q\frac{\hbar\omega}{\Delta}\Big\}, \tag{5.7.32}
$$

even when Δ/ε_F is as large as 0.5. The parameter ξ_q is equal to 1 at $q = 0$, and peaks at $q = q_0 = k_{F\uparrow} - k_{F\downarrow}$, after which it rapidly decreases ($\xi_q \simeq 0.25$ at $q = 2q_0$). For $\Delta/\varepsilon_F = 0.1$, the maximum value is about 4 and it decreases for increasing values of Δ, falling to about 3 at $\Delta/\varepsilon_F = 0.4$. Usually q_0 is much smaller than the length of any reciprocal-lattice vector, which means that the frequency dependence of the 'interband' term in the real part of $\widetilde{\mathcal{J}}(\mathbf{q}, \omega)$ can be neglected. The intra-band contribution is $2|j(\mathbf{q})|^2 \overline{\mathcal{N}}(\widetilde{\epsilon}_F)\xi_q \hbar\omega/\Delta$, and using

$$\left\{\hbar\omega + A + J\widetilde{\mathcal{J}}(\mathbf{0}, 0) - J\widetilde{\mathcal{J}}^*(-\mathbf{q}, -\omega)\right\}\langle\langle a_{-\mathbf{q}}^+ \, ; \, a_{\mathbf{q}}^+\rangle\rangle + B\langle\langle a_{\mathbf{q}} \, ; \, a_{\mathbf{q}}^+\rangle\rangle = 0,$$
$$(5.7.33)$$

which follows by symmetry from eqn (5.7.25), we may determine the spin-wave energies from the real part of $\widetilde{\mathcal{J}}(\mathbf{q}, \omega)$ to be

$$\hbar\omega = E_{\mathbf{q}}' = E_{\mathbf{q}}\left[1 + \xi_q\overline{\mathcal{N}}(\widetilde{\epsilon}_F)|j(\mathbf{q})|^2/j(\mathbf{0})\right]^{-1}, \qquad (5.7.34a)$$

to first order in $1/J$, with $E_{\mathbf{q}}$ given by (5.2.22). The extra factor, which originates from the frequency dependence of $\chi_{\mathrm{c.el.}}^{+-}(\mathbf{q}, \omega)$, differs from 1 by only a few per cent, and its $\mathbf{q}$-dependent contribution could scarcely be distinguished from that of $\mathcal{J}(\mathbf{q})$. However, the presence of this factor at $\mathbf{q} = \mathbf{0}$ means that the energy of the uniform spin-wave mode is no longer determined exclusively by the magnetic anisotropy of the bulk, according to (5.4.12) and (5.4.19), when the magnetoelastic effects are included, but instead the energy gap is

$$E_{\mathbf{0}}' = \frac{1}{N}\left(\frac{\partial^2 F}{\partial\theta^2}\frac{\partial^2 F}{\partial\phi^2}\bigg|_{\overline{\epsilon}}\right)^{\frac{1}{2}}\frac{1}{\langle J_z\rangle(1 + \frac{1}{2}\Delta g)}. \qquad (5.7.34b)$$

Although this modification is small, it demonstrates that the frequency dependence of $\chi_{\mathrm{c.el.}}^{+-}(\mathbf{q}, \omega)$ may cause small deviations between the static anisotropy parameters and those derived from the energy gap, as possibly detected in Tb in the form of a non-zero value of $\delta_6(-)$, defined by eqn (5.4.23a).

The dominant term in the real part of $\chi_{\mathrm{c.el.}}^{+-}(\mathbf{q}, \omega)$ is the frequency-independent contribution proportional to $\mathcal{F}(q/2k_F)$. Including only this contribution, and making the rather drastic simplifying assumption that $|j(\mathbf{q} + \boldsymbol{\tau})|$ in eqn (5.7.26c) is a constant $|j_0|$ at all wave-vectors, we may derive the exchange coupling in real space, which then depends only on the distance R between the different ions:

$$\mathcal{J}(R) = 2|j_0|^2\frac{V}{N(2\pi)^3}\int \overline{\mathcal{N}}(\widetilde{\epsilon}_F)\mathcal{F}\left(\frac{q}{2k_F}\right)e^{i\mathbf{q}\cdot\mathbf{R}}d\mathbf{q}.$$

The sum over $\boldsymbol{\tau}$ in (5.7.26c) corresponds to letting q vary between 0 and ∞, and the result is

$$\mathcal{J}(R) = 12\pi\nu|j_0|^2\overline{\mathcal{N}}(\widetilde{\epsilon}_F)\,\frac{\sin(2k_F R) - 2k_F R\cos(2k_F R)}{(2k_F R)^4}\,, \qquad (5.7.35)$$

where ν is the number of conduction electrons per ion; $\nu = Vk_F^3/3\pi^2 N$. Although this result is not directly applicable to realistic systems, it demonstrates explicitly that the indirect coupling mediated by the conduction electrons is long range, $\mathcal{J}(R) \propto R^{-3}$ for large R, and that it oscillates. The period of the oscillation is here $2\pi/2k_F$ whereas, in a real system, such oscillations may occur as a result of large parallel areas of Fermi surface, the separation of which determines an effective value of $2k_F$. It is interesting that $\mathcal{J}(R)$, derived from the excitation spectrum in Pr and shown in Fig. 1.18 on page 49, is reasonably well described by the above function, especially when $\mathbf{R}$ is in the basal plane, provided that an effective value of $2k_F$ of about $1.1\,\text{Å}^{-1}$ is used.

The magnetic scattering of the electron-hole pairs leads to a damping of the spin waves, which is determined by the imaginary part of the susceptibility (5.7.26b). The complementary result to eqn (5.7.31a) is then

$$\text{Im}\big[\chi^{+-}_{\text{c.el.}}(\mathbf{q},\omega)\big] =$$
$$-\frac{V}{(2\pi)^3}\frac{2\pi}{N}\int_0^\infty k^2 dk \int_{-1}^1 d\mu\,\pi\delta\Big(\hbar\omega - \Delta + \frac{(\hbar q)^2}{2m} - \frac{\hbar^2 kq}{m}\mu\Big)\,f_{\mathbf{k}\downarrow}$$
$$+\frac{V}{(2\pi)^3}\frac{2\pi}{N}\int_0^\infty k^2 dk \int_{-1}^1 d\mu\,\pi\delta\Big(\hbar\omega - \Delta - \frac{(\hbar q)^2}{2m} - \frac{\hbar^2 kq}{m}\mu\Big)\,f_{\mathbf{k}\uparrow}.$$

Because $-1 < \mu < 1$, the δ-function argument in the first term can only be zero if $\varepsilon_q \equiv (\hbar q)^2/(2m)$ lies between the two roots $\varepsilon_\pm = 2\varepsilon_k + \Delta - \hbar\omega \pm 2\big[\varepsilon_k(\varepsilon_k + \Delta - \hbar\omega)\big]^{1/2}$. For the second term, the same condition applies, except that the signs of Δ and $\hbar\omega$ are reversed, leading to the extra requirement that $\varepsilon_k > \varepsilon_K = \Delta - \hbar\omega$. If these conditions are satisfied,

$$\text{Im}\big[\chi^{+-}_{\text{c.el.}}(\mathbf{q},\omega)\big] =$$
$$-\frac{V}{N(2\pi)^2}\int_0^\infty \frac{\pi m}{\hbar^2 q}kf(\varepsilon_k + \tfrac{\Delta}{2})dk + \frac{V}{N(2\pi)^2}\int_K^\infty \frac{\pi m}{\hbar^2 q}kf(\varepsilon_k - \tfrac{\Delta}{2})dk,$$

where $f(\varepsilon) = 1/\big[\exp(\varepsilon - \varepsilon_F) + 1\big]$. By a suitable change of variables, the two integrals acquire the same limits and the same condition on ε_q, and they may therefore be combined in a single integral:

$$\text{Im}\big[\chi^{+-}_{\text{c.el.}}(\mathbf{q},\omega)\big] = \frac{V}{N(2\pi)^2}\frac{\pi m^2}{\hbar^4 q}\int_{\frac{\Delta - \hbar\omega}{2}}^\infty \big\{-f(\varepsilon + \tfrac{\hbar\omega}{2}) + f(\varepsilon - \tfrac{\hbar\omega}{2})\big\}d\varepsilon.$$

The integrand is only non-zero in a narrow interval of width $|\hbar\omega| \ll \Delta < \varepsilon_F$ around the Fermi surface, in which case the condition on ε_q can be written $k_{F\uparrow} - k_{F\downarrow} < q < k_{F\uparrow} + k_{F\downarrow}$ (if $\Delta = 0$ the lower boundary is replaced by $(\hbar\omega)^2/(4\varepsilon_F) < \varepsilon_q$). With this condition fulfilled,

$$\mathrm{Im}\big[\chi^{+-}_{\mathrm{c.el.}}(\mathbf{q},\omega)\big] = \frac{V}{N(2\pi)^2}\frac{\pi m^2}{\hbar^4 q}\hbar\omega,$$

independent of T (as long as $k_B T \ll \varepsilon_F$). Using

$$\mathcal{N}_\sigma(\varepsilon_F) = (V/N)(2\pi\hbar)^{-2}2mk_{F\sigma} \quad ; \quad (V/N)(2\pi)^{-2}\tfrac{2}{3}(k_{F\uparrow}^3 + k_{F\downarrow}^3) = \nu,$$

where ν is the number of conduction electrons per ion ($\nu = 3$), we may write the result:

$$\mathrm{Im}\big[\chi^{+-}_{\mathrm{c.el.}}(\mathbf{q},\omega)\big] = \frac{\pi}{3\nu}\mathcal{N}_\uparrow(\varepsilon_F)\mathcal{N}_\downarrow(\varepsilon_F)\frac{k_F}{q}\hbar\omega; \qquad (5.7.36)$$
$$k_{F\uparrow} - k_{F\downarrow} < q < k_{F\uparrow} + k_{F\downarrow},$$

neglecting corrections of second order in Δ/ε_F. In the zero-frequency limit considered here, q has to exceed the threshold value $q_0 = k_{F\uparrow} - k_{F\downarrow}$ before the imaginary part of $\chi^{+-}_{\mathrm{c.el.}}(\mathbf{q},\omega)$ becomes non-zero. This threshold value corresponds to the smallest distance in q-space between an occupied spin-down state and an unoccupied spin-up state, or vice versa, of nearly the same energy ($\simeq \varepsilon_F$). At $q = q_0$, the function makes a discontinuous step from zero to a finite value. The above result, combined with eqn (5.7.26), leads to

$$\mathrm{Im}\big[\widetilde{\mathcal{J}}(\mathbf{q},\omega)\big] = \zeta(\mathbf{q})\hbar\omega, \qquad (5.7.37a)$$

with

$$\zeta(\mathbf{q}) = \frac{2\pi}{3\nu}\mathcal{N}_\uparrow(\varepsilon_F)\mathcal{N}_\downarrow(\varepsilon_F)\sum_{\boldsymbol{\tau}}|j(\mathbf{q}+\boldsymbol{\tau})|^2\frac{k_F}{|\mathbf{q}+\boldsymbol{\tau}|}, \qquad (5.7.37b)$$

where the sum is restricted to $k_{F\uparrow} - k_{F\downarrow} < |\mathbf{q}+\boldsymbol{\tau}| < k_{F\uparrow} + k_{F\downarrow}$. The imaginary part of $\widetilde{\mathcal{J}}(\mathbf{q},\omega)$ gives rise to a non-zero width in the spin-wave excitations. If the above result is inserted in eqns (5.7.25) and (5.7.33), the denominator of the Green functions may approximately be written $(\hbar\omega)^2 - (E'_{\mathbf{q}})^2 + 2i\Gamma_{\mathbf{q}}\hbar\omega$, where $\Gamma_{\mathbf{q}}$ is half the linewidth of the spin waves at the wave-vector $\mathbf{q}$, and is found to take the form

$$\Gamma_{\mathbf{q}} = J\big[A + J\{\mathcal{J}(\mathbf{0}) - \mathcal{J}(\mathbf{q})\}\big]\zeta(\mathbf{q}) = JA_{\mathbf{q}}\,\zeta(\mathbf{q}). \qquad (5.7.38)$$
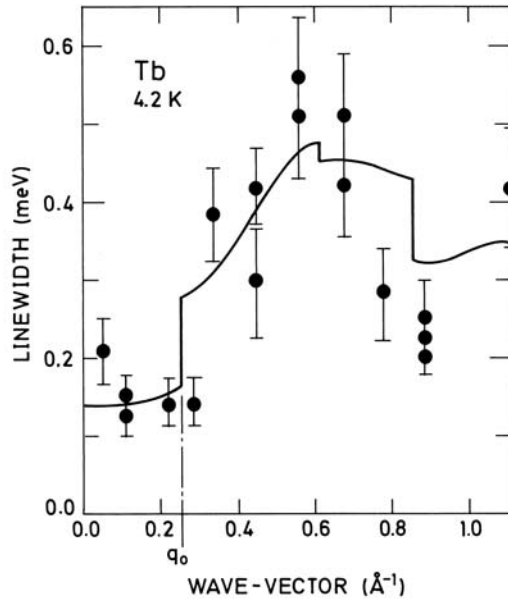
Fig. 5.13. The linewidths of magnons propagating in the c-direction of Tb at 4 K, compared with a theory based upon the nearly-free-electron model. The abrupt changes in the calculated lifetimes are due to the spin-splitting of the Fermi surface.

The lifetimes of the magnons propagating in the c-direction in Tb at 4 K, at which temperature the conduction electrons provide the dominant scattering process, were measured by Bjerrum Møller and Mackintosh (1979). As illustrated in Fig. 5.13, the linewidths are small, but non-zero, at small wave-vectors, rise abruptly at about a quarter of the way to the zone boundary, and fall again at large q. In order to interpret these results rigorously, it would be necessary to use eqn (5.7.27), with the correct band structure for Tb and realistic values for the exchange matrix elements $I(n'\mathbf{k}', n\mathbf{k})$. However, it is possible to obtain a semi-quantitative description by using the simple free-electron expression (5.7.37). As we shall see in the remainder of this section, this model, with an sf-interaction determined, for example, from the polarization of the conduction electrons (5.7.16–19), gives a surprisingly good account of the real scattering processes involving the interaction between the $4f$ and conduction electrons. Although the dominant d bands are far from parabolic in the rare earths, the nearly-free-electron Fermi surface for a trivalent hcp metal has a sheet with the form of a lens normal to the c-axis (Mackintosh *et al.* 1963), which mimics the Fermi-surface webbing

described in Section 1.3, and reproduces a number of observed features. In the calculations of Jensen (1982a), compared with the experimental results in Fig. 5.13, the spin-splitting of this surface gives rise to the critical value q_0 at which the linewidths abruptly increase. The finite lifetimes below this cut-off are due to interband transitions between states on sections of the Fermi surface with opposite spin, which intersect in the primitive Brillouin zone after translation through a reciprocal-lattice vector. These effects will also occur in calculations based on a realistic band structure, whereas the behaviour at higher q is much more dependent on the details of the energy bands.

5.7.2 The mass-enhancement of the conduction electrons

The processes in which the spin waves are scattered by the electron-hole pair excitations of the conduction electrons, and which therefore limit their lifetime, also have consequences for the conduction electrons. The energies of the conduction electrons are changed, and hence also their effective mass at the Fermi surface m^*, as measured directly by cyclotron resonance or the de Haas–van Alphen effect, or as determined from the low-temperature heat capacity. In the zero-temperature limit, the electronic part of the specific heat is

$$C = \gamma T = \frac{m^*}{m}\,\gamma_0 T \qquad ; \qquad \gamma_0 = \tfrac{1}{3}\pi^2 k_B^2 \big\{ \mathcal{N}_\uparrow(\widetilde{\varepsilon}_F) + \mathcal{N}_\downarrow(\widetilde{\varepsilon}_F) \big\} N, \quad (5.7.39)$$

where $m^* = (m_\uparrow^* + m_\downarrow^*)/2$ in the spin-polarized case. The use of $\widetilde{\varepsilon}_F$ instead of ε_F is meant to indicate that all the effects of the MF Hamiltonian, including the interband couplings in (5.7.7), are assumed to be incorporated in γ_0 or m.

In order to calculate m^*, we shall utilize the Green functions of the conduction electrons. Because these particles are fermions, it is convenient to introduce an alternative type of Green function, in which an anticommutator bracket replaces the commutator bracket occurring in the definition (3.3.12), so that, for instance,

$$G_\uparrow(\mathbf{k}, t - t') \equiv \langle\langle c_{\mathbf{k}\uparrow}(t)\,;\, c_{\mathbf{k}\uparrow}^+(t')\rangle\rangle_+ = -\frac{i}{\hbar}\theta(t - t')\langle\{c_{\mathbf{k}\uparrow}(t)\,,\, c_{\mathbf{k}\uparrow}^+(t')\}\rangle. \tag{5.7.40}$$

The Fourier transform obeys an equation of motion equivalent to eqn (3.3.14a), except that the commutator on the *right*-hand side of this equation is replaced by the anticommutator, or

$$\hbar\omega G_\uparrow(\mathbf{k}, \omega) - \langle\langle [c_{\mathbf{k}\uparrow}\,,\, \mathcal{H}]\,;\, c_{\mathbf{k}\uparrow}^+\rangle\rangle_+ = \langle\{c_{\mathbf{k}\uparrow}\,,\, c_{\mathbf{k}\uparrow}^+\}\rangle = 1. \tag{5.7.41}$$

If $\mathcal{H}$ is approximated by $\widetilde{\mathcal{H}}_s$, given by eqn (5.7.10), we obtain the non-interacting value of the Green function

$$G_\uparrow(\mathbf{k}, \omega) \simeq G_\uparrow^o(\mathbf{k}, \omega) = \frac{1}{\hbar\omega - \varepsilon_{\mathbf{k}\uparrow}} \tag{5.7.42}$$

(neglecting the minor difference between ε and $\widetilde{\varepsilon}$), showing that the poles of the Green function determine the energies of the conduction electrons. Considering the total Hamiltonian, in the approximation given by (5.7.20), we have instead

$$(\hbar\omega - \varepsilon_{\mathbf{k}\uparrow})G_\uparrow(\mathbf{k},\omega) + \sqrt{2J/N}\sum_{\mathbf{q}\tau}j(\mathbf{q}+\boldsymbol{\tau})\langle\langle c_{\mathbf{k}-\mathbf{q}-\tau\downarrow}a^+_{-\mathbf{q}}\,;\,c^+_{\mathbf{k}\uparrow}\rangle\rangle_+ = 1.$$

$$(5.7.43)$$

The equation of motion of the new Green function is determined from

$$[c_{\mathbf{k}-\mathbf{q}-\tau\downarrow}a^+_{-\mathbf{q}}\,,\,\mathcal{H}]$$
$$= \{\varepsilon_{\mathbf{k}-\mathbf{q}-\tau\downarrow} - A - J\widetilde{\mathcal{J}}(\mathbf{0},0)\}c_{\mathbf{k}-\mathbf{q}-\tau\downarrow}a^+_{-\mathbf{q}} - B\,c_{\mathbf{k}-\mathbf{q}-\tau\downarrow}a_{\mathbf{q}}$$
$$- \sqrt{2J/N}\sum_{\mathbf{k}'\tau'}j(-\mathbf{q}-\boldsymbol{\tau}')\Big[c^+_{\mathbf{k}'-\mathbf{q}-\tau'\downarrow}c_{\mathbf{k}-\mathbf{q}-\tau\downarrow}c_{\mathbf{k}'\uparrow}$$
$$+ \delta_{\mathbf{k}-\tau,\mathbf{k}'-\tau'}\,\langle a^+_{-\mathbf{q}}a_{-\mathbf{q}}\rangle c_{\mathbf{k}+\tau'-\tau\uparrow}\Big],$$

using an RPA decoupling procedure to obtain the last term. To proceed further, we have to calculate $\langle\langle c^+_{\mathbf{k}'-\mathbf{q}-\tau'\downarrow}c_{\mathbf{k}-\mathbf{q}-\tau\downarrow}c_{\mathbf{k}'\uparrow}\,;\,c^+_{\mathbf{k}\uparrow}\rangle\rangle_+$ and, within the RPA,

$$\langle\langle c^+_{\mathbf{k}'-\mathbf{q}-\tau'\downarrow}c_{\mathbf{k}-\mathbf{q}-\tau\downarrow}c_{\mathbf{k}'\uparrow}\,;\,c^+_{\mathbf{k}\uparrow}\rangle\rangle_+$$
$$= \delta_{\mathbf{k}'-\tau',\mathbf{k}-\tau}\,f_{\mathbf{k}-\mathbf{q}-\tau\downarrow}\langle\langle c_{\mathbf{k}+\tau'-\tau\uparrow}\,;\,c_{\mathbf{k}\uparrow}\rangle\rangle_+$$
$$- \sqrt{2J/N}\frac{j(\mathbf{q}+\boldsymbol{\tau}')\{f_{\mathbf{k}'\uparrow} - f_{\mathbf{k}'-\mathbf{q}-\tau'\downarrow}\}}{\hbar\omega - \varepsilon_{\mathbf{k}'\uparrow} - \varepsilon_{\mathbf{k}-\mathbf{q}-\tau\downarrow} + \varepsilon_{\mathbf{k}'-\mathbf{q}-\tau'\downarrow}}\langle\langle c_{\mathbf{k}-\mathbf{q}-\tau\downarrow}a^+_{-\mathbf{q}}\,;\,c^+_{\mathbf{k}\uparrow}\rangle\rangle_+.$$

Writing $\hbar\omega_1 = \hbar\omega - \varepsilon_{\mathbf{k}-\mathbf{q}-\tau\downarrow}$, we obtain from these equations

$$\{\hbar\omega_1 + A + J\widetilde{\mathcal{J}}(\mathbf{0},0) - J\widetilde{\mathcal{J}}^*(\mathbf{q},-\omega_1)\}\langle\langle c_{\mathbf{k}-\mathbf{q}-\tau\downarrow}a^+_{-\mathbf{q}}\,;\,c^+_{\mathbf{k}\uparrow}\rangle\rangle_+$$
$$+ B\langle\langle c_{\mathbf{k}-\mathbf{q}-\tau\downarrow}a_{\mathbf{q}}\,;\,c^+_{\mathbf{k}\uparrow}\rangle\rangle_+$$
$$= -\sqrt{2J/N}\sum_{\tau'}j(-\mathbf{q}-\boldsymbol{\tau}')\big(f_{\mathbf{k}-\mathbf{q}-\tau\downarrow} + \langle a^+_{-\mathbf{q}}a_{-\mathbf{q}}\rangle\big)\langle\langle c_{\mathbf{k}+\tau'-\tau\uparrow}\,;\,c^+_{\mathbf{k}\uparrow}\rangle\rangle_+.$$

$$(5.7.44)$$

In the sum, the terms with $\boldsymbol{\tau}' \neq \boldsymbol{\tau}$ only lead to higher-order corrections, of the same type as those arising from the difference between $c_{\mathbf{k}\uparrow}$ and $\widetilde{c}_{\mathbf{k}\uparrow}$, and they can be neglected. Calculating $\langle\langle c_{\mathbf{k}-\mathbf{q}-\tau\downarrow}a_{\mathbf{q}}\,;\,c^+_{\mathbf{k}\uparrow}\rangle\rangle_+$ in an equivalent way, and introducing the notation:

$$G_{m1}(\mathbf{q},\omega) = \langle\langle a_{\mathbf{q}}\,;\,a^+_{\mathbf{q}}\rangle\rangle \qquad ; \quad G_{m2}(\mathbf{q},\omega) = \langle\langle a^+_{\mathbf{q}}\,;\,a_{\mathbf{q}}\rangle\rangle = G^*_{m1}(\mathbf{q},-\omega)$$
$$G_{m3}(\mathbf{q},\omega) = \langle\langle a^+_{-\mathbf{q}}\,;\,a^+_{\mathbf{q}}\rangle\rangle \qquad\qquad\qquad\qquad\qquad\qquad (5.7.45)$$

for the magnon Green functions determined by (5.7.25) and (5.7.33), we obtain

$$\langle\langle c_{\mathbf{k}-\mathbf{q}-\tau\downarrow} a_{-\mathbf{q}}^+ ; c_{\mathbf{k}\uparrow}^+ \rangle\rangle_+ = \sqrt{2J/N}\, j(-\mathbf{q}-\boldsymbol{\tau}) G_\uparrow(\mathbf{k},\omega)$$
$$\times \left[\{f_{\mathbf{k}-\mathbf{q}-\tau\downarrow} + \langle a_{\mathbf{q}}^+ a_{\mathbf{q}}\rangle\} G_{m2}(\mathbf{q},\omega_1) - \langle a_{\mathbf{q}} a_{-\mathbf{q}}\rangle G_{m3}(\mathbf{q},\omega_1)\right]. \tag{5.7.46}$$

Defining the self-energy of the spin-up electrons by the relation

$$G_\uparrow(\mathbf{k},\omega) = \frac{1}{\hbar\omega - \varepsilon_{\mathbf{k}\uparrow} - \Sigma_\uparrow(\mathbf{k},\omega)}, \tag{5.7.47}$$

and using (3.1.10) to establish that

$$G_m(\mathbf{q},\omega) = \frac{1}{i\pi} \int \frac{G_m(\mathbf{q},\omega')}{\hbar\omega' - \hbar\omega} d(\hbar\omega'),$$

we obtain finally

$$\Sigma_\uparrow(\mathbf{k},\omega) = -\frac{2J}{N} \sum_{\mathbf{q}\tau} |j(\mathbf{q}+\boldsymbol{\tau})|^2 \frac{1}{i\pi} \int_{-\infty}^{\infty} \frac{d(\hbar\omega')}{\hbar\omega' - \hbar\omega + \varepsilon_{\mathbf{k}-\mathbf{q}-\tau\downarrow}}$$
$$\times \left[\{f_{\mathbf{k}-\mathbf{q}-\tau\downarrow} + \langle a_{\mathbf{q}}^+ a_{\mathbf{q}}\rangle\} G_{m2}(\mathbf{q},\omega') - \langle a_{\mathbf{q}} a_{-\mathbf{q}}\rangle G_{m3}(\mathbf{q},\omega')\right]. \tag{5.7.48}$$

This result corresponds to that deduced by Nakajima (1967), as generalized by Fulde and Jensen (1983).

The average effective mass of the spin-up electrons at the Fermi surface is determined by

$$\frac{1}{m_\uparrow^*} = \frac{1}{\hbar^2 \mathbf{k}} \frac{\partial \mathcal{E}_{\mathbf{k}\uparrow}}{\partial \mathbf{k}}\bigg|_{k=k_{F\uparrow}},$$

averaged over the direction of $\mathbf{k}$. Here $\mathcal{E}_{\mathbf{k}\uparrow} = \varepsilon_{\mathbf{k}\uparrow} + \mathrm{Re}\big[\Sigma_\uparrow(\mathbf{k},\mathcal{E}_{\mathbf{k}\uparrow})\big]$ is the corrected energy of the spin-up electrons. We can neglect the explicit $\mathbf{k}$-dependence of $\Sigma_\uparrow(\mathbf{k},\omega)$ in comparison to its frequency dependence, disregarding terms of the order $E_\mathbf{q}/\varepsilon_F$ in the derivative of $\mathcal{E}_{\mathbf{k}\uparrow}$, so that

$$\frac{\partial \mathcal{E}_{\mathbf{k}\uparrow}}{\partial \mathbf{k}} = \frac{\partial \varepsilon_{\mathbf{k}\uparrow}}{\partial \mathbf{k}} + \frac{1}{\hbar} \frac{\partial}{\partial \omega} \mathrm{Re}\big[\Sigma_\uparrow(\mathbf{k},\omega)\big]\bigg|_{\hbar\omega=\mathcal{E}_{\mathbf{k}\uparrow}} \frac{\partial \mathcal{E}_{\mathbf{k}\uparrow}}{\partial \mathbf{k}},$$

or

$$\frac{m_\uparrow^*}{m} = 1 - \frac{1}{\hbar} \frac{\partial}{\partial \omega} \mathrm{Re}\big[\Sigma_\uparrow(\mathbf{k}_{F\uparrow},\omega)\big]\bigg|_{\hbar\omega=\mathcal{E}_F}, \tag{5.7.49}$$

averaged over the Fermi surface. Within the same approximation, the terms in eqn (5.7.48) proportional to the magnon correlation-functions

can be neglected and, to leading order, $\hbar\omega = \mathcal{E}_F$ in the ω-derivative may be replaced by $\varepsilon_{\mathbf{k}\uparrow}$, with $\mathbf{k} = \mathbf{k}_{F\uparrow}$. In the limit of zero temperature, the free-electron model then gives

$$
\frac{m^*_\uparrow}{m} = 1 + \frac{2J}{N} \sum_{\mathbf{q}\boldsymbol{\tau}} |j(\mathbf{q}+\boldsymbol{\tau})|^2 \frac{1}{\pi} \int_{-\infty}^{\infty} d(\hbar\omega')
$$

$$
\times \frac{1}{2} \int_{-1}^{1} d\mu \frac{\mathrm{Im}\big[G_{m2}(\mathbf{q},\omega')\big]}{\left(\hbar\omega' + \Delta + \frac{(\hbar|\mathbf{q}+\boldsymbol{\tau}|)^2}{2m} - \frac{\hbar^2 k|\mathbf{q}+\boldsymbol{\tau}|}{m}\mu\right)^2},
$$

subject to the conditions that $k = k_{F\uparrow}$ and $|\mathbf{k} - \mathbf{q} - \boldsymbol{\tau}| < k_{F\downarrow}$. These conditions imply that $k_{F\uparrow} - k_{F\downarrow} < |\mathbf{q}+\boldsymbol{\tau}| < k_{F\uparrow} + k_{F\downarrow}$, and that the lower bound -1 of the μ-integral is replaced by $(\hbar^2 q^2 + 2m\Delta)/(2\hbar^2 k_{F\uparrow}|\mathbf{q}+\boldsymbol{\tau}|)$. Because $\mathrm{Im}\big[G_{m2}(\mathbf{q},\omega')\big]$ is odd in ω', the contribution due to the upper bound in the μ-integral can be neglected (it is of the order $\hbar\omega'/\varepsilon_F$). Since

$$
\frac{1}{\pi} \int_{-\infty}^{\infty} \frac{\mathrm{Im}\big[G_{m2}(\mathbf{q},\omega')\big]}{\hbar\omega'} d(\hbar\omega') = \mathrm{Re}\big[G_{m2}(\mathbf{q},0)\big] = -\frac{A_{\mathbf{q}}}{E_{\mathbf{q}}^2},
$$

the average mass-enhancement of the spin-up electrons at the Fermi surface is

$$
\frac{m^*_\uparrow}{m} = 1 + \frac{\mathcal{N}_\downarrow(\varepsilon_F)}{2k_{F\uparrow}k_{F\downarrow}} \int_{k_{F\uparrow}-k_{F\downarrow}}^{k_{F\uparrow}+k_{F\downarrow}} dq \int \frac{d\Omega_{\mathbf{q}}}{4\pi} q|j(\mathbf{q})|^2 \frac{2JA_{\mathbf{q}}}{E_{\mathbf{q}}^2}, \qquad (5.7.50)
$$

and, by symmetry, $m^*_\downarrow/m$ is given by the same expression, except that $\mathcal{N}_\downarrow(\varepsilon_F)$ is replaced by $\mathcal{N}_\uparrow(\varepsilon_F)$. We note that the mass-enhancement only depends on the static part of the susceptibility, i.e. $G_{m2}(\mathbf{q},0)$, and that the magnitude of the mass-renormalization is intimately related to the linewidth of the spin waves derived above in eqn (5.7.38). Utilizing this connection, we can write the specific heat, in the zero-temperature limit,

$$
C = \frac{\pi^2}{3} k_B^2 T \bigg[\mathcal{N}_\uparrow(\varepsilon_F) + \mathcal{N}_\downarrow(\varepsilon_F) + \frac{1}{N} \sum_{\mathbf{q}} \frac{2\Gamma_{\mathbf{q}}}{\pi E_{\mathbf{q}}^2} \bigg] N, \qquad (5.7.51)
$$

where again the $\mathbf{q}$-sum only extends over the primitive Brillouin zone. With typical values of $E_{\mathbf{q}}\mathcal{N}(\varepsilon_F) \approx 0.01$ and $2\Gamma_{\mathbf{q}}/E_{\mathbf{q}} \approx 0.05$, this expression predicts a doubling of the linear term in the heat capacity due to the interaction between the conduction electrons and the spin waves, which therefore has an appreciable effect on the effective mass of the electrons near the Fermi surface. More detailed analyses (Nakajima 1967; Fulde and Jensen 1983) show that the deformation of the electronic bands is

pinned to the Fermi surface, and occurs within a narrow interval with a width corresponding to the spin-wave energies. This implies that, even if the electronic energies $\varepsilon_{\mathbf{k}\sigma}$ appearing in the magnon Green-functions were replaced with $\mathcal{E}_{\mathbf{k}\sigma}$, due to higher-order processes, this modification would not be of much importance. The total electronic heat capacity is $C_e = \sum_{\mathbf{k}\sigma} \mathcal{E}_{\mathbf{k}\sigma} df_{\mathbf{k}\sigma}/dT$, when the imaginary part of the self-energy is neglected. The extra contribution due to the coupling to the spin waves is linear only at the lowest temperatures ($k_B T < 0.05 E_{\mathbf{q}}$), after which it increases more rapidly than linearly to its maximum at $k_B T \simeq 0.15 E_{\mathbf{q}}$. Above $k_B T \simeq 0.3 E_{\mathbf{q}}$, this contribution becomes negative and finally dies out when $k_B T \approx E_{\mathbf{q}}$. This variation with temperature was described by Fulde and Jensen (1983), and has been discussed in the context of the phonon interaction by Grimvall (1981). The bosons (magnons and phonons) do not contribute directly to the linear term in the heat capacity, which is thus a characteristic phenomenon of the Fermi gas. However, the departure from the linear variation when $k_B T > 0.05 E_{\mathbf{q}}$ may be influenced by the spin-wave contribution

$$
C_m = \sum_{\mathbf{q}} \frac{1}{\pi} \int_{-\infty}^{\infty} d(\hbar\omega) \frac{2\Gamma_{\mathbf{q}}(\hbar\omega)^3}{\left\{(\hbar\omega)^2 - E_{\mathbf{q}}^2(T)\right\}^2 + \left\{2\Gamma_{\mathbf{q}}\hbar\omega\right\}^2} \frac{d}{dT}\left(\frac{1}{1 - e^{-\beta\hbar\omega}}\right)
$$

$$
\simeq \sum_{\mathbf{q}} E_{\mathbf{q}}(T) \frac{d}{dT}\left(n_{\mathbf{q}} + \tfrac{1}{2}\right) + \frac{\pi^2}{3} k_B^2 T \sum_{\mathbf{q}} \frac{2\Gamma_{\mathbf{q}}}{\pi E_{\mathbf{q}}^2}\left[\frac{2}{5y^2} + \frac{4}{7y^4} + \cdots\right]_{y=\beta E_{\mathbf{q}}/2\pi},
$$
(5.7.52)

to first order in $\Gamma_{\mathbf{q}}/E_{\mathbf{q}}$. The first term is the RPA spin-wave contribution (5.3.3) derived before, which dominates strongly at elevated temperatures. However, in the low-temperature limit, the second term is of the same order of magnitude as the non-linear corrections to eqn (5.7.51). For comparison, the last term in this equation is multiplied by the factor $\left[1 + 3/(5y^2) + 5/(7y^4) + \cdots\right]$ when the higher-order temperature effects are included. The additional contribution due to the non-zero linewidth of the bosons is normally not considered in the literature. It may be added to the pure electronic contribution derived by Fulde and Jensen (1983), by replacing $yL'(y)$ with $2yL'(y)+L(y)$ in their eqn (17a). The mass-enhancement effect increases proportionally to the inverse of $E_{\mathbf{q}}$ ($\Gamma_{\mathbf{q}} \propto A_{\mathbf{q}}$). On the other hand, the interval in which the linear variation occurs is diminished correspondingly, requiring a more careful consideration of the higher-order modifications.

In the metals, the itinerant electrons also interact with the phonons, and this leads to an entirely equivalent enhancement of their mass. This effect has been calculated for the whole rare earth series by Skriver and Mertig (1990), who find an increase of the band mass due to coupling to the phonons of typically about 35% for the heavy elements. Assuming

the different contributions to be additive, we may write the total mass-enhancement

$$\frac{m^*}{m} = 1 + \lambda_{\text{tot}} = 1 + \lambda_{\text{sw}} + \lambda_{\text{ph}} + \lambda_{\text{c}} \qquad (5.7.53)$$

as a sum of contributions from the interactions with the spin waves and the phonons, and from the possible exchange and Coulomb interactions within the electron gas itself (λ_{c}). Although the different correlation effects may increase the effective mass derived from band structure calculations by a factor of two or more, it is difficult to isolate this enhancement in heat capacity measurements, because of the quite narrow temperature interval where a truly linear behaviour can be anticipated. This interval is bounded below because of the nuclear spins, which may give large contributions to the heat capacity in the mK-range. The upper bound is due partly to the higher-order temperature effects, but most importantly to the disturbance by the normal boson contributions, approximately proportional to $T^\alpha \exp(-E_{\mathbf{0}}/k_B T)$ and T^3 for the magnons and the phonons respectively, which completely dominate the heat capacity at elevated temperatures. Because of this limitation, the most reliable method of determining the mass-enhancement is by measuring the temperature dependence of the dHvA effect, which also allows a separation of the contributions from the different sheets of the Fermi surface. Using this method, and comparing with the results of band structure calculations, Sondhelm and Young (1985) found values of λ_{tot} varying between 0.2 and 1.1 for Gd. The theoretical results of Fulde and Jensen (1983) lie within this range, but these measurements point to the necessity of discriminating between states of different symmetry in considering the mass-enhancement of the conduction electron gas.

5.7.3 Magnetic contributions to the electrical resistivity

The electrical resistivity of a metal can be calculated by solving the *Boltzmann equation*. We shall not discuss the theory of transport properties in detail here, but instead refer to the comprehensive treatments of Ziman (1960), and Smith and Højgaard Jensen (1989). The non-equilibrium distribution function $g_{\mathbf{k}\sigma}$, generated by the application of an external electric field $\mathbf{E}$, is written in terms of the equilibrium distribution function, and is determined by the Boltzmann equation:

$$g_{\mathbf{k}\sigma} = f_{\mathbf{k}\sigma} + f_{\mathbf{k}\sigma}(1 - f_{\mathbf{k}\sigma})\psi_{\mathbf{k}\sigma}, \quad \text{where} \quad \frac{\partial g_{\mathbf{k}\sigma}}{\partial \mathbf{k}} \cdot \frac{d\mathbf{k}}{dt} = \frac{dg_{\mathbf{k}\sigma}}{dt}\bigg|_{\text{coll}}. \quad (5.7.54)$$

The electrical current-density is then determined as

$$\mathbf{j} = \overline{\overline{\sigma}} \cdot \mathbf{E} = -\frac{e}{V} \sum_{\mathbf{k}\sigma} \mathbf{v}_{\mathbf{k}\sigma} f_{\mathbf{k}\sigma}(1 - f_{\mathbf{k}\sigma})\psi_{\mathbf{k}\sigma},$$

with $\hbar\mathbf{v}_{\mathbf{k}\sigma} = \partial\varepsilon_{\mathbf{k}\sigma}/\partial\mathbf{k}$. In the linear regime, the left-hand side of the Boltzmann equation is

$$\frac{\partial g_{\mathbf{k}\sigma}}{\partial\mathbf{k}} \cdot \frac{d\mathbf{k}}{dt} \simeq -\frac{\partial f_{\mathbf{k}\sigma}}{\partial\varepsilon_{\mathbf{k}\sigma}}e\mathbf{v}_{\mathbf{k}\sigma}\cdot\mathbf{E} = e\beta f_{\mathbf{k}\sigma}(1-f_{\mathbf{k}\sigma})\mathbf{v}_{\mathbf{k}\sigma}\cdot\mathbf{E}.$$

The collision term on the right-hand side is

$$\frac{dg_{\mathbf{k}\sigma}}{dt}\bigg|_{\mathrm{coll}} = \sum_{\mathbf{k}'\sigma'}\big[g_{\mathbf{k}'\sigma'}(1-g_{\mathbf{k}\sigma})W(\mathbf{k}'\sigma',\mathbf{k}\sigma) - g_{\mathbf{k}\sigma}(1-g_{\mathbf{k}'\sigma'})W(\mathbf{k}\sigma,\mathbf{k}'\sigma')\big],$$

where $W(\mathbf{k}\sigma,\mathbf{k}'\sigma')$ is the probability per unit time for an electronic transition from an occupied state $|\mathbf{k}\sigma>$ to an unoccupied state $|\mathbf{k}'\sigma'>$. Linearizing the collision term, and using the principle of detailed balance, so that this term must vanish if $g_{\mathbf{k}\sigma} = f_{\mathbf{k}\sigma}$, we may reduce the Boltzmann equation to

$$e\beta f_{\mathbf{k}\sigma}(1-f_{\mathbf{k}\sigma})\mathbf{v}_{\mathbf{k}\sigma}\cdot\mathbf{E} = -\sum_{\mathbf{k}'\sigma'}(1-f_{\mathbf{k}\sigma})f_{\mathbf{k}'\sigma'}W(\mathbf{k}'\sigma',\mathbf{k}\sigma)\big(\psi_{\mathbf{k}\sigma} - \psi_{\mathbf{k}'\sigma'}\big).$$

It is possible to find an upper bound on the resistivity from this equation, with the use of a variational principle. Defining $\hat{\mathbf{u}}$ to be a unit vector along one of the principal axes of the resistivity tensor,

$$\rho_{uu} \leq \frac{V}{2\beta e^2}\frac{\sum_{\mathbf{k}\sigma}\sum_{\mathbf{k}'\sigma'}(1-f_{\mathbf{k}'\sigma'})f_{\mathbf{k}\sigma}W(\mathbf{k}\sigma,\mathbf{k}'\sigma')\big(\phi_{\mathbf{k}\sigma} - \phi_{\mathbf{k}'\sigma'}\big)^2}{\big[\sum_{\mathbf{k}\sigma}\mathbf{v}_{\mathbf{k}\sigma}\cdot\hat{\mathbf{u}}\,(1-f_{\mathbf{k}\sigma})f_{\mathbf{k}\sigma}\,\phi_{\mathbf{k}\sigma}\big]^2},$$

$$(5.7.55)$$

where $\phi_{\mathbf{k}\sigma}$ is an arbitrary trial function, and where the equality applies if $\phi_{\mathbf{k}\sigma} = \psi_{\mathbf{k}\sigma}$. In the case of the free-electron model, the Boltzmann equation possesses an exact solution, $\psi_{\mathbf{k}\sigma} \propto \mathbf{k}\cdot\hat{\mathbf{u}}$, if the scattering is purely elastic. As discussed, for instance, by Hessel Andersen *et al.* (1980), this trial function is still useful for treating possible inelastic scattering mechanisms, at least as long as the resistivity is dominated by elastic impurity scattering, so we shall use $\phi_{\mathbf{k}\sigma} = \mathbf{k}\cdot\hat{\mathbf{u}}$.

   In the Born approximation, the transition probability per unit time is given by the Golden Rule (4.1.1), which we may here write

$$W(\mathbf{k}\sigma,\mathbf{k}'\sigma') = \frac{2\pi}{\hbar}\sum_{if}P_i|<\mathbf{k}\sigma;i\,|\,\mathcal{H}_{\mathrm{int}}\,|\,\mathbf{k}'\sigma';f>|^2\delta(\hbar\omega + E_i - E_f),$$

where $\hbar\omega = \varepsilon_{\mathbf{k}\sigma} - \varepsilon_{\mathbf{k}'\sigma'}$. Instead of basing the derivation of the magnetic resistivity on the linearized spin-wave expression (5.7.20) for $\mathcal{H}_{\mathrm{int}}$, we shall be somewhat more general and use $\mathcal{H}_{sf}$ from eqn (5.7.6) as the

interaction Hamiltonian. We assume that the system is uniform, paramagnetic or ferromagnetically ordered, continue to utilize the simple free-electron model, and replace $(g-1)I(n'\mathbf{k}', n\mathbf{k})$ by $j(\mathbf{k}' - \mathbf{k} + \boldsymbol{\tau})$. The MF part (5.7.7) of the Hamiltonian may lead to a modification $\varepsilon_{\mathbf{k}\sigma} \to \widetilde{\varepsilon}_{\mathbf{k}\sigma}$ of the electronic band-states, but we can neglect this difference to leading order, and since the MF Hamiltonian does not lead to transitions between electronic states, we can replace J_{iz} by $\hat{J}_{iz} = J_{iz} - \langle J_z \rangle$ in $\mathcal{H}_{\text{int}}$, and obtain

$$W(\mathbf{k}\sigma, \mathbf{k}'\sigma') = \int_{-\infty}^{\infty} d(\hbar\omega)\delta(\hbar\omega - \varepsilon_{\mathbf{k}\sigma} + \varepsilon_{\mathbf{k}'\sigma'})$$

$$\times \frac{2\pi}{\hbar} \sum_{if} P_i \frac{1}{N^2} \sum_{jj'} |j(\mathbf{k}' - \mathbf{k})|^2 e^{-i(\mathbf{k}'-\mathbf{k})\cdot(\mathbf{R}_j - \mathbf{R}_{j'})}$$

$$\times \Big\{ <i|J_{j'}^-|f><f|J_j^+|i> \delta_{\sigma\uparrow}\delta_{\sigma'\downarrow} + <i|J_{j'}^+|f><f|J_j^-|i> \delta_{\sigma\downarrow}\delta_{\sigma'\uparrow}$$

$$+ <i|\hat{J}_{j'z}|f><f|\hat{J}_{jz}|i> (\delta_{\sigma\uparrow}\delta_{\sigma'\uparrow} + \delta_{\sigma\downarrow}\delta_{\sigma'\downarrow}) \Big\}\delta(\hbar\omega + E_i - E_f),$$
$$(5.7.56)$$

accounting explicitly for the condition on $\hbar\omega$ by the integral over the first δ-function. Using the same procedure as in the calculation of the neutron-scattering cross-section, when going from (4.1.16) to (4.2.1–3), we may write this:

$$W(\mathbf{k}\sigma, \mathbf{k}'\sigma') = \frac{2}{N\hbar} \int_{-\infty}^{\infty} d(\hbar\omega)\delta(\hbar\omega - \varepsilon_{\mathbf{k}\sigma} + \varepsilon_{\mathbf{k}'\sigma'}) \frac{1}{1 - e^{-\beta\hbar\omega}} |j(\mathbf{k} - \mathbf{k}')|^2$$

$$\times \Big\{ \chi''_{-+}(\mathbf{k} - \mathbf{k}', \omega)\delta_{\sigma\uparrow}\delta_{\sigma'\downarrow} + \chi''_{+-}(\mathbf{k} - \mathbf{k}', \omega)\delta_{\sigma\downarrow}\delta_{\sigma'\uparrow}$$

$$+ \chi''_{zz}(\mathbf{k} - \mathbf{k}', \omega)(\delta_{\sigma\uparrow}\delta_{\sigma'\uparrow} + \delta_{\sigma\downarrow}\delta_{\sigma'\downarrow}) \Big\}.$$

Introducing this expression into (5.7.55), and using $\phi_{\mathbf{k}\sigma} = \mathbf{k} \cdot \hat{\mathbf{u}}$ and $\mathbf{k}' = \mathbf{k} - \mathbf{q} - \boldsymbol{\tau}$, we proceed as in the derivation of eqn (5.7.36) for $\text{Im}\big[\chi^{+-}_{\text{c.el.}}(\mathbf{q}, \omega)\big]$, obtaining

$$\frac{1}{N} \sum_{\mathbf{k}} f_{\mathbf{k}\downarrow}(1 - f_{\mathbf{k}-\mathbf{q}\uparrow})\delta(\hbar\omega - \varepsilon_{\mathbf{k}\downarrow} + \varepsilon_{\mathbf{k}-\mathbf{q}\uparrow}) =$$

$$\frac{V}{N(2\pi)^2} \int_0^{\infty} dk\, k^2 \int_{-1}^{1} d\mu\, f(\varepsilon_{\mathbf{k}\downarrow})\big\{1 - f(\varepsilon_{\mathbf{k}\downarrow} - \hbar\omega)\big\}\delta\big(\hbar\omega - \Delta + \varepsilon_q - \mu\frac{\hbar^2 qk}{m}\big)$$

$$= \frac{V}{N(2\pi)^2} \int_{\frac{\Delta}{2}}^{\infty} d\varepsilon \frac{m^2}{\hbar^4 q} f(\varepsilon)\big\{1 - f(\varepsilon - \hbar\omega)\big\} = \frac{V}{N(2\pi)^2} \frac{m^2}{\hbar^4 q} \frac{\hbar\omega}{e^{\beta\hbar\omega} - 1},$$

where $k_{F\uparrow} - k_{F\downarrow} < q < k_{F\uparrow} + k_{F\downarrow}$ (when $k_B T \ll \varepsilon_F$). The denominator in (5.7.55) may be calculated in a straightforward fashion and

is $[N\nu/(\hbar\beta)]^2$, and we finally obtain the following expression for the resistivity, or rather its upper limit:

$$\rho_{uu}(T) \simeq \rho_0 \frac{3}{(4k_{F\uparrow}k_{F\downarrow})^2 \overline{j_u^2}} \int_{k_{F\uparrow}-k_{F\downarrow}}^{k_{F\uparrow}+k_{F\downarrow}} dq \int \frac{d\Omega_{\mathbf{q}}}{4\pi} \int_{-\infty}^{\infty} d(\hbar\omega)$$

$$\times |j(\mathbf{q})|^2 (\mathbf{q}\cdot\hat{\mathbf{u}})^2 q \frac{\beta\hbar\omega}{\sinh^2(\beta\hbar\omega/2)} \frac{1}{\pi} \sum_\alpha \chi''_{\alpha\alpha}(\mathbf{q},\omega), \quad (5.7.57a)$$

where

$$\rho_0 = \frac{3}{2} \frac{V}{N} \frac{\pi m}{\hbar e^2 \varepsilon_F} \overline{j_u^2} = \frac{m}{ne^2} \frac{\pi}{\hbar} \{\mathcal{N}_\uparrow(\varepsilon_F) + \mathcal{N}_\downarrow(\varepsilon_F)\} \overline{j_u^2}, \qquad (5.7.57b)$$

$n = \nu N/V$ is the electron density, and

$$\overline{j_u^2} = 4 \frac{3}{(2k_F)^4} \int_0^{2k_F} dq \int \frac{d\Omega_{\mathbf{q}}}{4\pi} |j(\mathbf{q})|^2 (\mathbf{q}\cdot\hat{\mathbf{u}})^2 q. \qquad (5.7.57c)$$

For cubic symmetry, ρ_{uu} is independent of u and $(\mathbf{q}\cdot\hat{\mathbf{u}})^2$ can be replaced by $q^2/3$. In the high-temperature limit, we have

$$\frac{1}{\pi} \int_{-\infty}^{\infty} d(\hbar\omega) \frac{\beta\hbar\omega}{\sinh^2(\beta\hbar\omega/2)} \sum_\alpha \chi''_{\alpha\alpha}(\mathbf{q},\omega) \simeq$$

$$\frac{1}{\pi} \int_{-\infty}^{\infty} d(\hbar\omega) \frac{4}{\beta\hbar\omega} \sum_\alpha \chi''_{\alpha\alpha}(\mathbf{q},\omega) = \frac{4}{\beta} \sum_\alpha \chi'_{\alpha\alpha}(\mathbf{q},0) = 4J(J+1),$$

recalling that $\chi'_{\alpha\alpha}(\mathbf{q},0) = \frac{1}{3}\beta J(J+1)$ in this limit. This result shows that the magnetic resistivity saturates at temperatures which are so high that the ions are uniformly distributed over the states in the ground-state J-multiplet, since the condition $k_B T \ll \varepsilon_F$ is always satisfied:

$$\rho_{uu}(T) \to J(J+1)\rho_0 \qquad \text{for} \quad T \to \infty, \qquad (5.7.58)$$

and $J(J+1)\rho_0$ is called the saturation value of the *spin-disorder* resistivity. Since ρ_0 contains the factor $(g-1)^2$, the spin-disorder resistivity is proportional to the de Gennes factor, as observed (Legvold 1972). If the crystal-field splitting of the energy levels is neglected, this factor also determines the relative magnitudes of the contributions of magnetic rare earth-impurities to the resistivity of a non-magnetic host (Kasuya 1959). However, in analysing the measurements of Mackintosh and Smidt (1962) of the resistivity changes produced by small amounts of heavy rare earths in Lu, Hessel Andersen (1979) found that such crystal-field effects are indeed important at $4\,\mathrm{K}$.

In a metal, the total collision rate $W(\mathbf{k}\sigma, \mathbf{k}'\sigma')$ in eqn (5.7.55) is actually the sum of contributions from several scattering mechanisms. If the trial function for elastic impurity-scattering still leads to a result reasonably close to that determined by the exact solution of the Boltzmann equation, then (5.7.55) implies that the different scattering mechanisms contribute additively to the total resistivity, in accordance with *Matthiessen's rule*:

$$\rho_{\text{total}}(T) = \rho_{\text{imp}} + \rho_{\text{m}}(T) + \rho_{\text{ph}}(T). \qquad (5.7.59)$$

Here ρ_{imp} is the residual resistivity due to elastic scattering of the electrons from impurities and from lattice defects. $\rho_{\text{m}}(T)$ is the contribution, calculated above, due to the magnetic excitations, whereas $\rho_{\text{ph}}(T)$ is the equivalent term due to the phonons. The two last terms, associated with the excitations in the metal, vanish in the limit of zero temperature, so that $\rho_{\text{total}}(T = 0) = \rho_{\text{imp}}$. The problem of distinguishing between the magnetic and phonon scattering can be approximately solved by estimating the latter from the temperature dependence of the resistivity of Lu, which has an electronic structure and phonon spectrum very similar to those of the magnetic heavy rare earths, but no magnetic moment. Using this method, Mackintosh (1963) was able to show that the magnetic scattering in Tb increases as $\exp(-E_\mathbf{0}/k_BT)$ at low temperatures, where the spin-wave energy gap $E_\mathbf{0}/k_B$ was estimated to be about 20 K, a value which was subsequently verified by neutron scattering. This analysis was refined by Hessel Andersen and Smith (1979), who used the free-electron model to show that the magnetic resistivity associated with the scattering by spin waves with an isotropic dispersion relation $E_\mathbf{q} = E_\mathbf{0} + \hbar^2 q^2/2m_{\text{sw}}$ is given by

$$\rho_{\text{m}}(T) = \frac{J}{4}\frac{m_{\text{sw}}^2}{m^2}\frac{E_\mathbf{0}k_BT}{\varepsilon_F^2}e^{-E_\mathbf{0}/k_BT}\Big(1 + 2\frac{k_BT}{E_\mathbf{0}} + \tfrac{1}{2}e^{-E_\mathbf{0}/k_BT} + \cdots\Big)\rho_0,$$
$$(5.7.60)$$

approximating the lower cut-off $k_{F\uparrow} - k_{F\downarrow}$ by 0 in (5.7.57a). A numerical calculation, utilizing the measured spin-wave energies and including one scaling parameter for the magnetic scattering and one for the phonon scattering, gave the excellent fit shown in Fig. 5.14. The disordered electric quadrupole moments of the $4f$-charge distributions can also provide a mechanism for the scattering of the conduction electrons. This is normally very difficult to distinguish from the magnetic scattering, but in TmSb, where the exchange interaction is relatively small and the electric quadrupoles large, the latter appear to dominate the electrical resistivity at low temperatures (Hessel Andersen and Vogt 1979).

Even though $k_BT \ll \varepsilon_F$, the residual resistivity ρ_{imp} is only independent of temperature as long as the ground-state properties of the
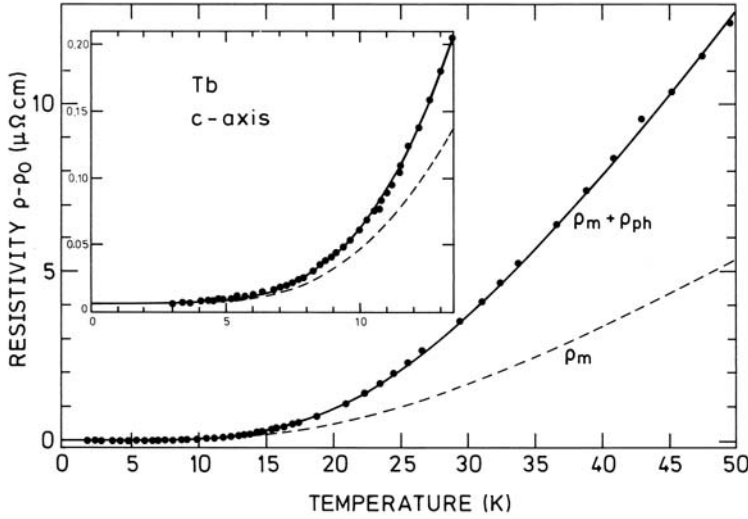
Fig. 5.14. A comparison of the measured and calculated resistivity of a Tb single crystal, as a function of temperature, after Hessel Andersen and Smith (1979). The residual resistivity has been subtracted from the experimental results. The full line includes the calculated contributions from both the magnon scattering and the phonons. The rapid increase around 20 K is predominantly due to the excitation of magnons across the energy gap.

electron gas remain unchanged. If the resistivity of the unpolarized electrons is $\rho^0_{\text{total}}(T)$ and their density of states at the Fermi surface is $\mathcal{N}(\varepsilon_F)$, the polarization (5.7.16) of the conduction electrons in the ferromagnetic state leads to a scaling of the *total* resistivity, which according to eqn (5.7.55) is

$$\rho_{\text{total}}(T) = \left\{1 + \zeta(T)\right\}\rho^0_{\text{total}}(T) \quad ; \quad \zeta(T) = \frac{\mathcal{N}_\uparrow(\widetilde{\varepsilon}_F) + \mathcal{N}_\downarrow(\widetilde{\varepsilon}_F)}{2\mathcal{N}(\varepsilon_F)} - 1.$$
(5.7.61)

In $\rho^0_{\text{total}}(T)$, the residual resistivity is temperature independent and the magnetic contribution is determined by the above result, if $\mathcal{N}_\sigma(\varepsilon_F)$ in (5.7.57b) is replaced by its paramagnetic value $\mathcal{N}(\varepsilon_F)$. The modification $\zeta(T)$, due to the polarization of the conduction electrons, depends on the temperature via the magnetization, and $\zeta(T) \propto \langle J_z \rangle^2$ at small magnetization.

The most important effect on the resistivity produced by the spin-polarization of the electronic states results from the change in the density of states at the Fermi surface, taken into account by $\zeta(T)$ in (5.7.61).

Since the other modification, the appearance of $k_{F\sigma}$ instead of the paramagnetic value k_F in (5.7.57b), generally only causes a minor correction to the value of the integral in this equation, the magnetic contribution to $\rho^0_{\text{total}}(T)$ is approximately independent of the spin-polarization, in this model. However, the spin-polarization in the real metals may be sufficiently great to alter the topology of the Fermi surface, as discussed in Section 1.4, so that the resistivity may change abruptly with temperature or magnetic field. Under these circumstances, the resistivity must be calculated from first principles, using a realistic model of the spin-polarized energy bands. The zz-contribution should be treated separately, as the q-integral for this case should go from 0 to $2k_F$, even when the electron spins are polarized, since no spin-flip is involved in the scattering process. This modification is, however, unimportant as the dominating contributions, in the ordered phase, arise from the perpendicular spin-wave components of the susceptibility.

The above results also apply, to a good approximation, when the moments are ordered antiferromagnetically, if the value of $\zeta(T)$ is calculated for a spatial modulation of the moments. The spin-polarization of the band electrons is determined by the MF Hamiltonian, and assuming $\langle J_{iz} \rangle = \langle J_z \rangle \cos(\mathbf{Q} \cdot \mathbf{R}_i)$, we may replace (5.7.7) by

$$\mathcal{H}_{sf}(\text{MF}) = -\sum_{nn'} \sum_{\mathbf{kk'}} (g-1) I(n'\mathbf{k'}, n\mathbf{k}) \big(c^+_{n'\mathbf{k'}\uparrow} c_{n\mathbf{k}\uparrow} - c^+_{n'\mathbf{k'}\downarrow} c_{n\mathbf{k}\downarrow} \big)$$
$$\times \frac{1}{2} \big(\delta_{\mathbf{k'},\mathbf{k}+\mathbf{Q}+\tau} + \delta_{\mathbf{k'},\mathbf{k}-\mathbf{Q}+\tau} \big) \langle J_z \rangle, \qquad (5.7.62)$$

showing that the modulated moments induce a coupling between the band electrons at the wave-vectors $\mathbf{k}$ and $\mathbf{k} \pm \mathbf{Q} + \tau$. In the same way as the periodic lattice potential lifts the degeneracy of the band states at the Brillouin-zone boundaries (passing through $\mathbf{k} = \tau/2$), the above MF Hamiltonian gives rise to energy gaps at the *superzone boundaries*, the planes perpendicular to, and passing through, the vectors $\mathbf{k}_s = (\pm\mathbf{Q} + \tau)/2$. If $\mathbf{k}_s$ is along the c-axis, the value of the energy gap δ is $(g-1)|I(n\mathbf{k}, n - \mathbf{k})|\langle J_z \rangle$ in the nth band. The importance of the superzone gaps for the resistivity was first pointed out by Mackintosh (1962), and detailed theories were developed by Elliott and Wedgwood (1963) and Miwa (1963). These theories utilized the free-electron model and the *relaxation time* approximation, $dg_{\mathbf{k}\sigma}/dt|_{\text{coll}} = -(g_{\mathbf{k}\sigma} - f_{\mathbf{k}\sigma})/\tau_{\mathbf{k}\sigma}$, giving a conductivity

$$\sigma_{uu} = \frac{e^2 \beta}{V} \sum_{\mathbf{k}\sigma} \tau_{\mathbf{k}\sigma} \big(\mathbf{v}_{\mathbf{k}\sigma} \cdot \hat{\mathbf{u}} \big)^2 f_{\mathbf{k}\sigma} \big(1 - f_{\mathbf{k}\sigma} \big)$$

or, if the relaxation time $\tau_{\mathbf{k}\sigma}$ is assumed to be constant over the Fermi

surface,

$$\sigma_{uu} \simeq \frac{e^2\tau}{(2\pi)^3\hbar^2} \sum_{\sigma} \int_{\varepsilon_{\mathbf{k}\sigma}=\varepsilon_F} \left(\frac{\partial\varepsilon_{\mathbf{k}\sigma}}{\partial k_u}\right)^2 \frac{1}{|\nabla_{\mathbf{k}}\varepsilon_{\mathbf{k}\sigma}|} dS, \qquad (5.7.63)$$

where dS is a surface element of the Fermi surface. Even without detailed calculations, this expression shows that the conductivity may be reduced substantially if the superzone gaps are able to eliminate significant areas of the Fermi surface. Furthermore, the Fermi-velocity factor puts different weight on the various regions of the Fermi surface in the different components of the conductivity tensor. If $\mathbf{k}_s$ is parallel to the c-axis, as in the heavy rare earths, and if its length is close to that of the Fermi wave-vector in the c-direction, only the cc-component of the conductivity is appreciably affected by the superzone boundary. For instance, an internal field of $2\,\text{kOe}$ in the basal plane of Ho at 4 K, which eliminates the superzone energy gaps by inducing a transition from the cone to ferromagnetic ordering, increases the conductivity along the c-axis by about 30%, while decreasing the b-axis component by only about 1% (Mackintosh and Spanel 1964). As illustrated in Fig. 5.15, the anomalous increase in the resistivity in the helical phase of Tb is eliminated by a magnetic field which is large enough to suppress this structure, leaving only a weak maximum similar to that observed in Gd, which has been ascribed to critical scattering of the conduction electrons by magnetic fluctuations (de Gennes and Friedel 1958). This anomalous increase is not observed in the basal plane and the resistivity is little affected by a magnetic field (Hegland *et al.* 1963).

The theoretical calculations of the superzone effects within the free-electron model give a semi-quantitative account of the experimental observations, with a small number of adjustable parameters. For example, a superzone boundary normal to the c-axis, which intersects the Fermi surface, gives a positive contribution to $\zeta_{cc}(T)$ in (5.7.61) which is proportional to δ/ε_F, while $\zeta_{bb}(T)$ decreases like $(\delta/\varepsilon_F)^2$. Bearing in mind the analogy between the real and free-electron Fermi surfaces mentioned above, this corresponds well with the observations in, for example, Ho. In addition, the model calculations suggest that the superzone gaps are important for the value of the ordering wave-vector $\mathbf{Q}$, at which the exchange energy has its maximum (Elliott and Wedgwood 1964; Miwa 1965), by predicting a gradual reduction of the length of $\mathbf{Q}$ with the increase of the size of the superzone gaps, which are proportional to $\langle J_z \rangle$ below the Néel temperature. Hence the exchange coupling $\mathcal{J}(\mathbf{q})$ is somewhat dependent on the magnetization, because the nearly elastic intra-band contributions to the exchange interaction depend on the density of states near the Fermi surface, as is also true in the ferromagnetic case, according to (5.7.21).
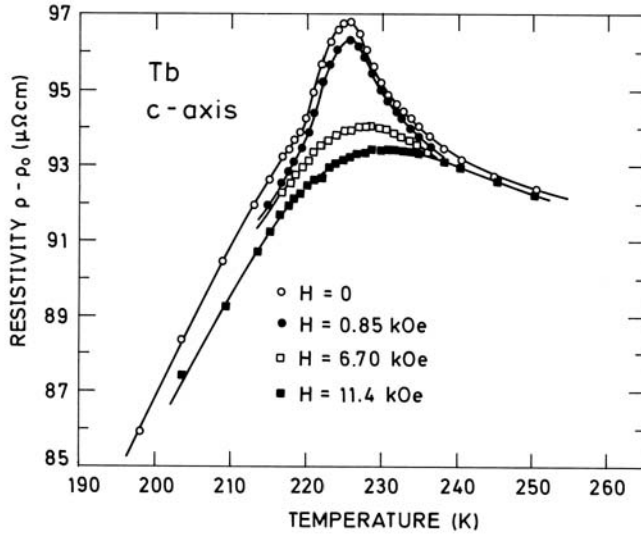
Fig. 5.15.   The *c*-axis resistivity of Tb in the vicinity of $T_N = 230\,\mathrm{K}$, after Hegland *et al.* (1963). As the helical ordering develops, the magnetic superzones cause a sharp increase in the resistivity, which disappears at $T_C = 220\,\mathrm{K}$. The superzones may also be eliminated by a magnetic field in the *b*-direction, which suppresses the helical structure.

The agreement obtained between simple model calculations of the variation of **Q** and that observed experimentally is surprisingly good, to some extent fortuitously so. The band electrons are far from free-electron-like in the rare earth metals, and the approximation in which $I(n'\mathbf{k}', n\mathbf{k})$ is replaced by $j(\mathbf{k}' - \mathbf{k} + \boldsymbol{\tau})$ is rather crude. The effective free-electron model, with $j(\mathbf{q})$ proportional to a form factor $\left[1 + (A\,q)^2\right]^{-1}$ where $A \approx 0.2\,\text{Å}$ and $2k_F \approx 2.8\,\text{Å}^{-1}$, leads to a maximum in $\mathcal{J}(\mathbf{q})$ at $\mathbf{q} \simeq 0.3\,\text{Å}^{-1}$ parallel to the *c*-axis, in the paramagnetic phase. In this model, $\frac{1}{N}\sum_{\mathbf{q}} \widetilde{\mathcal{J}}(\mathbf{q})$ is found to be an order of magnitude larger than $\mathcal{J}(\mathbf{0})$, and the same is the case with the interband contributions ($\boldsymbol{\tau} \neq \mathbf{0}$) to the exchange interaction, compared to the intra-band contributions. However, various estimates indicate that all these terms are of the same order of magnitude. Lindgård *et al.* (1975) have made the only existing *ab initio* calculation of $\mathcal{J}(\mathbf{q})$ in a rare earth metal, considering the simplest case of Gd, and they obtained a reasonable account of the dependence on wave-vector, even though the magnitude differed by as much as a factor of four from that determined experimentally. Their calculations show that the exchange integral is dominated by the

contributions of the d-like band electrons, as is the density of states at the Fermi surface. Although the effective free-electron model is not adequate for determining the exchange interaction, other quantities derived above which depend on real scattering processes close to the Fermi surface (i.e. the contributions to the spin-wave linewidths, the mass enhancement, and the resistivity), may be more trustworthy, particularly if the actual density of states of the band electrons is substituted for the free-electron value. This should especially be true for the linewidth and mass-enhancement, but the strong polarization effect (5.7.60) on the resistivity in the ferromagnetic phase, for which the maximum effect occurs in Gd, with $\zeta(T)$ approaching -0.5 in the zero temperature limit (Fulde and Jensen 1983), may be somewhat exaggerated, because the conductivity is strongly influenced by the sp-band electrons.